CITY UNIVERSITY OF HONG KONG
香港城市大學

Routing and Spectrum Allocation for Multicast Traffic in Elastic Optical Networks
彈性光網絡中多播業務的路由和頻譜分配

Submitted to
Department of Electronic Engineering
電子工程系
in Partial Fulfillment of the Requirements
for the Degree of Doctor of Philosophy
哲學博士學位

by

CAI Anliang
蔡安亮

March 2018
二零一八年三月

Abstract

Internet traffic has been experiencing an enormous growth in the past few decades. This growth will continue with the increasing demand for and popularity of new services such as cloud computing. In particular, cloud service providers (CSP), such as Google and Facebook, transport and replicate their data between geographically distributed datacenters using inter-datacenter wide area networks. How to improve the network throughput in order to sustain growth has emerged as an important research problem.

The traditional Wavelength-Division Multiplexing (WDM) optical networks may not provide a viable solution since their frequency-grid follows the ITU-T standards and is therefore coarse and fixed, leading to inflexibility in spectrum resource allocation and low spectrum efficiency. For example, it is a waste of spectrum to allocate 50-GHz bandwidth to a 10-Gb/s connection. To mitigate these drawbacks, Elastic Optical Networks (EONs) have been proposed finer granularity and to allow for partial spectrum overlapping. EONs have many advantages, e.g., the support of high speed transmissions beyond 100 Gb/s, and new features, e.g., distance-adaptive transmission. These features make it a promising candidate for next-generation optical transport networks. This thesis focuses on efficient designs of EONs for multicast services, as could be, required by the aforementioned data replication.

Three technologies, namely, lightpath, light-tree, and light-trail, can be utilized for the provision of multicast services. As the latter two are inherent to support

optical multicasting, a multicast can be provisioned either by a single light-tree/light-trail or multiple light-trees/light-trails, each connecting the source to a subset of the destinations, while for the lightpath technology, a multicast is provisioned by lightpaths, each connecting the source to a destination. We made a comprehensive comparison among these five schemes in the context of EONs taking into account their distance-adaptive transmission capability. Numerical results illustrate their performances for a range of cases.

We then adopt the light-tree scheme as is simple but efficient, and address the problem of accommodating multiple multicast demands in EONs. For this problem, we provide a Mixed Integer Linear Programming (MILP) formulation for the small-size problems. We also propose an efficient heuristic algorithm for large instances, and compare it to existing approaches. Moreover, since heuristics accommodate demands in a sequence order and different sequences yield varied performances, we investigated the impact of sequences on the heuristic performance by proposing a couple of ordering strategies for good solutions. Numerical results show that the proposed algorithm achieves better performance than the existing ones in the various cases, and approaches the optimum obtained by the MILP algorithm.

We also consider protection in the EON design in the event of single-link failures. We provision each multicast demand by a light-tree, and protect these light-trees against any single-link failure. Given an EON and a set of multicast demands, the objective is to minimize the bandwidth requirement under the condition that all the demands are accommodated by distance-adaptive spectrum allocation. For the static traffic model, we provide a MILP formulation and propose an efficient heuristic algorithm for the protection scheme. We also consider a dynamic traffic model where a Markov-chain simulation is used to evaluate the performance of the proposed algorithm. Numerical results demonstrate the effectiveness of the proposed algorithm.

CITY UNIVERSITY OF HONG KONG
Qualifying Panel and Examination Panel

Surname: CAI

First Name: Anliang

Degree: PhD

College/Department: Department of Electronic Engineering

The Qualifying Panel of the above student is composed of:

Supervisor(s)
Prof. ZUKERMAN Moshe — Department of Electronic Engineering, City University of Hong Kong

Qualifying Panel Member(s)
Dr. CHAN Chi Hung Sammy — Department of Electronic Engineering, City University of Hong Kong

Dr. WONG Wing Ming Eric — Department of Electronic Engineering, City University of Hong Kong

This thesis has been examined and approved by the following examiners:

Dr. CHAN Chi Hung Sammy — Department of Electronic Engineering, City University of Hong Kong

Dr. YEUNG Kai Hau Alan — Department of Electronic Engineering, City University of Hong Kong

Prof. ZUKERMAN Moshe — Department of Electronic Engineering, City University of Hong Kong

Prof. WOSINSKA Lena — School of Information and Communication Technology, KTH Royal Institute of Technology

I would like to dedicate this thesis to my mother and to the memory of my father.

Acknowledgements

Foremost, I would like to express the highest appreciation to my supervisor, Prof. ZUKERMAN Moshe. He is my role model as a researcher. His invaluable guidance helps my research and writing all the time. Without his enthusiastic support and extreme patience, I could not have completed my Ph.D. program and this thesis.

I offer my heartfelt gratitude to Prof. SHEN Gangxiang at Soochow University, China. Without him, I would never have the opportunity to start this wonderful journey.

I would also like to give thanks to Prof. SHEN Gangxiang, Prof. CHAN Chun-Kit, Dr. LIN Rongping, Dr. GUO Jun and Dr. FAN Zheyu for their constructive comments and substantial contributions to the papers which constitute an important part of this thesis.

I wish to thank Prof. MUKHERJEE Biswanath at the University of California, Davis, for the valuable mentoring and time spent during my visit there. Many thanks also go to Dr. ZHAO Yongli, Dr. LI Yongcheng, Dr. WANG Xinbo, Miss WANG Lin, Mr. WU Yu, and Mr. WANG Wei for their kind help in Davis.

I express the warmest thanks to my fellow Ph.D. students, Mr. XU Kai, Mr. LI Fan, Mr. WANG Qing, Mr. YU Weiwen, and Miss XING Chang for stimulating discussions and happy moments.

Last but not least, I thank my grandparents, parents, sisters, and my wife XU Xin for their spiritual supports and encouragements.

The work described in this thesis was supported by a grant from the Research Grants Council of the Hong Kong Special Administrative Region, China [CityU 11216214].

Table of contents

List of figures

List of tables

Acronyms

AFA Adaptive Frequency Assignment.

BPSK Binary Phase-Shit Keying.

BV-OXC Bandwidth-Variable Optical Cross-Connect.

BV-WSS Bandwidth-Variable Wavelength Selective Switch.

BV-WXC Bandwidth-Variable Wavelength Cross-Connect.

BVT Bandwidth-Variable Transponder.

CO-OFDM Coherent Optical Orthogonal Frequency-Division Multiplexing.

DAC Digital-to-Analog Converter.

DCMCT Distance-Constrained Minimum-Cost Tree.

DPP Dedicated Path Protection.

DSP Digital Signal Processing.

EON Elastic Optical Network.

FDM Frequency-Division Multiplexing.

FS Frequency Slot.

FWDM Flexible Wavelength-Division Multiplexing.

ILP Integer Linear Programming.

ITU-T International Telecommunication Union-Telecommunication Standardization Sector.

MC Multicast-Capable.

MC-RMSA Multicast-Capable Routing, Modulation and Spectrum Assignment.

MI Multicast-Incapable.

MILP Mixed Integer Linear Programming.

MPH Minimum-cost Path Heuristic.

MS Modulation Scheme.

OEO Optical-Electrical-Optical.

OFDM Orthogonal Frequency-Division Multiplexing.

OSNR Optical Signal-to-Noise Ratio.

OXC Optical Cross-Connect.

PDM Polarization-Division Multiplexing.

QAM Quadrature Amplitude Modulation.

QPSK Quadrature Phase-Shit Keying.

RMSA Routing, Modulation, and Spectrum Assignment.

ROADM Reconfigurable Optical Add/Drop Multiplexer.

RSA Routing and Spectrum Assignment.

RWA Routing and Wavelength Assignment.

SBPP Shared Backup Path Protection.

SBVT Sliceable Bandwidth-Variable Transponder.

SD Source-Destination.

SLICE Spectrum-Sliced Elastic Optical Path Network.

SPT Shortest-Path Tree.

SSS Spectrum Selective Switch.

SW Spectrum Window.

SWP Spectrum-Window Plane.

TaC Tap-and-Continue.

WDM Wavelength-Division Multiplexing.

WSS Wavelength Selective Switch.

WXC Wavelength Cross-Connect.

Chapter 1

Introduction

1.1 Motivations

Internet traffic has experienced enormous growth in the past few decades. This growth is continuing unabated due to the increasing demand and popularity of new services. These services include ultrahigh-definition TV and cloud computing, and typically require large bandwidth. Cisco predicted that the annual global IP traffic will be over one Zettabyte in 2016 [1] and will reach 2.3 Zettabytes by 2020 at a compound annual growth rate of 22 percent as shown in Fig. 1.1.

Besides this rapid growth, future traffic will become much more dynamic over time. Within a day, the traffic pattern in the daytime is different from that in the evening. In the daytime, the traffic is believed to be very high due to the very large number of users, while in the evening, the traffic is anticipated to be low as there are far fewer users involved [9]. Such traffic variations should be considered for efficiently designing future networks.

As content and cloud service providers compete in the service market, traffic type will also become more diverse. To provide cloud services, resources in datacenters, e.g., computing capabilities, are virtualized to support millions of users. Users are usually allocated to certain virtual machines. The users can operate their virtual

machines to perform various functionalities. They can install different applications and use the virtual machines as storage for all kinds of data, e.g., photos and videos. These various services have a wide range of bandwidth requirements. As noted by Cisco, the annual global datacenter traffic reached 4.7 Zettabytes in 2015, and will grow three-fold over the next 5 years reaching 15.3 Zettabytes in 2020 [10]. The operations of datacenter networks do not need to be placed outside the operators' network, and can be part of it to provide services by, for example, network function virtualization [11].

Traffic patterns have changed due to the newly emerging services, some of them will require larger bandwidth than current services. Future traffic is expected to reach Tb/s class [12]. Also, the traffic will become more dynamic over time and will have a higher percentage of multicast, e.g., live Internet video was predicted by Cisco to increase from 3% in 2016 to 13% in 2021 [13]. How to enhance the network in order to sustain such traffic patterns has become an important research problem.

To better support emerging traffic patterns, EONs have been proposed to provide cost-effective solutions. Compared to traditional WDM optical networks, EONs provide better flexibility by allocating elastic bandwidth adaptively to connections rather than a fixed amount of bandwidth in WDM networks. This flexibility is well suited to the future demands that have diverse requirements and time varying of data rates. EONs have been shown to be advantageous over WDM optical networks for both unicast and multicast traffic [14, 15].

In this thesis, we consider performing multicast operations at the optical layer, instead of at the network layer as in today's Internet, since optical layer multicasting of large volume traffic assumed in this thesis is more cost-effective. Multicasting at the optical layer does not require router operations and Optical-Electrical-Optical (OEO) conversion in intermediate nodes while these are required at the network layer. Thus, the associated buffer and OEO converters are saved which are expensive. Also, without the need of frequently going through OEO conversion, multicasting at

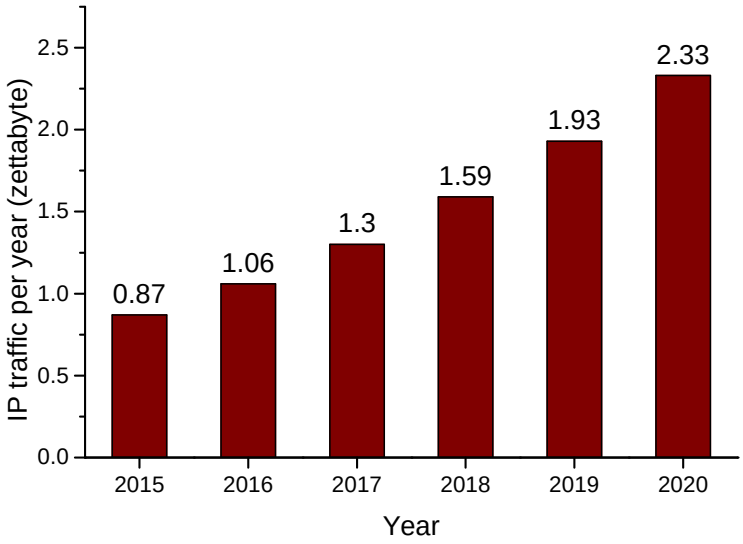

Fig. 1.1 Global IP Traffic, 2015–2020 [1].

the optical layer significantly reduces power consumption. Moreover, multicasting at the optical layer can provide better real-time and delay-sensitive services, e.g., multiplayer video gaming and live video streaming, since it eliminates the store-and-forward processing of packet-switched technology that introduces significant delay. There is extensive literature on provisioning multicast services in WDM optical networks [16–18]. However, the algorithms and schemes proposed in that context cannot be directly applied to EONs since EONs bring additional flexibility and introduce unique constraints [19]. Thus, the algorithms proposed for the WDM optical networks need to be re-evaluated for EONs.

1.2 Organization

This thesis focuses on the provision of multicast services in EONs. The outline of the thesis is as follows.

Prior to the introduction of our work we present the background in Chapter 2. We start by pointing out the known drawbacks of traditional WDM optical networks. We then move on to EONs and introduce degrees of flexibility that deal with the

drawbacks existing in the WDM networks. After that, we provide the node architectures of EONs based on which we introduce one of the key problems in EONs—RSA where traffic between two end nodes is routed via an optical channel with appropriate bandwidth—which is a fundamental problem of the work to be presented in this thesis. Finally, based on the RSA, we briefly survey the techniques that can enhance EONs.

Chapter 3 compares the performance of various schemes based on the three technologies, namely, lightpath, light-tree, and light-trial, that can be applied to the provision of multicast services in EONs. We first provide a survey of studies on the provisioning schemes of multicast services. Then, we present MILP formulations for the problems of minimizing resource usage by these multicast approaches in EONs. We make a comprehensive performance comparison of these schemes through various test cases. Numerical results demonstrate their efficiency in EONs.

In Chapter 4, we study the problem of provisioning multiple multicast demands by the light-tree technology in EONs. We provide a MILP formulation; due to its intractability, we also propose an efficient heuristic algorithm that is polynomial-time and compare it to state-of-the-art approaches. Numerical results demonstrate the effectiveness of the proposed algorithm.

Chapter 5 further considers protection for light-trees used for provisioning multicast in EONs. First, we review the state-of-the-art on this topic. Then, we propose and address the optimization problem associated with designing EONs with the minimum bandwidth requirement. For this problem, we provide a MILP formulation and propose an efficient heuristic algorithm. Numerical results demonstrate the performance of the algorithm.

Chapter 6 closes the thesis with a summary of the results and a discussion of potential directions for future work.

1.3 Contributions

The main contribution of this thesis are now outlined.

- We derive a MILP formulation for multicast provisioning using light-trail technology in EONs with distance-adaptive transmission. This MILP is applicable for cases where a multicast demand is provisioned by a single light-trail or by multiple light-trails (Section 3.5.3).

- For the provision of a single multicast, we make a comprehensive comparison among various schemes supported by the existing technologies, namely, lightpath, light-tree, and light-trail. We also evaluate, in EONs, the benefit of having distance-adaptive transmission for these schemes (Chapter 3).

- We propose a heuristic algorithm for the restricted shortest path problem that applies to the routing of both unicast and anycast traffic (Section 4.3.1).

- For the provision of multiple multicast demands, we provide a MILP based on a node-arc formulation, which, compared to other such existing formulations, has the additional flexibility to allow the provision of a multicast by multiple light-trees. Also, we propose a polynomial-time heuristic algorithm without the requirement that trees be precomputed for the provision of multicast demands, and compare it to the optimal MILP and existing approaches (Chapter 4).

- We consider the problem of protecting light-trees for multicast services in EONs with distance-adaptive transmission. To the best of our knowledge, this is the first work on the problem of provisioning light-trees with protection in EONs involving distance-adaptive transmission. For this problem, we derived a MILP formulation and proposed a heuristic algorithm. We study network cases with static traffic, where demands are known *a priori*, and dynamic traffic, where connection demands arrive sequentially (Chapter 5).

1.4 Publications

The following are publications and submissions by the author of this thesis during his period as a PhD candidate. Some of the material in these papers is not included in this thesis.

1.4.1 Journal Papers

- A. Cai, J. Guo, R. Lin, G. Shen, and M. Zukerman, "Multicast routing and distance-adaptive spectrum allocation in elastic optical networks with shared protection," *IEEE/OSA Journal of Lightwave Technology*, vol. 34, no. 17, pp. 4076–4088, Sep. 2016.

- Y. Li, A. Cai, G. Qiao, L. Shi, S. K. Bose, and G. Shen, "Multi-objective topology planning for microwave-based wireless backhaul networks," *IEEE Access*, vol. 4, pp. 5742–5754, Oct. 2016.

- A. Cai, Z. Fan, K. Xu, C. K. Chan, and M. Zukerman, "Elastic versus WDM networks with dedicated multicast protection," *IEEE/OSA Journal of Optical Communications and Networking*, vol. 9, no. 11, pp. 921–933, Nov. 2017.

- R. Lin, S. Luo, J. Zhou, S. Wang, A. Cai, W.-D. Zhong, and M. Zukerman, "Virtual network embedding with adaptive modulation in flexi-grid networks," *IEEE/OSA Journal of Lightwave Technology*, to appear.

1.4.2 Conference Papers

- A. Cai, M. Zukerman, R. Lin, and G. Shen, "Survivable multicast routing and spectrum assignment in light-tree-based elastic optical networks," in *Proc. Asia Communications and Photonics Conference*, Nov. 2015, pp. ASu4E-1.

- M. Wang, L. Hou, E. W. M. Wong, J. Guo, J. Liu, F. Li, A. Cai, H. Mehrvar, D. Wang, D. Geng, E. Bernier, and M. Zukerman, "Design implications of the add/drop ratio in transparent photonic networks," in *Proc. 17th International Conference on Transparent Optical Networks*, Jul. 2015.

Chapter 2

Background

Optical fibers have been widely adopted as a transmission medium due to their various merits, in particular, low loss and huge capacity. To exploit the huge bandwidth potential, WDM technology, which is essentially the same as Frequency-Division Multiplexing (FDM) in radio communications, has been proposed for high capacity networks.

2.1 Traditional WDM Optical network

In traditional WDM optical networks [20], the spectrum resource of an optical fiber is carved up into multiple non-interfering wavelength bands. Each of these wavelength bands can provide a wavelength channel operating at a desired rate. Current backbone networks are based on the WDM technology, where multiple wavelengths are multiplexed onto a single fiber and transmitted in parallel through the same fiber. Figure 2.1 shows an example of WDM optical networks consisting of four Wavelength Cross-Connect (WXC) nodes and four fiber links interconnecting the WXCs. The WXC routes signals from an input port to an output port based on the wavelength [21]. Each WXC connects its client node via transponders, which work as an interface between the client and the network. It converts a client signal

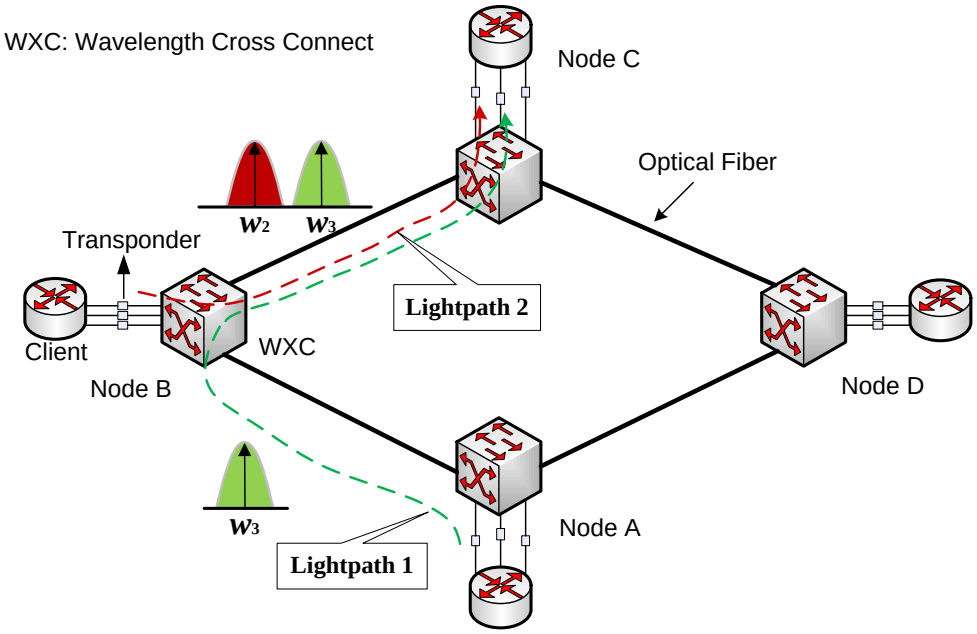

Fig. 2.1 An example WDM optical network.

into a signal that can be transmitted in the network and also converts a signal from the network into a signal that is suitable for the client. When a client node wants to send data to another node in the network, the transponder at the transmitter side first launches the designate data onto an optical signal; then the optical signal is transmitted to the destination node via a *lightpath*; and finally when the signal reaches its destination, the transponder at the receiver side converts it for the client. A lightpath is an optical channel from a source node to a destination node, and may span multiple physical links. For example, in Fig. 2.1, the communication between node A and node C is provisioned via lightpath 1 traversing links (A,B) and (B,C). Similarly, the data transmission from node B to node C is supported by lightpath 2.

Traditional WDM optical networks [20] follow the fixed frequency grid defined by the International Telecommunication Union-Telecommunication Standardization Sector (ITU-T) [22], e.g., 50 GHz as shown in Fig. 2.2. The coarse and rigid grid granularity of WDM networks leads to inflexible spectrum allocation and therefore to low spectrum utilization. This is because a wavelength is assigned to a connection

even when the requested data rate is significantly lower than the capacity of the wavelength channel leading to bandwidth waste, and also a large portion of the wavelength bandwidth is wasted to reduce inter-channel interference. An example is the allocation of wavelength w_1 as shown in Fig. 2.3. Such rigid spectrum allocations are not suitable for the future demands that have diverse data rate requirements.

Considerable efforts were made to enhance WDM networks in the past decades. Most of today's WDM systems deployed in optical backbone networks support transmissions at 40 Gb/s. Moreover, 100-Gb/s interfaces are now commercially available and are expected to be deployed in a few years. However, future optical networks are expected to support transmissions of Tb/s [12]. The traditional WDM technology is not an efficient solution for long distance transmissions at high data rates although a high-speed transmission may be supported by breaking it into multiple flows, each carried via its own wavelength. For example, as shown in Fig. 2.3, a 300-Gb/s transmission necessitates three wavelengths, namely, w_2, w_3, and w_4, each of which provides a capacity of 100 Gb/s. However, it consumes an excessively large spectral bandwidth. This is because traditional WDM transponders operate at a fixed bit rate and the spectral bandwidth of a wavelength cannot be larger than the channel spacing defined by ITU-T. Furthermore, considering the channel limitations, e.g., dispersion and nonlinearities, the channel spacing is set more than twice the spectral bandwidth of the wavelength channel so that the signal can be successfully filtered [23]. In this regard, WDM optical networks are not suitable for large-bandwidth requirements. All these are obstacles of WDM optical networks on the road to become a candidate for next generation optical transport networks.

2.2 EONs

In conventional WDM optical networks, demands are accommodated in the same manner—the channel spacing is fixed, the bit rate that the transponder operates is

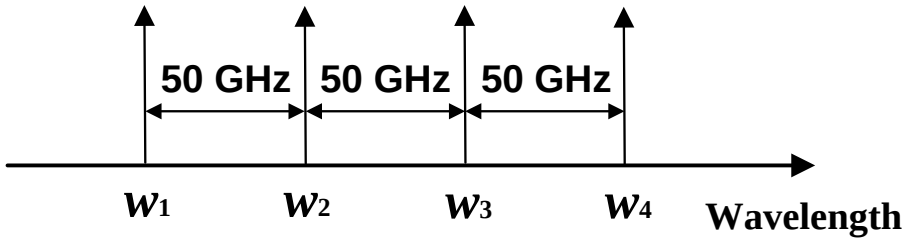

Fig. 2.2 ITU-T fixed-frequency grid.

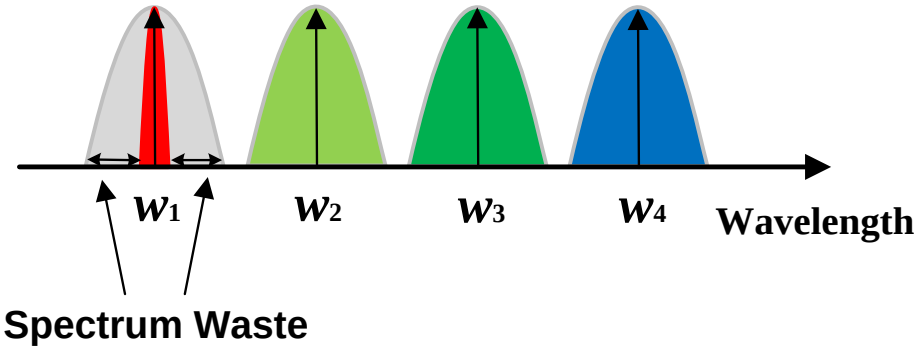

Fig. 2.3 Wavelength allocation in WDM networks.

fixed, the maximum transmission distance that the signal can reach, the so-called *transparent reach*, is fixed. This inflexibility leads to the various aforementioned drawbacks, leading to low throughput of the traditional WDM optical networks. To enhance network throughput, future optical networks are expected to go beyond the limitations of the fixed assignment and to have additional desirable features, e.g., flexible resource allocation, low energy consumption, reduced cost, and high scalability. Recent advances in transmission technologies such as Coherent Optical Orthogonal Frequency-Division Multiplexing (CO-OFDM) [24] and Nyquist WDM [25] push forward the network evolution to build a new generation of optical networks, i.e., *EONs* [2, 14], where the usage of network resources are more flexible than the network in force. Thus, EONs are more spectrum efficient than the traditional WDM networks. More than 30% spectrum saving has been demonstrated in real network topologies [15, 26]. Please note that in the literature, the terms "flexible," "flex-grid," "flexi-grid," "tunable," "gridless," and "elastic" are used interchangeably to denote the systems that do not follow the ITU-T fixed frequency grid [27].

2.2.1 Enabling Transmission Technologies

As coherent detection technologies are getting mature, higher-level MSs, e.g., 16-Quadrature Amplitude Modulation (QAM), are used to increase the spectrum efficiency but at the cost of shorter transmission distances for higher Optical Signal-to-Noise Ratio (OSNR) required. Alternatively, reducing the channel spacing also can achieve higher spectral efficiency. Among all the transmission technologies, Nyquist WDM and OFDM are two potentials that attract the most attention [28]. Nyquist WDM aims to minimize the spectrum usage of each channel by maximally reducing the spectrum used as guard bands between adjacent channels, while for the OFDM scheme, subcarriers adjacent to each other partially overlap in the frequency domain without introducing interference, and require no guard bands between them.

Nyquist WDM

In theory, the signal using the Nyquist WDM technology has a sinc pulse shape in the time domain and a rectangle spectrum in the frequency domain. For Nyquist WDM, signals are spectrally shaped so that they occupy a bandwidth equal to the symbol rate. However, setting the channel spacing equal to the symbol rate leads to significant power penalties. To obtain desired performance, forward error correction is required, resulting in a tradeoff between spectrum efficiency and inter-carrier interference [14]. In practical implementations, the channel bandwidth is allowed to increase slightly. To avoid inter-carrier interference, filters are also required at the transmitter side. Optical Nyquist WDM and digital Nyquist WDM are the two techniques that implement the spectrum shaping optically and digitally, respectively [29]. Long distance transmissions were demonstrated for both optical and digital Nyquist WDM technologies [30, 31].

For the optical Nyquist WDM, an optical filter is utilized to band-limit the signal from transmitters. Multiple wavelengths of Nyquist signals can then be multiplexed to generate a superchannel where the subchannels are closely packed. To achieve high spectral efficiency, the analog filters require to be steep enough so that it does not introduce crosstalk between adjacent subchannels. The performance of optical Nyquist WDM is limited by the development of photonic integrated circuit. The optical Nyquist WDM has been demonstrated to achieve 96×112-Gb/s with Polarization-Division Multiplexing (PDM)-Quadrature Phase-Shit Keying (QPSK) at spectrum efficiency of 3 b/s/Hz over a transmission of 10,610 km [30].

For the digital Nyquist WDM, the spectrum shaping is performed in the digital domain. To obtain a near-rectangle spectrum, Digital-to-Analog Converters (DACs) are required to have very high sampling speed and resolution. The higher the sampling speed is, the higher symbol rate can it achieve. Also, the resolution of the DAC limits the maximum number of bits per symbol that can be supported. The

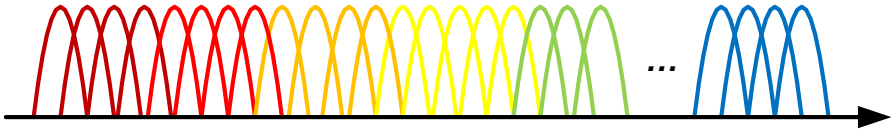

Fig. 2.4 OFDM subcarriers in an optical fiber.

main drawback of the digital Nyquist WDM is the requirements of costly devices, e.g., high speed Digital Signal Processing (DSP) and DACs, for a good spectral shape. With the help of digital Nyquist WDM, a transmission of 21.2 Tb/s over 10,290 km was achieved [31].

OFDM

OFDM technology was first introduced in wireless communications and has been extensively applied in wireless (e.g., WiFi) and wired (e.g., digital subscriber loop) environments. For the great success, it has recently been introduced to optical transmissions [32, 33]. The OFDM technology belongs to the multicarrier modulation scheme, where a high-speed data stream is sliced into multiple low-speed ones and these low-speed streams are transmitted over separate subcarriers. These OFDM subcarriers are spaced at the symbol rate and are orthogonal to each other. Although they partially overlap, in theory, no cross-talk is introduced. Figure 2.4 shows OFDM subcarriers in an optical fiber.

Optical OFDM has the enhanced scalability and flexibility in supporting applications with various requirements of data rates, e.g., sub-wavelength and super-wavelength. Since OFDM is a multicarrier modulation scheme, various bandwidth can be achieved by simply changing the number of subcarriers. Figure 2.5 shows an example OFDM-based EON, where flexible elements, e.g., BVTs and BV-OXCs, are

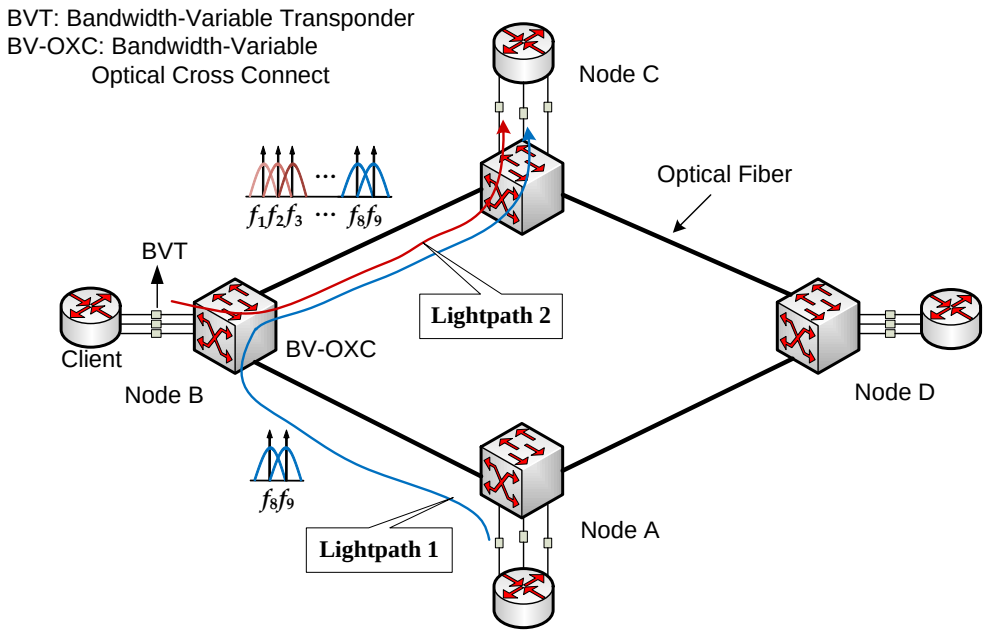

Fig. 2.5 An example OFDM-based EON.

used to provide various degrees of flexibility. In this EON, two lightpaths are assigned different numbers of FSs to efficiently support different data-rate requirements.

The major advantages of using OFDM are that it precisely tailors signals to the channel characteristics, e.g., by using high-level MSs on subcarriers with good channel conditions [33], and that OFDM subcarriers, though required to be frequency-locked, can be seamlessly multiplexed to form a superchannel. The main disadvantage is the high peak-to-average power ratio due to the symbol synthesis of multiple parallel subcarriers causing signal distortion [24]. A transmission of 3×485 Gb/s using the CO-OFDM technology was demonstrated to achieve 4-b/s/Hz spectrum efficiency over a distance of 4,800 km [34].

Nyquist WDM and OFDM have their own pros and cons, and comparisons have been made between them [35], however, no clear tendency is visible [36]. Building on these two spectrally efficient transmission technologies, several EON architectures were proposed, e.g., SLICE [2], flexible WDM [37], data-rate elastic [38], and digital subcarrier optical networks [39]. The last one is for opaque networks where optical

signals are converted to digital signals in intermediate nodes, while the former three have additional applications in all-optical networks where lightpaths do not experience OEO conversion in intermediate nodes. This thesis mainly focuses on all-optical networks, in the following, we only discuss the all-optical network architectures.

2.2.2 EON Architectures

SLICE

Based on OFDM technology, Jinno *et al.* [2] proposed an EON architecture named SLICE with the following desirable features that traditional WDM optical networks cannot offer.

Bandwidth Segmentation: Traditional WDM optical networks assign a wavelength channel to a connection even when the requested bandwidth is a small fraction of the capacity, which leads to spectrum waste. To increase efficiency, SLICE can support low data-rate connections in a spectrally efficient way. It allocates a just-enough amount of spectrum to a demand according to the requested data rate. The allocated spectrum varies by adjusting the number of subcarriers for different data rates. This flexible spectrum allocation in SLICE presents a significant benefit over WDM networks. For example, to provision a 40-Gb/s connection, the required bandwidth could be 25 GHz for the EON with a granularity of 12.5 GHz rather than 50-GHz for the WDM network with a channel spacing of 50 GHz. For a 100-Gb/s connection, SLICE may only need to allocate a spectrum of 37.5 GHz.

Bandwidth Aggregation: The flexible spectrum allocation capability also gives rise to efficient accommodation of demands with diverse bandwidth requirements. In particular, SLICE can support *superchannels*. The superchannels are flows requiring data rates beyond the capacity of a single wavelength and are generated and transported in the optical domain as a single entity. For legacy WDM optical

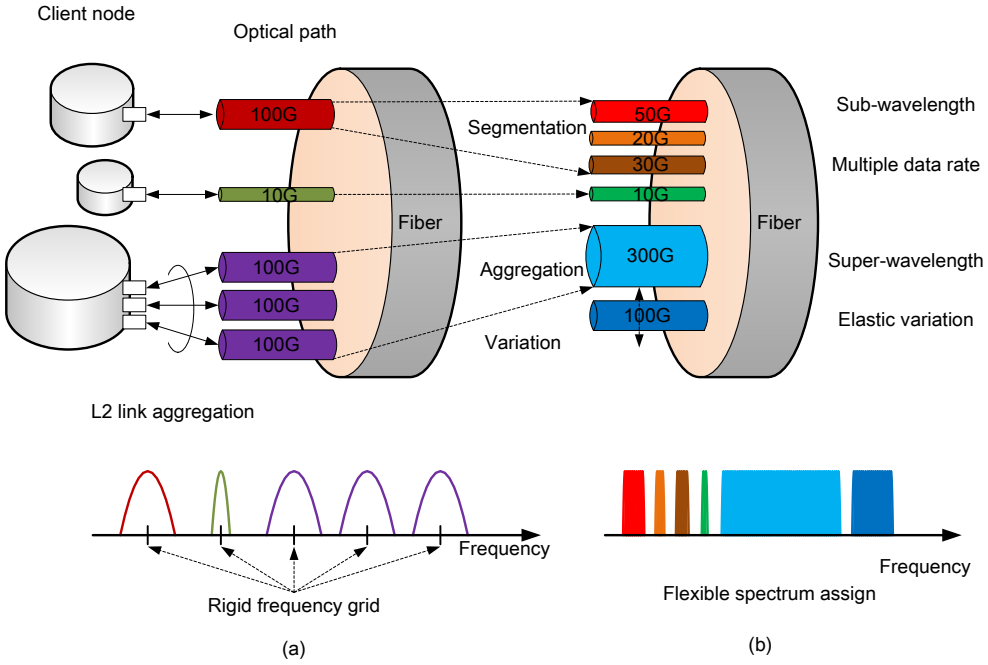

Fig. 2.6 Comparison between traditional WDM and SLICE optical networks [2].

networks, a high-capacity transmission is supported by multiple separate wavelength channels where a large guard-band exists between two neighboring channels to avoid inter-channel interference when the channels are cross connected in the intermediate nodes along their routing paths. However, in SLICE, guard-bands are not necessary since the transmission is supported via a single channel, and within the channel, subcarriers adjacent to each other are orthogonal. Compared to the WDM network, SLICE is spectrally more efficient to support high-speed transmissions. For example, Figure 2.6 shows a comparison between traditional WDM and SLICE optical networks. A 300-Gb/s channel is supported via three wavelength channels each at 100 Gb/s in the WDM network; while in SLICE, it is provisioned by a superchannel at 300 Gb/s.

Multiple Data Rates: SLICE is based on OFDM technology which allows its subcarriers to be modulated by different schemes, allowing channels of diverse rates to coexist.

Distance-Adaptive Spectrum Allocation [40]: SLICE is able to support distance-adaptive spectrum allocation which further increases the spectrum utilization. In distance-adaptive spectrum allocation, a minimum amount of spectrum is allocated to an optical channel according to its physical condition. Signals with different transmission distances may be modulated by different schemes since they may have varied channel conditions. This is an enhanced characteristic that further reduces spectrum use when compared to the fixed spectrum allocation of conventional WDM networks.

Energy Savings: SLICE is energy-efficient in that it can turn off subcarriers that are not in use to reduce power consumption since the OFDM subcarriers can be individually operated.

Network Virtualization [41]: Network virtualization can be supported by allowing the network visualizing OFDM subcarriers as virtual links.

These degrees of flexibility brought by the SLICE present significant advantages over traditional WDM optical networks with fixed spectrum allocation, and require enhanced features that are beyond the reach of node architectures in traditional WDM optical networks. Advanced node architectures, e.g., data-rate/bandwidth-variable transponders and BV-OXCs, should be deployed accordingly for the flexibility.

Flexible WDM Optical Network

Patel *et al.* [37] proposed the FWDM architecture to support dynamic traffic whose data rate changes over time by changing the line rate or adjusting the allocated spectral bandwidth. Thus, spectrum can be shared between two neighboring flexible channels in time domain thereby achieving enhanced spectrum efficiency. Similar to the SLICE, FWDM also breaks the fixed grid limitation, and supports flexible resource allocation. The difference is that FWDM supports both single-carrier modulation and OFDM-based multi-carrier modulation scheme, and represents an

enhanced evolution of the WDM optical network architecture. The transponders required by FWDM are different from those by the SLICE. Current node architectures for WDM-based optical networks cannot be applied to the FWDM optical networks, and should be replaced by flexible nodes, e.g., by BVTs and BV-OXCs.

Data-Rate Elastic Optical Network

Traditional WDM networks are usually equipped with transceivers of the same type, which operate at a fixed data rate, e.g., 10 Gb/s. With such an equipment setting, the network cannot efficiently handle heterogeneous traffic with various requirements leading to underutilized network resources. Alternatively, networks with a mix of transceiver types can achieve better performance. However, accurate forecast of traffic evolutions is required since once the transceivers are deployed, there is little space allowing for reconfiguration due to the inflexible data rates. To deal with this situation, Rival and Morea [38] proposed a data-rate-elastic optical network architecture. It employs a type of data-rate tunable transponder that can operate at various data rates with the support of versatile modulation formats. The advantage of this architecture is that it is fully compatible with the existing WDM optical networks and can provide increased flexibility. However, it is a single-carrier transmission, and operates at fixed-frequency grids, thereby suffering the low spectrum utilization due to inflexible spectrum allocation.

Fig. 2.7 shows the scope of the three EON architectures. FWDM supports both single- and multi-carrier transmission schemes, SLICE is based on the multi-carrier modulation, i.e., OFDM, while the data-rate elastic optical network uses the single-carrier modulation. The flexibility brought by the data-rate elastic optical network lies in its ability to vary the data rate of the optical channel. The other two architectures further support flexible spectrum allocation which has many merits such as the support of superchannels.

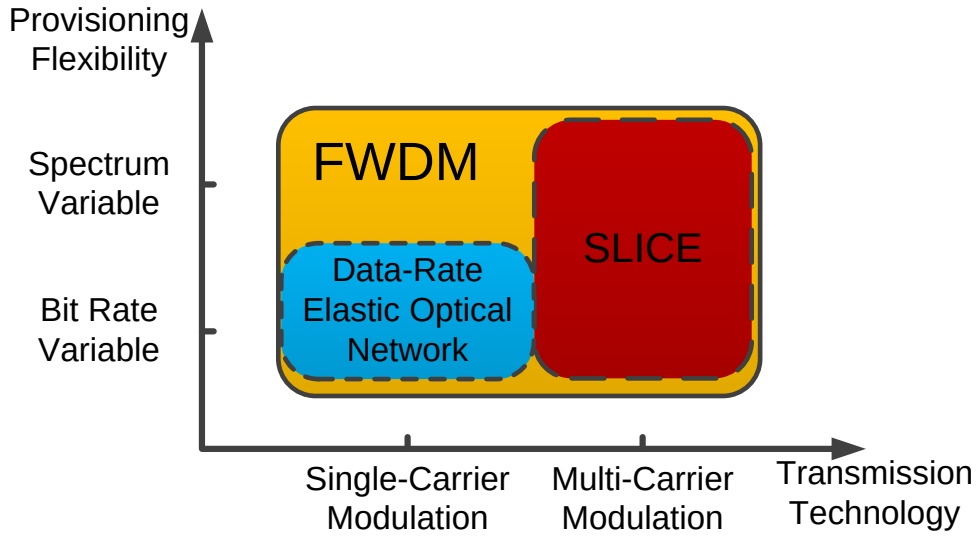

Fig. 2.7 Scope of SLICE, FWDM and data-rate elastic optical networks.

2.3 Enabling Elements of EONs

In this section, we introduce the EON architectures [2, 42] that are different from those of the nodes currently deployed in the WDM networks due to they lack of the flexibility.

2.3.1 BVT and SBVT

BVTs constitute an enhanced architecture over the transponders in traditional WDM optical networks [19]; it supports differentiated data rates by adjusting the assigned spectral bandwidth and can therefore meet the diverse bandwidth requirement of future demands. As shown in Fig. 2.8, a connection requesting a higher transmission rate is assigned with an increased number of subcarriers. This flexibility also presents a potential for enhanced spectral efficiency in provisioning the time-varying connection whose requested data rate dynamically changes over time [43, 44]. Rather than be allocated a fixed amount of spectrum corresponding to the peak requested rate, time-varying traffic may be supported by changing the number of subcarriers

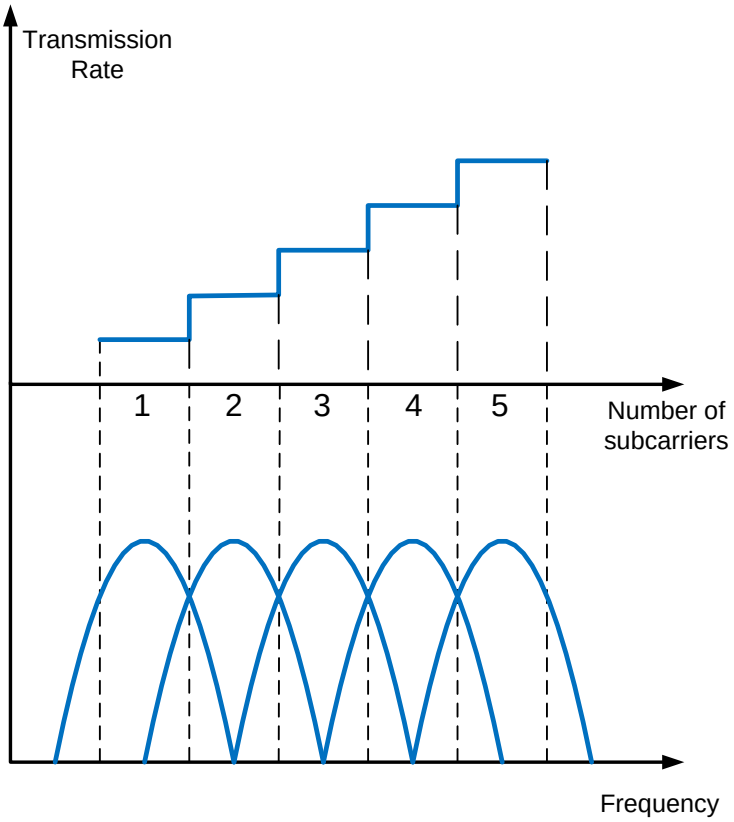

Fig. 2.8 Relationship between transmission rate and number of subcarriers [3].

used for the connection according to its requested rate. When the requested rate is high, the connection is assigned a large number of subcarriers, and when the rate drops, some of the allocated subcarriers may be released. The spectral bandwidth occupancy in the fibers changes according to the adjustment of the spectrum in the transponder allocated to the connection since the connection occupies the same amount of spectrum in the links along its transmission path. When the BVT reduces the launched subcarriers, the connection occupies less bandwidth in the traversed links. The released bandwidth in the BVT can be used by other connections. In this way, better spectral utilization can be anticipated.

EONs can also achieve increased spectral efficiency by differentiating the MSs used for the assigned spectral bandwidth for varied transmission distances, whereas in the WDM network, all wavelength bands are constrained to use the same MS which is selected for the worst case, e.g., the longest distance among the lightpaths. For instance, it is spectrally efficient to assign a higher-order MS, e.g., 64-QAM, to a shorter lightpath, while a lightpath of a longer distance should be assigned a less efficient MS, e.g., QPSK or even Binary Phase-Shit Keying (BPSK), due to the physical layer impairments. In this regard, the BVT enables distance-adaptive spectrum allocation by changing the MS and the amount of bandwidth.

The BVT has a high capacity, usually of the order of several hundreds of Gb/s to Tb/s, and is much more expensive than fixed-rate transponders. Therefore, it is a waste when a BVT is dedicated to a connection that requests a rate lower than the capacity of the BVT. Although the capacity utilization can be improved by *traffic grooming* which aggregates multiple flows to form a high-speed flow [45, 46], it involves operations in higher layers and eliminates some of the gains of the EON [47].

To overcome capacity waste of the BVT, an SBVT architecture has been investigated in [48, 49]. This type of architecture can be viewed as multiple virtual BVTs operating at relatively low rates. It presents increased flexibility that allows these virtual BVTs assigned to one or multiple flows that may aim for different destina-

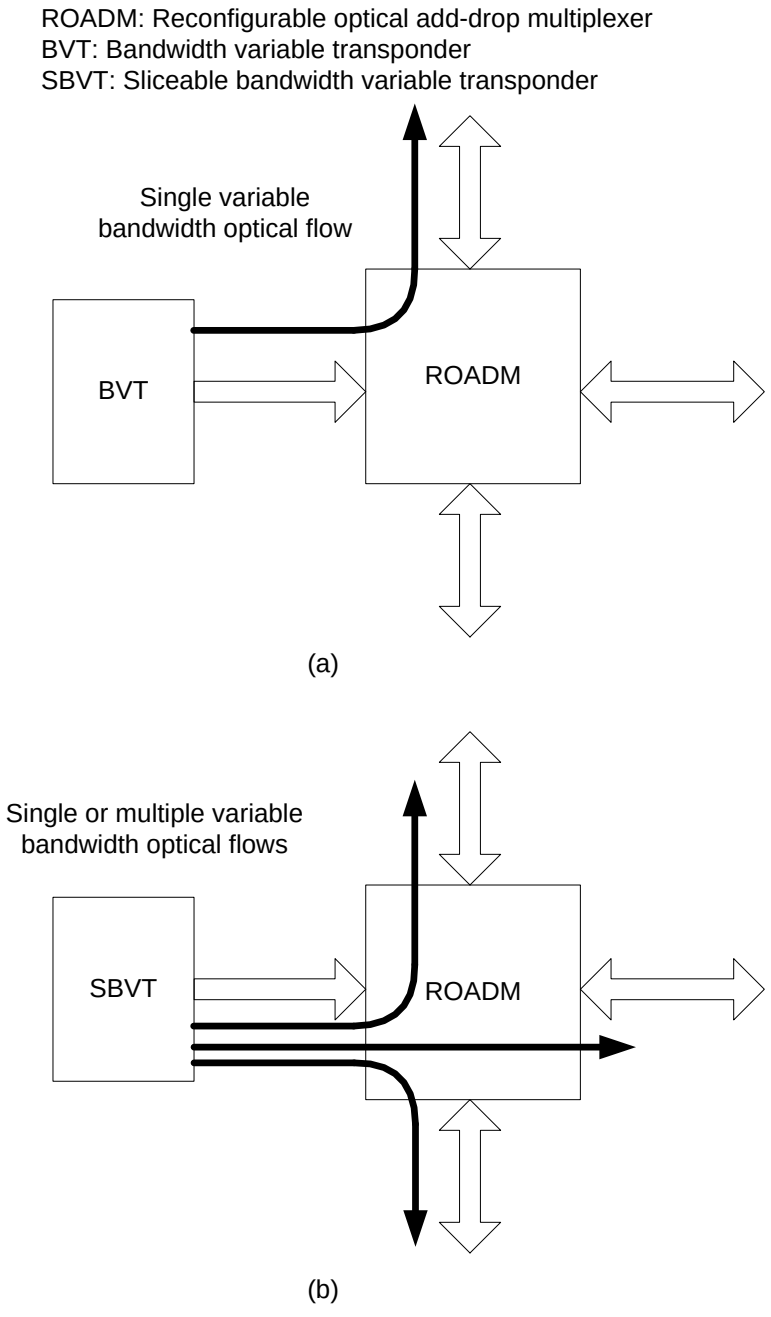

Fig. 2.9 Functionalities of (a) BVT; (b) SBVT [4].

tions. This adds another dimension of flexibility and gives rise to the technology of *optical grooming* where multiple flows are aggregated in the optical domain to form an optical tunnel [50, 51]. Optical grooming improves cost-effectiveness by allowing multiple flows sharing the capacity of the same SBVT. Figure 2.9 gives the functionalities of BVT and SBVT. In the figure, BVT only generates a single flow to a destination while SBVT generates three optical flows destined for different nodes. The flows are added to the network via a Reconfigurable Optical Add/Drop Multiplexer (ROADM). ROADMs are used to add a signal to or drop a signal from the network in an economic way while signals to other destinations pass through it requiring no OEO conversion. In summary, the sliceability of the SBVT provides a desirable feature to improve utilization of the costly transponder.

2.3.2 BV-OXC

Different from the lightpath with a fixed spectral bandwidth in WDM optical networks, the spectral bandwidth of the lightpaths vary in the EON. To support lightpaths with variable spectral bandwidth, BV-OXCs should be able to cross connect the input of optical signals with differentiated amounts of spectral bandwidth to outputs. This requires the BV-OXC to be capable of flexibly configuring the spectrum switching window suitable for the optical signal. An example implementation of the BV-OXC [2] is shown in Fig. 2.10. The $N \times N$ BV-OXC presented in the figure is based on a broadcast-and-select architecture. An input optical signal goes through the light splitter which splits the signal into $N+1$ identical copies. Each of the N output ports is fed with one copy, and the other one copy is for possible drop to the local station. Also, local signals that need to be transmitted to other nodes of the network are added and broadcast to the output ports also by a light splitter. To support the add-and-drop function for signals, BV-WSSs are utilized. BV-WSSs, also called Spectrum Selective Switch (SSS) in the literature [52], provide grooming and routing

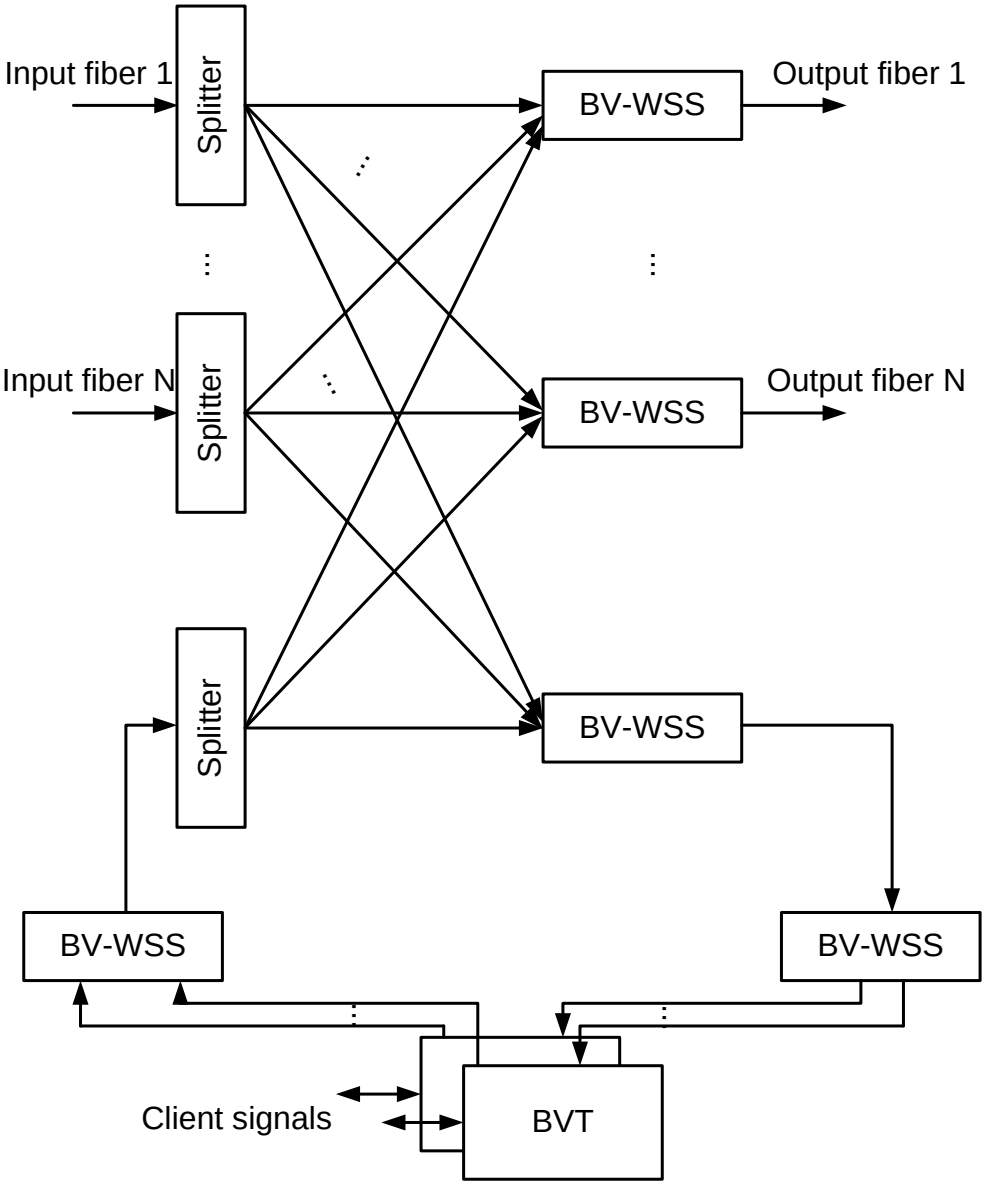

BV-WSS: Bandwidth-variable wavelength selective switch
BVT: Bandwidth-variable transponder

Fig. 2.10 BV-WXC [2].

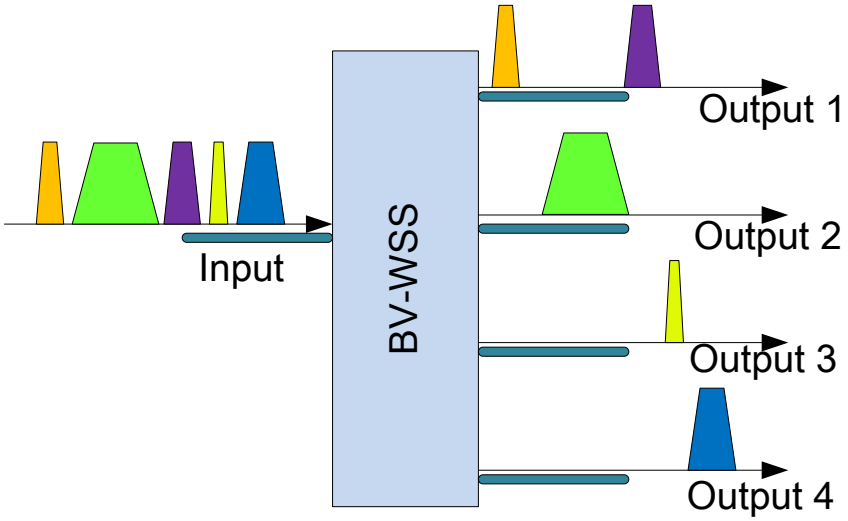

Fig. 2.11 BV-WSS Functionality.

functions for transit signals. The BV-WSS in the EON has the same functions of the Wavelength Selective Switch (WSS) for the fixed spectral bandwidth in traditional WDM networks however supports a flexible configuration of the spectral bandwidth. Generally speaking, WSSs make use of integrated spatial optics to provide functions, e.g., wavelength multiplexing/demultiplexing and switching. An input light is demultiplexed into its constituent spectral components by a dispersive element. Inversely, the multiplexing function is implemented by focusing the spatially separated spectral bandwidths on a one-dimensional mirror array and redirecting them to the designated output fiber. Diverse spectral bandwidth functionality of BV-WSSs can easily be incorporated by adopting the liquid crystal on silicon or micro-electro-mechanical systems technologies [53, 54]. As shown in Fig. 2.11, the input signals with diverse spectral bandwidths are routed to the outputs.

2.3.3 Node Architectures

There are several node architectures proposed for EONs.

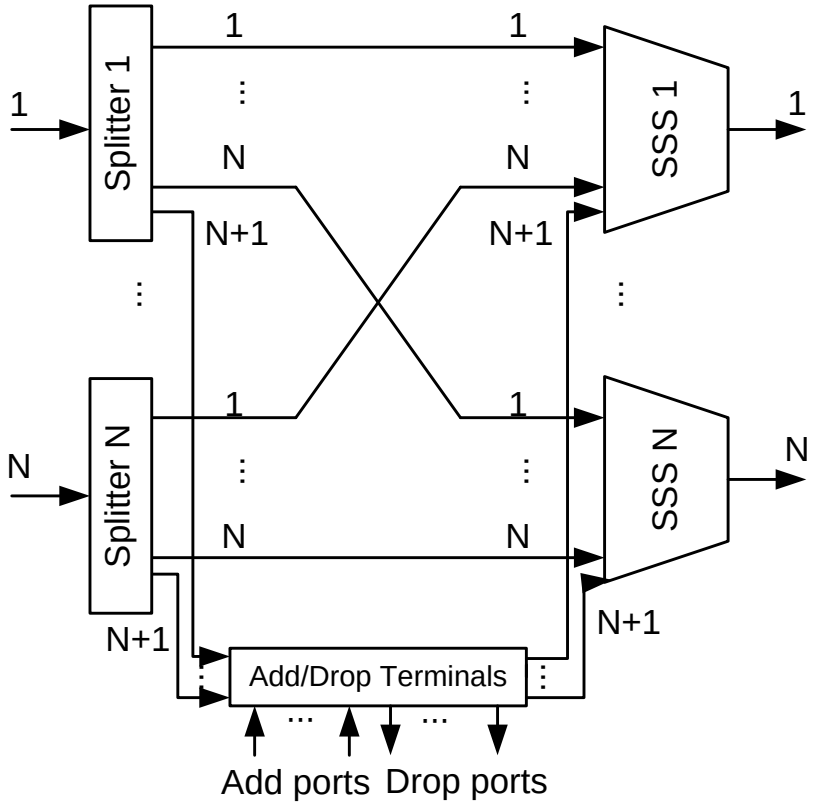

Fig. 2.12 Broadcast-and-select architecture [4].

1) Broadcast-and-Select

The broadcast-and-select has been investigated in [2, 55] for EONs where SSSs have been incorporated. Figure 2.12 shows an $N \times N$ architecture of the broadcast-and-select. Input signals going through the light splitters generate $N+1$ replications. The N replications are then sent to the SSSs of the N outputs for demultiplexing/multiplexing and routing purposes, respectively, while the remaining replication is sent to the add/drop terminals and is dropped if it contains signals that are destined for the present node. Also, a local signal can be added and sent to SSSs for grooming and routing operations. The add/drop terminals may be equipped with the features of colorlessness, directionlessness, and contentionlessness for better performance [56].

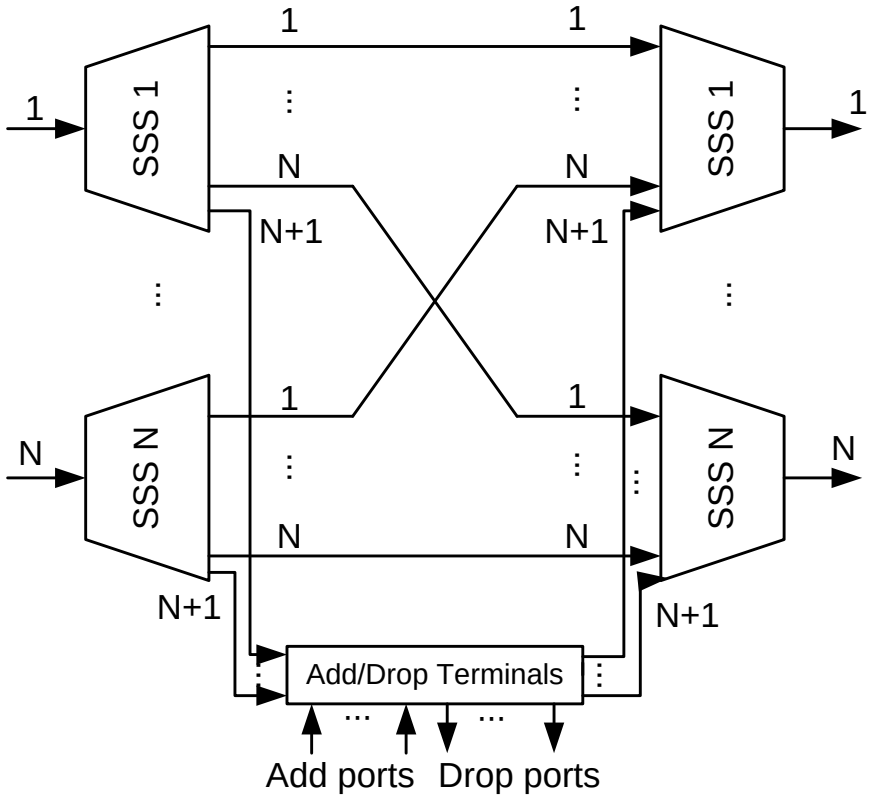

Fig. 2.13 Spectrum routing architecture [4].

This type of node architecture inherently provides optical multicasting. Indeed an incoming signal from any input of the node can produce identical copies via the light splitter, each of the SSSs at all outputs and the add/drop network being fed one copy. These copies can be handled individually, and thus can be switched to one or more outputs and/or the drop port. Because of the light splitting for the various ports, the copies only have a fraction of the power of the original signal, and with the increase of the node degree, the power of a copy decreases. To achieve long distance transmission, amplifiers may be required to power up the signals.

2) Spectrum Routing

To deal with the drawbacks of the broadcast-and-select architecture, spectrum routing is introduced where SSSs are utilized to replace the splitters at the inputs as shown in Fig. 2.13. Instead of splitting a signal, the SSS performs filtering and switching functions. The SSS filters the light from an input fiber into separate spectral components and routes them to their designated ports. Without splitting the signal into multiple identical copies, the loss of a signal going through the node does not depend on the node degree. However, this type of architecture is more costly than the broadcast-and-select architecture since it requires a larger number of expensive SSSs. Moreover, no dynamic functionalities are supported such as spectrum defragmentation [57].

3) Switch and Select with Dynamic Functionality

In order to provide dynamic functions such as spectrum defragmentation and regeneration which the previous two architectures, namely, broadcast-and-select and spectrum routing, cannot offer, the architecture of switch and select with dynamic functionality has been introduced. In this architecture, the signal at an input port is first sent to a light splitter to generate multiple copies. These copies together with the possible local signals then go through an optical switch, and are directed either to the SSSs or functionality modules that provide dynamic functions or to the local drop port. Signals that are accepted by the modules will then feed to the SSS for filtering and multiplexing to its corresponding output. Figure 2.14 presents an $N \times N$ architecture of switch and select with dynamic functionality. The signal from an input port is split into $N+P$, $(P \geq 1)$, copies, where N copies directly feed to the SSSs of the N output fibers, one to the local drop, and the other $P-1$ copies are fed to the modules for possible requirements of dynamic functions. Choices of functionality include regeneration, time multiplexing and spectrum defragmentation,

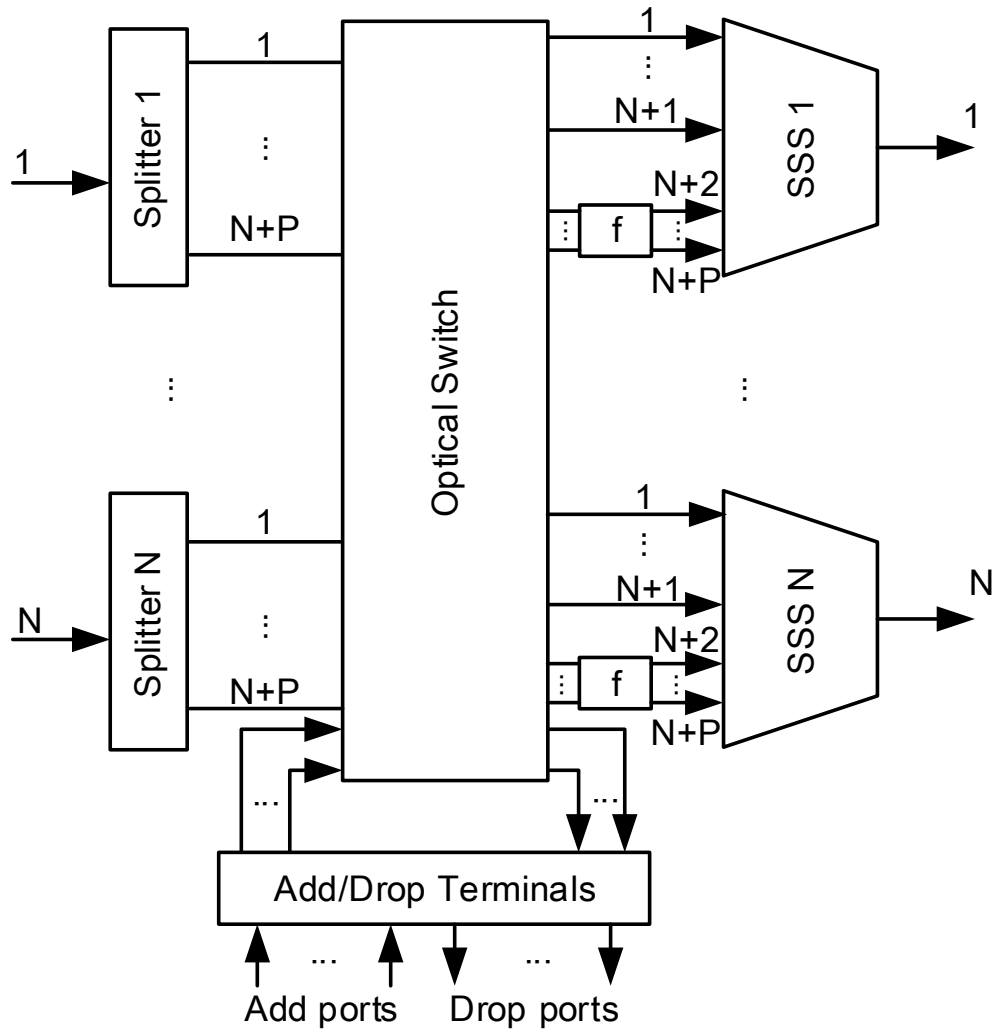

Fig. 2.14 The architecture of switch and select with dynamic functionality [4].

etc. This type of architecture is costly since an optical switch with a large number of ports, i.e., $N \times (N+P)$ inputs/outputs, is required. The input/output port count can be reduced to $N \times P$ when each SSS is directly fed by a signal copy from each of the N splitters and a locally added signal without going through a switch.

2.4 RSA in EONs

Previously, we have introduced the EON and node architectures. In this section, we introduce one of the key functionalities in EONs, RSA that are based on the architectures. The RSA problem is similar to the Routing and Wavelength Assignment (RWA) in WDM-based optical networks [58], where the requested connection is established by finding an appropriate path from the source to the destination and assigning to it a proper wavelength in the links along the path. Due to the elastic characteristics provided by the EON, the additional degrees of flexibility make RSA more complicated than the RWA in WDM networks. For example, a flexible amount of spectral bandwidth in EONs is allocated to a connection rather than a fixed wavelength in WDM networks.

2.4.1 RSA Problems

The research on the RSA problem can be divided into two categories, namely, static and dynamic routing and spectrum assignments. For the static case, assumptions are as follows. A network topology is given and a set of long-live demands is also given *a priori* together with their source and destination information and the requirements of specific data rates or spectrum resources. The objective of the static problem is typically to minimize the maximum spectrum resources in the network links such that all the demands are accommodated. For the dynamic RSA case, a capacitated network with limited resources, e.g., spectrum, is given and demands

arrive sequentially and randomly. The demands may be either *admitted* or *blocked* in the network. A demand is said to be admitted when the residual network resources at the moment are sufficient and specific resources are occupied for the establishment of a connection; otherwise, it is blocked and no network resources are allocated. A connection then holds for a certain period after its establishment and departs after the completion of its service. If a connection departs, the occupied network resources are released accordingly. The establishments and departures of connections dynamically change the residual resources in the network, thereby affecting the admission and blocking of demands that arrive afterwards. The objective of this dynamic problem is typically to minimize the blocking probability, which is defined as the ratio of the total number of blocked demands to that of total arrived demands.

Like the RWA problem in WDM optical networks, the RSA problem in EONs can also be divided into two subproblems, namely, routing and spectrum allocation. In the following, we will introduce the two subproblems.

2.4.2 Routing

To set up a communication connection between two nodes in a network, a routing path from a source to a destination is essential to transmit the data. There are several routing algorithms that search for proper routes for connections. We introduce three major algorithms as follows.

1) Fixed Routing

Fixed routing is the simplest and most straightforward algorithm where a fixed path is provided for a given Source-Destination (SD) pair. In fixed routing, the fixed paths for all SD pairs are calculated offline. The most commonly used algorithms are shortest path algorithms, e.g., Dijkstra's algorithm, where for each SD pair, the path calculated is shortest among all possible paths. When a lightpath demand arrives,

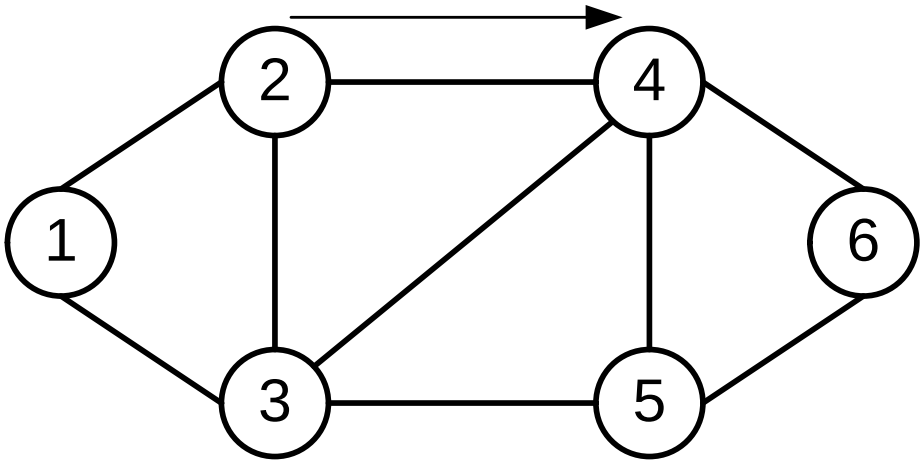

Fig. 2.15 Fixed routing from node 2 to node 4.

the network attempts to accommodate it by allocating the required spectrum in each link of the pre-calculated path. The fixed routing algorithm is simple and requires no timely calculation of paths in the control plane. However, it brings potential disadvantages that it may lead to a high requirement of spectrum resources for the static RSA, or a high blocking probability in the dynamic case. Moreover, it cannot handle network failures, e.g., a link failure. To provide survivability, the network should either be equipped with alternate paths or have the capability of routing dynamically. Fig. 2.15 shows fixed routing using the shortest path algorithm. The routing path from node 2 to node 4 is $2 \rightarrow 4$. If link $(2,4)$ gets cut, connections whose paths traverse this link will be lost.

2) Fixed Alternate Routing

Instead of one path for each SD pair in the fixed routing, fixed alternative routing provides multiple paths. In fixed alternative routing, each network node maintains for each of the other nodes a routing table where the multiple paths are usually organized in increasing order of cost. As in the fixed routing, these paths are also

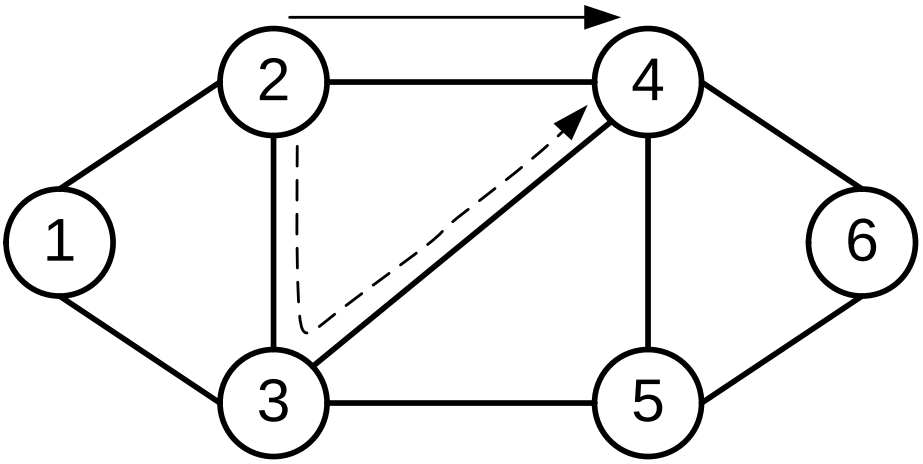

Fig. 2.16 Fixed alternative routing from node 2 to node 4.

precalculated. As an example shown in Fig. 2.16, the routing table from node 2 to node 4 contains two paths, namely, $2 \rightarrow 4$ and $2 \rightarrow 3 \rightarrow 4$.

For the dynamic problem, when a demand arrives, the source attempts to establish a connection by trying the sequenced paths in the routing table until a path is selected if the spectrum requirements are met. Then, a spectrum allocation method is adopted to accommodate the demand. If no path meets the resource requirements, the demand is blocked. For the static problem, a proper path may be selected to establish a connection so that the requirements of spectrum resources in the network links are balanced.

The disadvantages of fixed alternative routing are that it has higher complexity than fixed routing, and may not use the optimal paths. However, it provides significantly lower blocking probabilities than fixed routing. Also, having multiple paths for each SD pair provides, to some extent, fault tolerance of link failures to the connections. For example, in Fig. 2.16, when link $(2,4)$ fails, path $2 \rightarrow 3 \rightarrow 4$ could be used to set up a connection from node 2 to node 4.

3) Adaptive Routing

In adaptive routing, the computation of the path from a source node to a destination node is performed in real time based on the network state. The network state is determined by the connections that currently exist in the network, and dynamically changes after a new connection is established or an existing connection departs. In fixed routing and fixed alternative routing, in order to establish the connection for a given SD pair, a path is selected from the routing table, which has a limited number of paths and is fixed once given, while in adaptive routing, the paths are computed dynamically and may vary if the network state changes. Thus adaptive routing has the potential to find any possible path for a given SD pair. The commonly used adaptive routing in optical networks with wavelength conversion capability is adaptive shortest path routing [20], where a cost is assigned to each network link. The cost is set with regard to the availability of required spectrum resources. The cost of a link is set to one if the required spectrum resources are available for use; otherwise is set to ∞. Figure 2.17 shows an example network with link costs. When a demand arrives, the shortest path algorithm attempts to find the shortest path for the SD pair. The demand is blocked if a path that satisfies the spectrum requirements is not found by the algorithm. If there are more than one path with the same cost, one is picked at random among them.

Adaptive routing achieves a lower blocking probability compared to fixed routing and fixed alternative routing due to its potential of finding any possible path. As shown in Fig. 2.17, if links $(2,4)$ and $(3,4)$ do not meet the spectrum requirements, a path, i.e., $2 \rightarrow 3 \rightarrow 5 \rightarrow 4$, is found and can be used to establish a connection from node 2 to node 4 by adaptive routing, while no connection established would be under either of the previous two routing algorithms. However, in adaptive routing, the path computation is performed in a dynamic manner based on the real-time

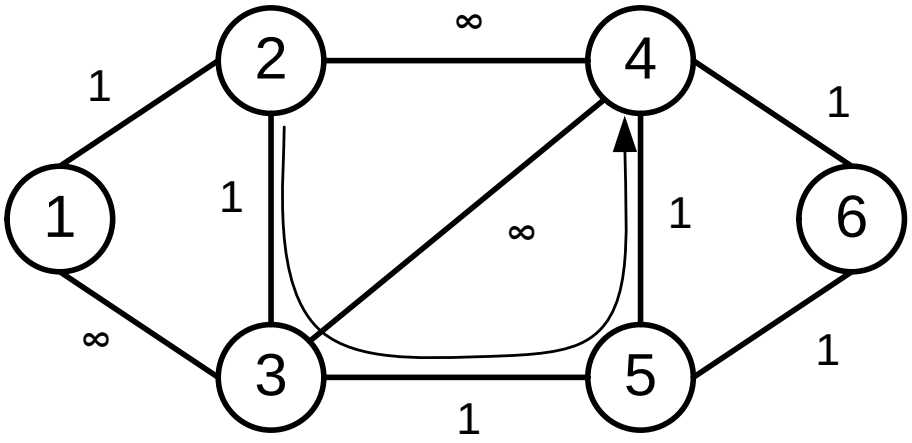

Fig. 2.17 Adaptive routing from node 2 to node 4.

network state, and this requires extensive support, e.g., rapid update of the link state information, from the control and management protocols.

2.4.3 Spectrum Allocation

To establish a connection between a given SD pair, spectrum resources should be allocated to carry the traffic. For the spectrum allocation, there are three major constraints that should be satisfied in EONs, namely, spectrum continuity, spectrum contiguity and spectrum non-overlapping. The spectrum continuity and spectrum non-overlapping constraints are similar to the wavelength continuity and non-overlapping constraints in WDM optical networks, while the spectrum contiguity constraint is new and unique to EONs. In fixed-grid WDM optical networks, a single wavelength is allocated to a connection, while EONs may allocate diverse amounts of spectrum to connections requiring various data rates. The spectrum contiguity constraint forces the FSs in a link allocated to a connection to be contiguous. The spectrum contiguity constraint is also called spectrum consecutiveness constraint in the literature. As shown in Fig. 2.5, lightpath 2 from node B to node C traverses link (B,C), three FSs,

i.e., f_1, f_2 and f_3, that are consecutive in link (B,C) are allocated to the lightpath. If the network nodes are incapable of spectrum conversion, the spectrum continuity constraint should be guaranteed for those lightpaths that traverse multiple links. The spectrum continuity ensures that a connection uses the same spectrum resources in all the links of its path. The spectrum continuity constraint can be relaxed when spectrum converters are available. For example, in Fig. 2.5, lightpath 1 traverses links (A,B) and (B,C), and uses the same two FSs, i.e., f_8 and f_9, in both links. However, if node B supports full spectrum conversion, lightpath 1 can use any two free contiguous FSs, e.g., f_5 and f_6, in link (B,C) that are different from the FSs allocated in link (A,B). The spectrum non-overlapping constraint guarantees that any spectral bandwidth in a link will not be allocated to two distinct connections. This constraint should be present when the paths of two connections share one or more common links. In Fig. 2.5, the FSs, i.e., f_8 and f_9 in link (B,C), are dedicated to lightpath 1, no other connections can use the FSs in the link. This is the same for f_1, f_2 and f_3 in link (B,C) to lightpath 2. In other words, both lightpaths traverse link (B,C), but they use different FSs in this common link.

There are several methods to assign spectrum resources to connections. We introduce three common methods.

Random Fit: In random fit, to allocate spectrum for the establishment of a connection, the entire spectrum space is reached for all the spectral bands of the required amount that meet the spectrum requirements, e.g., the above three constraints. After the spectrum bands are found, randomly select one of them to establish the connection. For example, assume that a demand requests two FSs, and the path used to set up the connection traverses links (A,B) and (B,C). Given also that the network does not support spectrum conversion, where the spectrum continuity constraint should be guaranteed. Figure 2.18a shows the FS utilization of the two links. In Fig. 2.18b, all the possible allocations of spectrum bands that meet the requirements are indicated by rounded rectangles. One of these spectral bands is randomly selected, e.g., a

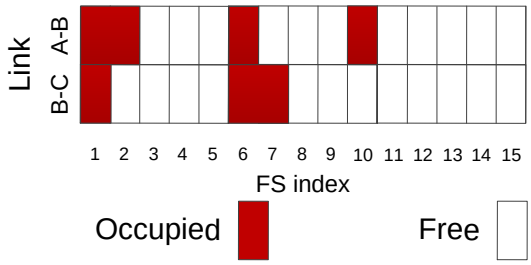

(a)

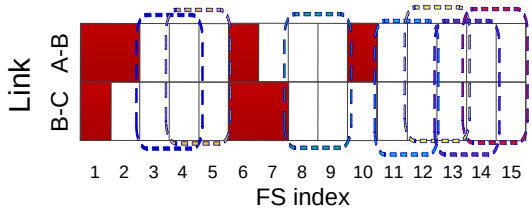

(b)

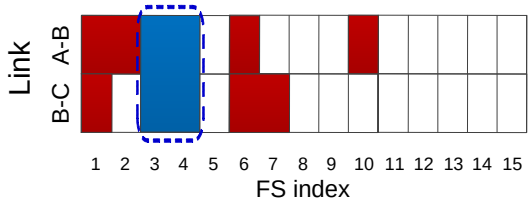

(c)

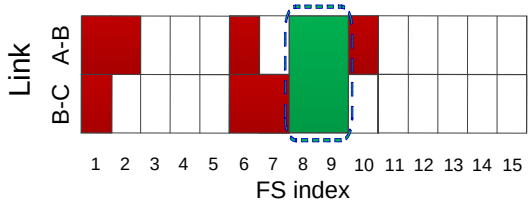

(d)

Fig. 2.18 Example accommodations of a connection that requests two FSs and traverses links (A,B) and (B,C) using the three scheme: (a) FS utilization in links (A,B) and (B,C); (b) all possible allocations by random fit; (c) first fit; (d) exact fit.

rounded rectangle covering FSs 13 and 14, for accommodating the connection in random fit scheme.

First-Fit: In first-fit scheme, the FSs are indexed by consecutive numbers, and the FSs with lowest indices that meet the spectrum requirements of a given demand are selected for the allocation. This scheme searches for the required spectrum resources indexed from low to high. Once the scheme finds spectrum that meets the requirements, it stops searching and allocates the spectrum to the connection. The main idea is to use the spectrum in one end (or head) of the entire spectrum leaving a large amount of unused contiguous spectrum towards the other end (or tail). The unused and contiguous spectrum can lead to a higher probability of successful accommodations of future connection demands because the large and contiguous spectrum is more probable in satisfying the three constraints. Moreover, as this scheme does not search all the possible solutions of the entire spectrum space, its computation complexity is low. For these reasons the first-fit scheme is preferred in practice. As shown in Fig. 2.18c, to accommodate the same demand as in random fit, the first fit scheme searches the spectrum space until the first spectral band and stops after the spectral band of FSs 3 and 4 is found in the two traversed links. The two FSs in the links are allocated to set up the connection.

Exact Fit [59]: To accommodate a demand, exact fit searches for the free spectrum block whose bandwidth is exactly the required size. This spectral block is then allocated to the connection. Here, the free spectrum block is defined as a band of contiguous spectra, where the entire spectra are free for usage and the spectra adjacent to both ends of the band are occupied. If a free spectral block matching the exactly-required size is not available, the first largest free spectrum block is allocated to the connection [59]. Exact fit is a unique spectrum allocation policy in EONs as WDM channels occupy a fixed spectral bandwidth. In Fig. 2.18d, the spectrum block of FSs 8 and 9 is allocated to the same connection that requires two FSs and traverses the two links.

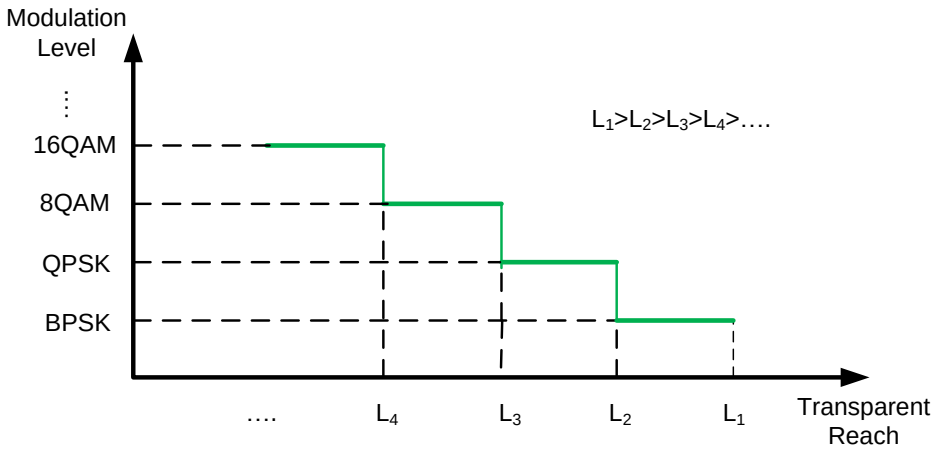

Fig. 2.19 Relationship between modulation scheme and transparent reach [5].

Distance-Adaptive Spectrum Allocation

In traditional WDM optical networks, all the connections are allocated with the same amount of spectral bandwidth without considering the physical layer impairments such as dispersion and nonlinear effects, which leads to low spectrum utilization [60]. To overcome this drawback, distance-adaptive spectrum allocation has been introduced in EONs. In distance-adaptive spectrum allocation, connection demands are accommodated with minimum spectral bandwidth and various MSs are adaptively applied to the signals such that the requirements of OSNRs are met [14, 40]. In general, a signal can be modulated by a higher level scheme, when it has a shorter distance to travel, requiring a narrower spectral bandwidth since a higher-level MS carries more bits per symbol. For example, two connections require the same bit rate, i.e., 100 Gb/s. One connection has a distance of 4,000 km, the signal is modulated by BPSK and requires 100 GHz spectrum. The other connection over a distance of 2,000 km may be modulated by a higher level scheme, QPSK, and thus requires only 50 GHz since QPSK carries twice the number of bits per symbol than BPSK. This distance-adaptive spectrum allocation provides a way to enhance spectrum efficiency by using higher level modulation schemes to shorter distance connections

for allocating reduced spectrum. Figure 2.19 shows the relationship between modulation schemes that apply to an optical signal and transparent reaches (or maximum distance that the optical signal can reach) under certain requirements, e.g., OSNR. An optical signal modulated by a higher level scheme has a shorter transparent reach. Signals modulated by QPSK has a transparent reach of L_2, while those modulated by a lower level modulation scheme, BPSK, can be transmitted maximally to a distance of L_1, where $L_2 < L_1$.

Brief Survey on RSA

The flexible features of EONs have attracted extensive attention on the topic of RSA problems. We classify the studies into static and dynamic RSA problems.

For the static RSA, Wang *et al.* [61–63] developed an Integer Linear Programming (ILP) model based on the node-arc formulation [64] and two heuristic algorithms were proposed to minimize the number of required FSs. Christodoulopoulos *et al.* [3, 5] considered k-shortest paths between each pair of nodes and developed an arc-path ILP model [64] to minimize the required number of FSs. They first derived an ILP formulation using a one-step approach where the routing and the spectrum allocation are jointly considered. To reduce the problem size of the joint ILP model, they divided the problem into two sequential sub-problems, namely the routing and the spectrum allocation. Heuristic algorithms were also proposed. Velasco *et al.* [65] provided two ILP formulations to solve the capacitated RSA problem. One is arc-path, and the other is node-arc; to shorten model-solving times, two relaxed ILP models were also evaluated. Cai *et al.* [66] also developed a node-arc ILP formulation with fewer variables and constraints, and proposed a one-step heuristic algorithm where the routing and the spectrum allocation are considered jointly. Numerical results show that the running time for solving the ILP is significantly shorter than the previous ones and the proposed algorithm requires reduced spectral

bandwidth. For the same RSA problem, Klinkowski *et al.* [67] provided an arc-path ILP formulation using binary variables, and proposed a heuristic algorithm.

For the dynamic RSA case, Wan *et al.* [68] proposed two one-step algorithms to achieve efficient spectrum resource utilization and low lightpath blocking. The work in [69] considered multiple constraints, namely, the spectrum continuity, transmission distance limitation, and the relationship between bitrate and signal bandwidth. Liu *et al.* [70] proposed a grid-based spectrum-scan routing scheme, which is similar to the traditional waveplane approach [71] for WDM networks. It is shown to achieve better blocking performance compared to the existing RSA methods. An upgraded version, discrete spectrum-scan routing algorithm, was also proposed in [72], and is capable of supporting a gridless optical network.

2.5 Survivability

Occurrence of failures in optical networks poses great challenges to network operators. As EONs achieve a high network throughput where each fiber can carry 10–100 Tb/s, any failure in the network, e.g., fiber cut or node failure, can disconnect connections leading to millions of users being isolated. This significant impact on the network could cause huge revenue loss. For instance, network failures that occurred in 2004 resulted in $500 million loss of the Gartner research group [73]. To protect the network, one method is to use strong cables with high quality ducts in the physical layer. However, this does not guarantee 0% failure. Even with the most advanced physical layer protection, the cable can still become damaged in some sense. Also, laying better cables introduces significant consumption in time and labor.

To enable networks to continue operation under failures, survivability has been incorporated in optical networks [64, 74]. As we quote from [75], network survivability is defined as "*the set of capabilities that allows a network to restore affected*

traffic in the event of a failure." A network is survivable if the network is able to continue providing service in the presence of failure [76]. Compared to protection in the physical layer and other layers, survivability in the optical layer seems more appealing and beneficial in many aspects, e.g., faster recovery speed, effective use of spare capacity, and simpler operations than that in higher layers [74].

Like in WDM optical networks, there are generally two types of the survivability mechanisms in EONs, namely, protection [77] and restoration [78]. When a failure occurs, the protection scheme switches optical signals carried via primary paths to backup paths. The backup paths are preplanned, and the spectrum resources along the backup paths are also reserved. The resources reserved along the backup paths are used to hand over the connections from the affected primary paths. For the restoration, backup paths could be preplanned but the spectrum resources are usually not reserved for connections prior to failure occurrence. The computation of spectrum resources for recovery is invoked after failures occur, and is adaptive to the dynamically changing network state. The protection scheme usually provides a faster recovery than the restoration scheme since all the required resources are preplanned, while the restoration can achieve a higher spectrum efficiency since it uses residual resources in the network for recovery [76]. In this thesis, we focus on the investigation of networks with protection schemes, since restoration schemes can be derived accordingly but in the dynamical manner.

In optical networks, a connection between two nodes usually traverses multiple nodes and links, and any of the elements along its path may fail. In general, the failures can be divided into two categories, node and link failures [76]. When a node fails, the entire node is down and the links connecting to it also fail. For a link failure, only the link fails while its two end nodes maintain operation. To survive from the failure of a given node in the primary path, the connection requires that the backup path does not traverse the node. Similarly, to survive from the failure of a given link

in the primary path, the connection requires that a backup path does not traverse the link.

There are several protection schemes to enable the connections to continue operating after a failure occurs. As single link failures are dominant in failure scenarios, in this thesis, we focus on the protection for any link failure.

2.5.1 Path, Link, and Subpath Protection

Considering different rerouting schemes, the protection scheme can be divided into *path-based protection*, *link-based protection* and *subpath-based protection*. In path-based protection, a connection is secured from failures on the basis of the path [8]. To survive from any link failure, a backup path that shares no common link with the primary path is utilized. The primary and backup paths are called *link-disjoint* from each other. In link-based protection, signals are rerouted around the failed link. Link-based protection enables a faster recovery than its path-based counterpart as it handles failures at the two end nodes of the failed link, but at the cost of higher spectrum usage [79]. For link-based protection, there are several schemes, e.g., ring cover [79], and p-cycle [64]. In ring cover technique, a ring rather than a path is used to protect the links on the ring. When a link on the ring fails, ring cover provides fast recovery by rerouting the traffic via a path obtained by excluding the failed link from the ring. Extending ring cover that aims for the failure of a link on the ring, p-cycle also protects straddling links which are not on the ring but their two end nodes are. The p-cycle provides a comparable recovery speed to ring cover as the resources are preconfigured [80]. Trading off between recovery time and resource utilization, subpath-based protection, proposed in [81], lies between the link-based and path-based protection schemes. It partitions a primary path into multiple subpaths and protects each of the subpaths separately.

2.5.2 Dedicated and Shared Protection

Regarding the resources utilized as backup, protection can be dedicated or shared. For the *dedicated protection*, backup resources reserved are dedicated to a connection in case of a failure and cannot be utilized for other connections. When a failure occurs, signals are rerouted using the reserved backup resources. Based on dedicated protection, $1+1$ protection transmits two copies of the signal via two disjoint paths simultaneously, respectively. This capability is enabled by the dedicated backup resources which no other connection can use. Backup resources can also be shared to protect multiple connections as long as the backup resources are not invoked to restore multiple connections simultaneously. Shared protection achieves better spectrum efficiency than dedicated protection. However it requires a longer recovery time than the dedicated protection since backup resources are shared and need to be configured along preplanned paths after a failure occurs while the resources are preconfigured beforehand in dedicated protection.

Figure 2.20 shows the comparison between DPP and SBPP. Both are path-based protection schemes, but with different resource reservation. DPP uses dedicated protection while SBPP is based on shared protection. As shown in Fig. 2.20a, two lightpaths require two and three FSs, respectively, and are protected on the basis of the whole path. For example, the primary path $1 \rightarrow 2 \rightarrow 4$ of lightpath 1 is protected by a link-disjoint backup path, i.e.,$1 \rightarrow 3 \rightarrow 4$, with a reservation of three FSs in each of the traversed link. The two backup paths share a common link $(3,4)$ but use different spectrum resources to protect their primary connections, leading to a requirement of five FSs in link $(3,4)$. Figure 2.20b shows an example of the two lightpaths protected by SBPP. Their backup paths can share the FSs in link $(3,4)$, and only three FSs are required to protect both lightpaths. This is because their primary paths do not share any common link, and thus will not fail simultaneously in the event of any link failure. And the three FSs reserved in link $(3,4)$ are sufficient

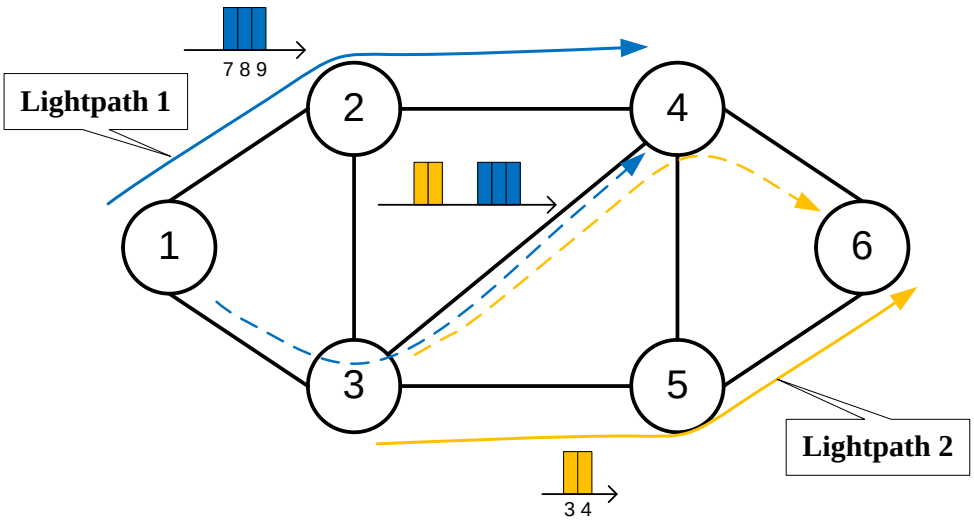

(a)

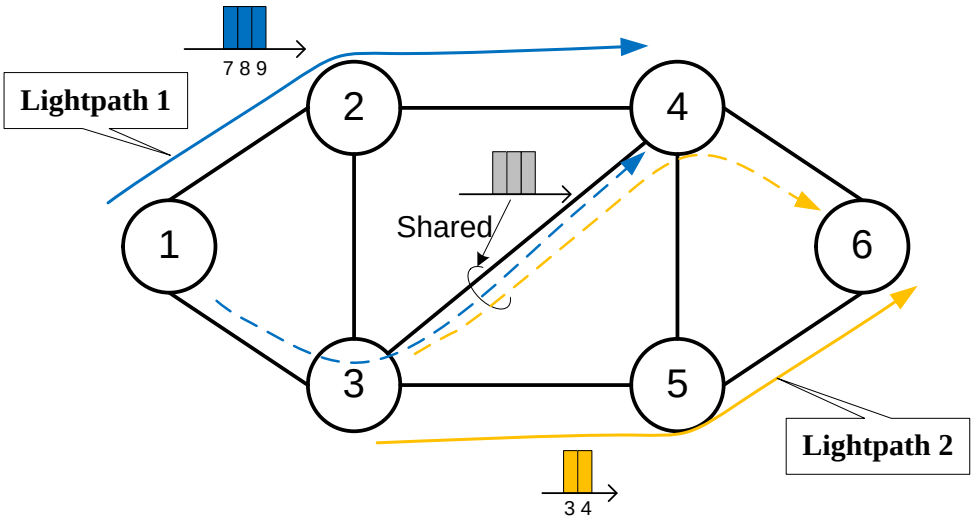

(b)

Fig. 2.20 Comparison between two protection schemes: (a) DPP; (b) SBPP.

to recover either of the two lightpaths. Compared to the requirement of five FSs in link $(3,4)$ in DPP, SBPP is more spectrally efficient.

Extensive studies have been conducted on the survivability of optical networks. SBPP in EONs is more complicated than that in fixed grid WDM optical networks,

since the backup resources of one connection can be shared as a whole by other connections, and in part by multiple connections with different bandwidth [82]. To minimize the required spectrum resources, Shen *et al.* [83, 84] provided ILP formulations for both SBPP and $1+1$ dedicated protection. In [85], different spectrum conversion capabilities, namely, no conversion, partial conversion, and full conversion, are considered in designing EONs with link protection technique. DPP [86–88], SBPP [8], ring cover [89], *p*-cycle [90, 91] and link-based [92] protection schemes were also investigated in EONs.

2.6 Grooming

Traffic grooming has been extensively studied in WDM-based optical networks where a number of low-speed connections are packed together to share a high-speed wavelength channel [93, 94]. A wavelength channel is generally too large for a single low speed connection and it is wasteful to use an entire wavelength bandwidth for each low speed connection. By aggregating low-speed electronic signals onto a wavelength, traffic grooming can improve spectrum utilization.

Although in EONs, a demand is accommodated by allocating a just-enough spectral bandwidth to the connection, traffic grooming can still be utilized for enhanced resource utilization for the following reasons [45, 46, 95, 96]. From the perspective of improved capacity utilization in transponders, BVTs in EONs are designed to have large capacities, say to support superchannels, and are usually very expensive. From the perspective of high spectrum efficiency in fiber links, traffic grooming reduces the usage of guard bands between channels because it decreases the number of channels by aggregating multiple data streams into an entity transmitted via a single channel instead of one channel per data stream.

The data streams that are aggregated onto a large optical channel may aim for different destinations. In other words, an end-to-end transmission may span

multiple lightpaths. Thus, it may go through OEO conversion. To reduce the electronic processing bottleneck and to provide better flexibility, *optical grooming* has been introduced where multiple flows are groomed in the optical domain. Based on optical grooming, source grooming has been investigated in [50, 51] where multiple optical flows that have the same sources are groomed in the optical domain. This technique can be supported by SBVT as mentioned earlier. Similarly, optical grooming improves the utilization of both transponders and of the fiber spectrum.

2.7 Spectrum Defragmentation

In EONs, demands of various data-rate requirements are flexibly allocated with diverse spectral bandwidths. In dynamic scenarios, connections undergo a birth-and-death process, that is, demands arrive sequentially and randomly for possible connection establishments, the established connections are then held for certain periods, and finally depart. This dynamic pattern and flexible spectrum allocation together with the enforcement of the three constraints lead to the spectrum being fragmented into small-size blocks. For example, when a connection occupying a spectral bandwidth completes its service, the spectrum bandwidth is then released for future demands. Connections requiring smaller bandwidths can be established by utilizing parts of the released spectrum leaving the remaining parts of the spectrum unused. The left spectrum parts are usually small-size and may not be utilized for future connection setups, which are called *spectrum fragments* [27]. Due to the fact that the small-size spectrum fragments can hardly be used, the fragmentation leads to low spectrum utilization and increased blocking probabilities. To address this problem, *spectrum defragmentation* techniques were investigated that makes room for future demands by rearranging the existing connections.

Defragmentation mechanisms can be divided into two directions, reactive and proactive. For the reactive mechanism, defragmentation is invoked when a demand

cannot be admitted for the spectrum usage of the network status. In the proactive mechanisms, defragmentation is invoked periodically or triggered to fulfill a certain requirement to prepare resources for future demands.

To address the defragmentation problem, a reoptimization approach was proposed in [97] that can be implemented as reactive and proactive mechanisms. In reoptimization techniques, existing connections are allowed to be reconfigured by changing their paths and/or allocating different spectral bandwidth. The authors formulated the spectrum defragmentation problem to first maximally consolidate the available spectral bandwidth and then minimize the number of interrupted connections. Two heuristic algorithms were proposed for the problem. This reoptimization technique indeed improves spectrum utilization. However it introduces interruptions to the connections, and is thus time-inefficient. To alleviate the impact on connection disruptions and for better time-efficiency, the authors in [57] presented a make-before-break technique based on the reactive mechanism for the spectrum defragmentation problem considering distance-adaptive spectrum allocation. For each demand that cannot be admitted by the network, this technique tries to reroute the existing connections that conflict with the accommodation of the demand. For each of the conflicting connection, the replacement is achieved by relocating an alternative route and/or assigning different spectral bandwidth in the make-before-break manner. The bandwidth and/or the alternative route are reserved, then switch the transmission to the lightpath using the reserved route and/or the reserved bandwidth and release the resources of the original connection. The make-before-break provides a faster defragmentation process and minimizes the impact on connection disruption, but it requires extra transmitters. Push-pull and hop tuning techniques that alter only the spectrum of conflicting lightpaths were investigated in [98] and [99], respectively. Both techniques perform defragmentation in a *hitless* manner without traffic disruption, and shift only the central frequency by exploiting the tuneability of the lasers in transponders. Based on the hitless technique, the authors in [100] proposed

heuristic algorithms for the defragmentation problem for both reactive and proactive mechanisms.

In another direction, fragmentation-aware algorithms were also investigated that keep existing connections intact but allocate spectrum resources in a cautious way with reduced creation of fragments. The authors in [101] proposed fragmentation-aware algorithms that select one of the candidate paths which creates fewest spectrum fragments. Compared to the existing algorithms, the fragmentation-aware algorithms achieve enhanced blocking performance. Sub-band virtual concatenation has been introduced to CO-OFDM-based EONs, which improves blocking performance for the dynamic RSA problem [102, 103]. It breaks a CO-OFDM channel into multiple sub-bands, and transmits these sub-bands separately to the destination. Similarly, multipath routing was introduced to deal with the spectrum defragmentation problem in [104] where the sub-bands are transmitted via multiple paths with bounded delay difference. Enhanced blocking performance is also achieved when a proper number of paths are considered.

Chapter 3

Optimization for a Multicast Demand

In the previous chapter, we introduced EONs focusing on the accommodation of unicast (one-to-one) demands. Instead of the one-to-one connection, in this thesis, we aim to address RSA problems for one-to-many multicast demands. One-to-many multicast involves a source and multiple destinations rather than a single destination for unicast. A multicast connection involves transmitting a signal from the source to multiple destinations. In this thesis, we denote a multicast session by $\langle s; \{d_1, d_2, \ldots, d_n\} \rangle$ where s is the source node, and $\{d_1, d_2, \ldots, d_n\}$ are the set of n destination nodes. A multicast demand mentioned in this thesis is a request for multicast service. The request includes a set of attributes, which are the source and destination nodes, the bit-rate and the holding time. Such one-to-many multicast have many applications, e.g., synchronization of databases among geographically distributed datacenters and ultra-high-definition TV delivery. Here, the source and destinations may not be exactly the end users, but are routers. And the traffic generated at the source may not be from a single user but aggregated from many users. We denote a multicast demand r by $\langle s_r; \mathbf{F}_r; t_r \rangle$, requesting a data transmission from the source s_r to the set of destinations $\mathbf{F}_r$ at the requested bit rate t_r. In the network design problem that we solve, we make the simplifying assumption that the holding times are unlimited. However, in Section 5.5.2, we apply the proposed approach also

to the dynamic case with limited holding times and show good performance also in the dynamic case.

There are generally three structures, namely, lightpath, light-trail, and light-tree, to provision a multicast demand depending on the multicasting capabilities of network nodes. When the node architecture only supports unicast capability, e.g., the spectrum routing architecture mentioned in the previous chapter, the lightpath scheme is used to accommodate the multicast demand. For this structure, a multicast demand is considered as a set of unicast demands, each requiring a transmission of the data from the source to a destination. When the node architecture is *Multicast-Capable (MC)*, the multicast demand can be provisioned using the light-tree structure by a single light-tree or multiple light-trees. An example is based on the broadcast-and-select architecture mentioned in the previous chapter, while the discussion on non-blocking architectures with multicasting capability in the context of WDM networks was presented in [105]. Here, a light-tree is an optical channel from a source to multiple destinations which is an extension of the concept of lightpath [106]. For a light-tree, the signal is transmitted in the optical domain along a tree structure that connects the source to the destinations. The optical signal is split into multiple copies at a splitting node of the tree and each of the copies feeds an egress link at the node. In particular, a lightpath can be considered a special case of a light-tree that has only one destination. Thus, for the MC architecture, to accommodate a multicast, we can use a single light-tree, or a combination of light-tree(s) and/or lightpaths. The third structure is the light-trail [107, 108], where the nodes between the two end nodes of the trail can also receive the signal by tapping a small portion of the power, while switching the remainder to the output. The light-trail structure requires the network node to be *Multicast-Incapable (MI)* with Tap-and-Continue (TaC) functionality [109]. Similar to the light-tree, the light-trail can also support optical multicasting by allowing multiple nodes along the trail to receive the signal. Also, the lightpath is a special case of the light-trail where only the end node of the

trail receives the signal. Therefore, for the TaC-based node architecture, a multicast may be provisioned by a single light-trail or a combination of light-trail(s) and/or lightpath(s).

Similar to lightpath-based RSA in EONs, the light-tree-based and light-trail-based RSA that do not consider spectrum conversion capability are also required to satisfy the three constraints of *spectrum continuity*, *spectrum contiguity*, and *spectrum non-overlap*. The spectrum continuity constraint ensures that the same FSs should be utilized in all fiber links that are included in a light-tree/light-trail. The spectrum contiguity constraint ensures that the FSs in each fiber link assigned to a light-tree/light-trail are contiguous. Then, the spectrum non-overlapping constraint prevents any FS in a fiber link from being allocated to two or more connections.

Distance-adaptive spectrum allocation is an important feature that improves spectrum efficiency [14, 40]. Distance-adaptive transmission entails the choice of MS for a signal that is adaptive to the transmission distance of the optical path. Thus, the RSA problem is extended into a more flexible and complex problem involving Routing, Modulation, and Spectrum Assignment (RMSA) [5, 8, 110]. Similarly, the light-tree-based MC-RSA/light-trail-based MI-RSA are extended to be MC- and MI-RMSA, respectively.

3.1 Related Work

Extensive studies on provisioning multicast services have been reported for optical networks in the literature. The authors in [16] presented a tutorial on multicast routing algorithms and related protocols for packet-switched networks. The authors in [111] formulated analytical models to compare the lightpath scheme, the light-tree scheme, and a hybrid approach of the lightpath and light-tree with and without wavelength conversion capability in the context of traditional WDM optical networks. Benefits of employing multicasting capability in the provision of multicast services

were also examined in [112]. The author in [17] discussed the fundamental principles and enabling components for multicasting in the optical layer. Moreover, the authors in [18, 113] surveyed various aspects of provisioning multicast services in WDM optical networks.

Solutions based on the light-trail have also been proposed for provisioning multicast demands [114–118]. The authors in [118] provided an ILP formulation to provision a single multicast by light-trails in the context of WDM networks. The authors in [115, 117] studied the problem of minimizing the number of required light-trails for a given multicast demand. Also, light-trail-based solutions were investigated for the traffic grooming of sub-wavelength connections in WDM networks [116]. Moreover, for WDM sparse-splitting networks with a mix of MC and MI nodes, algorithms were proposed [119, 120]. The light-trail has been also studied in the context of EONs however for unicast demands [121].

The study on provisioning multicast demands attracts attentions for EONs. The authors in [122] considered provisioning multicast demands in an overlay network where the multicast in the application layer is accommodated by lightpaths in the optical layer. Recent studies focus on provisioning multicast connections in EONs using light-tree based on the assumption that the network nodes are MC. Experiments of light-trees with and without conversion capabilities have been demonstrated in [123] for EONs. The authors in [124] investigated benefits of multicasting in EONs over WDM networks. Yu *et al.* [125] considered a network with modulation-enabled nodes, where the MSs of the input and output signals can be different. Their simulation results show that with one modulation-enabled node, the blocking probability drops significantly. Ruiz and Velasco [126] considered a similar problem to the one we presented in this chapter. They evaluated the three schemes for multicast demands, namely, path, tree, and subtree. However, they omitted the distance-adaptive spectrum allocation, which is an important feature for improving spectrum efficiency in EONs and could bring the lightpath scheme spectrum savings

over the light-tree scheme as we will show in this chapter. Also, they did not compare with schemes using the light-trail technology for the multicast demands, which we do in this chapter. The authors of [127] formulated ILP models for distance-adaptive resource allocation in EONs using light-tree technology on an SD pair basis, where a tree is constructed by multiple paths, each of which starts from the source and ends at a destination. They also developed heuristic algorithms for both the static and dynamic cases. In [128], the authors formulated a flow multicast model for a similar problem. Due to the high computation complexity, they also formulated a candidate tree model and proposed a heuristic algorithm, both based on pre-calculated candidate trees. As the performance of the algorithm is highly affected by the pre-calculated trees, the authors in [129] further discussed the selection metrics on the candidate trees. Moreover, the impact of the degree limitation of a multicast tree node was investigated in [130], and has been demonstrated to be relatively small in terms of spectrum consumption. In the same paper, the authors also considered the transmission reach reduction due to optical signal splitting in EONs with distance-adaptive resource allocation. Such reduction requires more regenerators, while the spectrum usage remains almost unchanged. Following that, with similar constraints in the physical layer, a light-forest that consists of multiple light-trees rather than a single light-tree is utilized to provision a multicast demand in EONs [131]. While these studies are aimed mainly at the optical layer, the authors in [132] investigated the impact of the number of MC nodes and the multicast degree on the network design problem of minimizing the spectrum requirement in links. The authors in [133] considered using the multi-light-tree scheme for provisioning multicast demands and applied network coding in the design. The authors in [134] proposed an efficient algorithm using the multi-light-tree scheme for the provision of multicast services in a dynamic environment. The authors in [135] also provided an arc-path ILP formulation for the static MC-RMSA problem and compared the performance of using multiple light-trees to that of using a single light-tree for a multicast. However,

they did not compare to the schemes using lightpaths or light-trails which we do in this chapter. Ruiz and Velasco [136] considered serving multicast demands in multiple layers.

In this chapter, we focus on comparing various schemes using lightpath, light-tree and light-trail to provision multicast services in the context of EONs. In the following, we introduce preliminaries in Section 3.2. Section 3.3 elaborates the schemes that are compared in this chapter. We state the problem in Section 3.4, and in Section 3.5 we provide the MILP formulations for the schemes. Section 3.6 presents the numerical results and finally we summarize this chapter in Section 3.7.

3.2 Preliminaries

In this section, we present the network model we use in this thesis and the distance-adaptive transmission we consider for the network.

3.2.1 Network Model

The EON is represented by a directed graph $G = (\mathbf{V}, \mathbf{L})$ where $\mathbf{V}$ is the set of nodes and $\mathbf{L}$ is the set of directed links. Every two adjacent nodes i and j are connected by two directed links in opposite directions, each of which corresponds to a unidirectional fiber link, denoted by (i, j) for the one from node i to node j and (j, i) for the one from node j to node i. Let ℓ_{ij} denote the weight of fiber link (i, j) representing its physical length. We assume $\ell_{ij} = \ell_{ji}$ for all $(i, j) \in \mathbf{L}$ without loss of generality. Let $\mathcal{G}$ denote the bandwidth of an FS in units of GHz. The set of MSs considered is $\mathbf{M}$. For $m \in \mathbf{M}$, we denote by τ_m^r the transparent reach of a given multicast demand r modulated by MS m, and by $\mathcal{C}_m$ the capacity per FS modulated by MS m. Let g denote an integer number of FS that are used as the guard band placed between two neighboring channels to avoid interference.

3.2.2 Distance-Adaptive Transmission

To efficiently utilize the spectrum resources, we consider distance-adaptive spectrum resource allocation in EONs, where minimum spectrum resources are adaptively allocated to an all-optical channel according to its physical condition [137–139]. As in [8, 137, 140], the condition of a lightpath is measured by its physical transmission distance. In this context, a more spectrally efficient (or higher-order) MS implies less spectrum for serving a demand but is associated with a shorter transparent reach. As an example, Table 3.1 provides the transparent reach and the capacity per FS of three MSs, namely, BPSK, QPSK and 8-QAM. These values are used in [8] based on [137].

If the transmission distance of a connection is longer than the transparent reach of the assigned MS, regenerators are required to regenerate the signal. This indicates a fundamental tradeoff between the cost of the transparent reach and the spectrum usage in choosing an MS. Accordingly, in distance-adaptive spectrum allocation, among the available MSs whose transparent reaches are longer than the transmission distance of the connection, the highest-order one is chosen. If no MS is available, regenerators are required in the network. In this form of distance-adaptive transmission [141], the number of regenerators required in the network can be minimized, while the spectrum usage is kept at a reasonable level.

For a regenerator-free optical network, the transmission distance of a lightpath cannot exceed the transparent reach of the assigned MS as no regeneration is applied to the signal. As a lightpath is a one-to-one connection, only the path distance is used to determine the MS assignment. However, different from a lightpath, a light-tree transmits a signal to multiple destinations and has multiple paths from the source to the destinations along the tree. A light-tree can only be assigned one MS as it is a single optical entity. To determine the MS assignment, the longest distance among the paths is usually used [127, 128, 132, 135, 142]. Similarly, a light-trail is also a

Table 3.1 Transparent Reach and Capacity per FS for Each MS [8]

MS	Transparent Reach [km]	Capacity per FS [Gb/s]
BPSK	4000	12.5
QPSK	2000	25
8QAM	1000	37.5

single entity and the signal is transmitted via the light-trail from a source to multiple destinations. Likewise, the distance from the start node to the end node of the trail can be utilized to determine the MS.

3.3 Schemes for Multicast Demands

In this section, we describe five schemes, namely, lightpath, light-tree, multi-light-tree, light-trail, and multi-light-trail, to provision a given multicast demand $r = \langle s_r; \mathbf{F}_r; t_r \rangle$ where $\mathbf{F}_r = \{d_1, d_2, \ldots, d_n\}$.

3.3.1 The Lightpath Scheme

The lightpath method is firstly to treat the multicast demand as multiple unicast demands $r_i = \langle s_r; \{d_i\}; t_r \rangle$, $i = 1, 2, \ldots, n$, each from the source to one of the destinations requiring the same data rate as the original multicast demand. Then, the multicast demand is accommodated when separate lightpaths are established for the unicast demands. The accommodation of a multicast demand is transformed into the accommodation of the several end-to-end lightpaths. Thus the RMSA for a multicast demand is changed into RMSA for the multiple lightpaths. This lightpath scheme occupies n transmitters at the source node and one receiver at each destination node, in total n receivers in the accommodation of the multicast demand.

Figure 3.1 shows the lightpath approach that is used to provision an example multicast demand, $\langle A; \{B, C, D\}; 30 \text{ Gb/s} \rangle$. The multicast demand is consid-

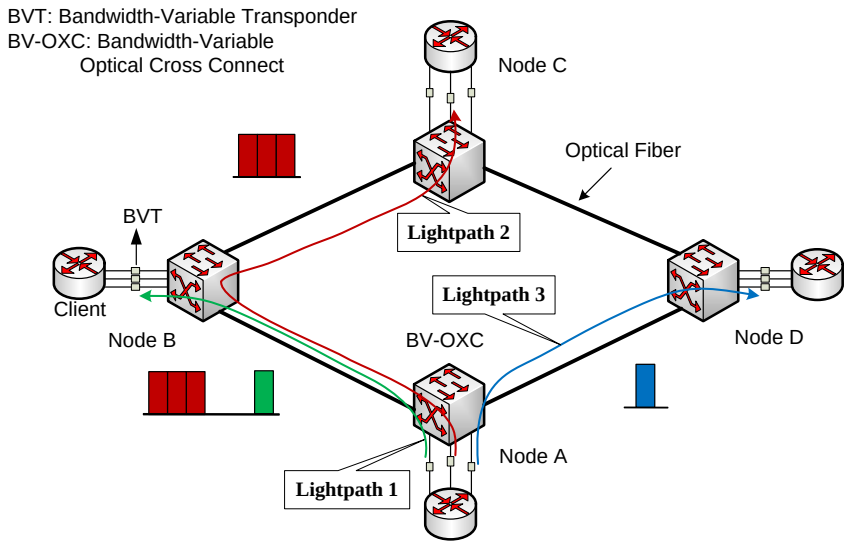

Fig. 3.1 The lightpath scheme for a multicast demand $\langle A;\{B,C,D\};30\text{ Gb/s}\rangle$.

ered as three unicast demands, namely, $\langle A;\{B\};30\text{ Gb/s}\rangle$, $\langle A;\{C\};30\text{ Gb/s}\rangle$, and $\langle A;\{D\};30\text{ Gb/s}\rangle$. These unicast demands are provisioned by three separate lightpaths. In the figure, we note that the three lightpaths aim for the same capacity, but occupy different numbers of FSs. This is because lightpaths are accommodated based on distance-adaptive spectrum allocation, where a shorter path implies that less spectrum is required. Thus we assume that lightpath 2 requires three FSs since it has a longer path while the other two lightpaths require only one FS. The multicast demand is accommodated using the lightpath scheme by a total of eight FSs and three transmitters.

3.3.2 The Light-Tree Scheme

For the light-tree method, the multicast demand is considered as a whole and is accommodated by a single light-tree. This light-tree technology requires the network nodes to be MC with optical multicasting capability. An example Optical Cross-Connect (OXC) node is the splitter-and-delivery switch [143]. The accommodation of multicast demands by the light-tree scheme requires only one transmitter at the

source node and one receiver at each of the n destinations which entails transmitter savings over the lightpath scheme.

A single light-tree is spectrum efficient in EONs with a fixed modulation. Assume that all the light-trees are using the same modulation scheme, and thus occupy the same amount of bandwidth in each traversed link for a given data rate. A light-tree is considered more spectrum efficient to provision a multicast than multiple lightpaths [106] as the lightpaths traverse more links in total and therefore occupy more spectral bandwidth than the light-tree. This high spectrum efficiency of a light-tree for multicast is achieved by allowing spectrum sharing among the transmissions from the source to the destinations.

However, a single light-tree for a multicast may not be that efficient in EONs with distance-adaptive spectrum allocation. When choices on MS are available to connections, which breaks the limitation of the uniform modulation usage, a single light-tree may not be a very good choice. It may even be worse than the lightpath scheme in some cases as we will show in the following example and the numerical results. This is due to the fact that a light-tree is required to use a single scheme to modulate a signal so that the quality of transmission is guaranteed for the worst case, e.g., the farthest destination from the source. And the utilized modulation scheme is usually of a low level (i.e., spectrum inefficient) as it is subject to the longest distance of paths to the destinations, which raises the spectrum requirement in links traversed. This introduces excessive spectrum consumption because the transmission of a shorter distance to a destination, if provisioned separately, could use a more spectrum-efficient modulation with less spectrum consumption. The problem of excessive spectrum consumption can be solved by the multi-light-tree scheme at the cost of a higher transmitter usage where multiple light-trees can be utilized for multicast as we will show later.

In Fig. 3.2, we provide an example of using the light-tree approach to accommodate the same multicast demand as mentioned in the lightpath scheme. Here the

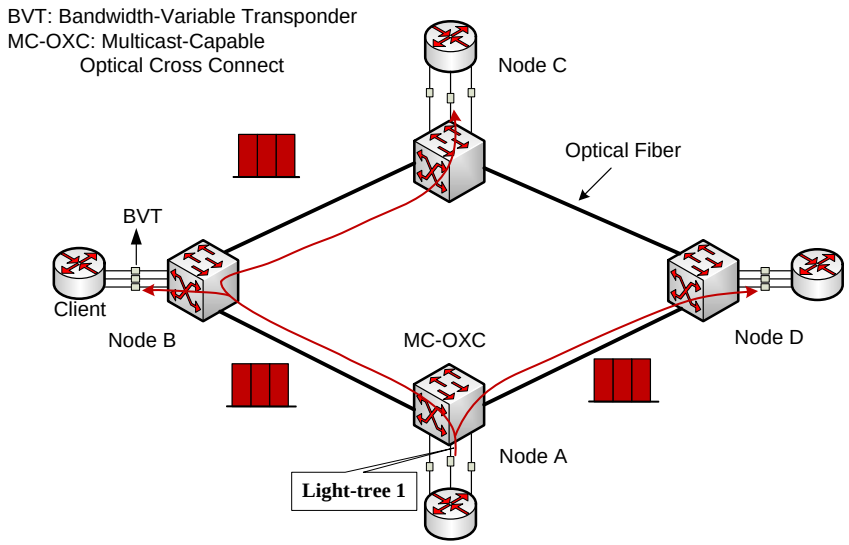

Fig. 3.2 The light-tree scheme for a multicast demand $\langle A;\{B,C,D\};30\text{ Gb/s}\rangle$.

network nodes are assumed to be MC. The multicast demand is accommodated as a single entity by a light-tree that connects the source node to all its destination nodes. The signal is split into two copies at node A, one copy transmitted via link (A,D) and dropped at node D, the other via link (A,B). When the signal arrives at node B, it again is split into two copies, one dropped at node B, the other transmitted via link (B,C) and dropped at node C. The accommodation of the multicast demand using the light-tree scheme requires a total of nine FSs and one transmitter. Compared to the lightpath scheme, the light-tree scheme saves two transmitters but uses one additional FS. Note that if the signal is modulated by the same MS for the lightpaths and the light-tree, it is intuitive that the total amount of spectrum utilized by the light-tree scheme is less than or equal to that used by the lightpath scheme as discussed previously. However, when distance-adaptive spectrum allocation is applied, the light-tree scheme does not necessarily provide spectrum savings over the lightpath scheme as we show in this case.

3.3.3 The Multi-Light-Tree Scheme

The multi-light-tree approach is to separate the set of destinations of the given multicast demand into m, $1 \leq m \leq n$, subsets of destinations $\bar{\mathbf{F}}_r{}^j$, $j = 1,2,\ldots,m$, which are mutually exclusive and collectively exhaustive, i.e., $\bar{\mathbf{F}}_r{}^x \cap \bar{\mathbf{F}}_r{}^y = \emptyset$, where $x \neq y, x, y = 1,2,\ldots,m$, and $\cup_{j=1}^{m} \bar{\mathbf{F}}_r{}^j = \mathbf{F}_r$. Then, the multicast demand can be considered as multiple sub-demands, $\langle s_r; \bar{\mathbf{F}}_r{}^j; t_r \rangle$, $1 \leq j \leq m$, which have the same source and requires the same data rate as the original demand, but aimed at different subsets of the destinations. Each of the sub-demands is implemented by a single entity, i.e., either a single light-tree if it has multiple destinations or a lightpath if it has only one destination. Thus, the multi-light-tree scheme provisions a multicast demand by a combination of lightpath(s) and/or light-tree(s). Solutions provided by the multi-light-tree scheme can be classified to be pure lightpaths each to one destination as provided by the lightpath scheme, a single light-tree covering all destinations as by the light-tree scheme, multiple light-trees each covering different sets of destinations, and a mixed of lightpath(s) and light-tree(s). The solutions provided by the lightpath and light-tree methods can be considered as special cases of the multi-light-tree scheme, i.e., when $m = n$ and $m = 1$, respectively. Thus the multi-light-tree method is flexible in provisioning multicast demands and can be considered a generalization of the lightpath and light-tree methods. The multi-light-tree approach requires m, $1 \leq m \leq n$, transmitters at the source node and one receiver at each destination node.

In the same MC network as used for the single light-tree approach, for the multi-light-tree scheme, the multicast demand is partitioned into two sub-demands, namely, a smaller-size multicast demand $\langle A; \{B,C\}; 30 \text{ Gb/s} \rangle$ and a unicast demand $\langle A; \{D\}; 30 \text{ Gb/s} \rangle$. The smaller-size multicast demand is served by a light-tree and the unicast demand by a lightpath as shown in Fig. 3.3. The multi-light-tree scheme uses two transmitters and seven FSs in total achieving the least spectrum

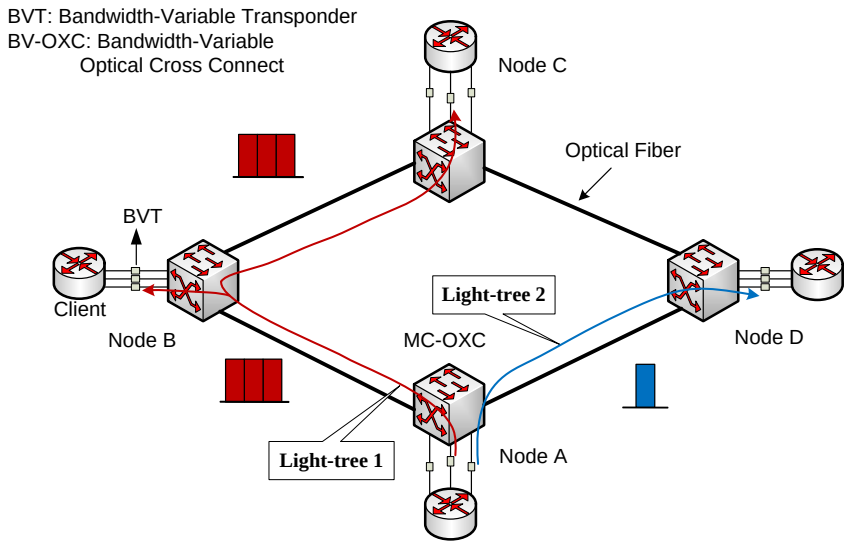

Fig. 3.3 The multi-light-tree scheme for a multicast demand $\langle A; \{B, C, D\}; 30 \text{ Gb/s} \rangle$.

consumption with a moderate usage of transmitters compared to the previous two approaches.

3.3.4 The Light-Trail Scheme

The light-trail technology was proposed in [107] to allow multiple nodes to share its spectral bandwidth. Similar to a lightpath, a light-trail is a unidirectional optical circuit. However, for the light-trail, signals are transmitted via a physical trail where the intermediate nodes can also receive the data. Here, a trail is an extension of a path by allowing repeated visits of nodes but not directed links in a directed graph. Thus, a lightpath can be also considered as a special case of a light-trail. If network nodes are equipped with TaC functionality [109], a light-trail can be used as a means to support optical multicasting by traversing all the destination nodes. The TaC functionality enables the node to tap a small portion of an input signal for local usage that causes negligible degradation to the signal and to switch the remainder to one output port. In this way, all the destination nodes can receive the signal via a single light-trail. Also, the TaC-based node architecture is more cost-effective than the architecture for light-tree technology as it does not require the massive use of light-splitters and

amplifiers. However, finding a trail with the optimum cost that starts from the source and covers all the destinations is proven to be NP-complete [144]. Moreover, a light-trail that covers all the destinations entails a long transmission distance. Due to power budget limitations, such a light-trail for a multicast demand may not meet the quality of transmission requirements, for which a set of light-trails may be used. Similar to a light-tree, a light-trail requires only one transmitter at the source and one receiver at each covered destination.

A light-trail also provides spectrum sharing among the transmissions to multiple destinations as the destinations receive the signal at different points of the trail. However, for the sake of covering the destinations, a light-trail may repeatedly visit some nodes that form cycles leading to excessive spectrum consumption. This makes the light-trail scheme not as spectrum-efficient as the light-tree and possibly worse than the lightpath method. This is because for a light-trail associated with a multicast connection in a TaC-based multicast-incapable network, there is an equivalent light-tree in the corresponding MC network assuming that both the light-tree and light-trail require the same amount of spectral bandwidth in each traversed link. For a light-trail with cycles, a light-tree can be derived by removing some of the links that cause the cycles, while an equivalent light-trail solution without cycles is a light-tree using the same links. Also, the transmission distance of a light-trail is longer than or equal to that of an equivalent light-tree. Thus, if distance-adaptive resource allocation is present, the light-trails may use less spectrum-efficient modulations due to the longer transmission distances and therefore consume more spectrum in each traversed link than the light-trees and possibly the lightpath method as well. These entail solutions of multiple light-trails for a multicast in multicast-incapable networks like the multi-light-tree scheme in MC networks.

For the same multicast demand, Fig. 3.4 shows the light-trail scheme in a multicast-incapable network. The signal is transmitted via a trail $A \rightarrow D \rightarrow A \rightarrow B \rightarrow C$. The trail changes its direction at node D leading to a revisit at node A.

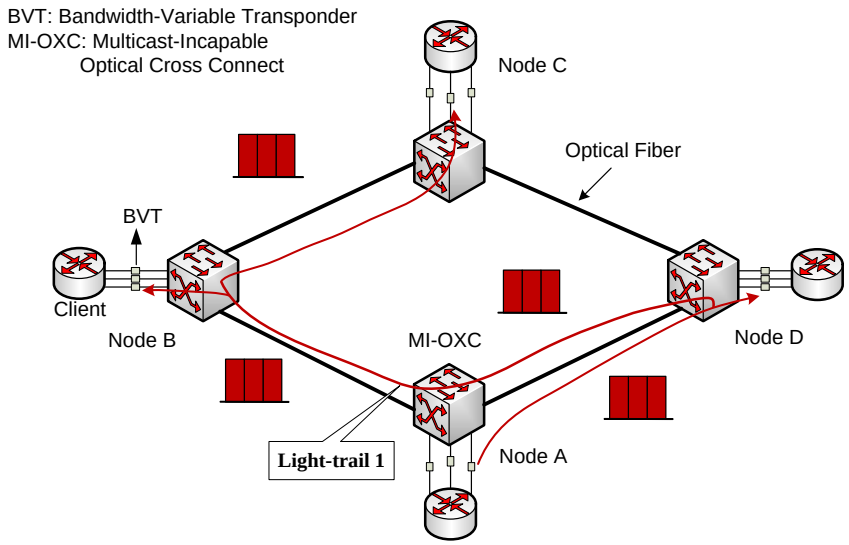

Fig. 3.4 The light-trail scheme for a multicast demand $\langle A; \{B, C, D\}; 30 \text{ Gb/s} \rangle$.

Destination nodes D and B tap the signal from the light-trail for local usage. Assume that the light-trail occupies three FSs in each traversed link. The light-trail in total uses 12 FSs to provision the demand and one transmitter at node A.

3.3.5 The Multi-Light-Trail Scheme

Similar to the multi-light-tree scheme, the multi-light-trail scheme uses multiple light-trails to provision a multicast. It also splits the multicast demand into multiple, say h ($1 \leq h \leq n$), sub-demands, each with the same source and bit rate but mutually exclusive and collectively exhaustive sets of destinations. Each sub-demand is provisioned by a single light-trail. With h varying from 1 to n, the multi-light-trail scheme can also be classified as (i) pure lightpaths each to one destination ($h = n$) as provided by the lightpath scheme, (ii) a single light-trail ($h = 1$) as provided by the light-trail scheme, and (iii) a mixture of light-trails and/or lightpaths ($1 < h < n$). The multi-light-trail method requires h, $1 \leq h \leq n$, transmitters at the source node and a total of n receivers each at a destination node.

For the same multicast demand, Fig. 3.5 shows the multi-light-trail scheme in the same multicast-incapable network as used in the light-trail scheme. Like the multi-

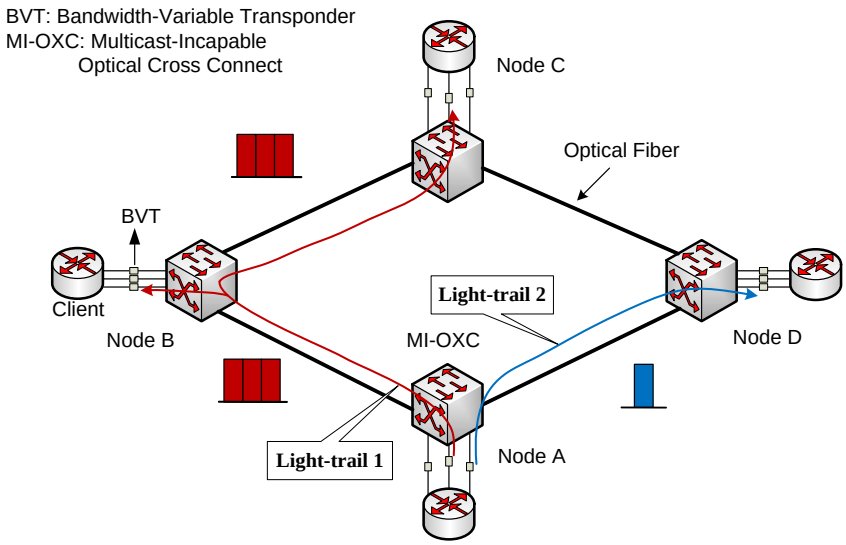

Fig. 3.5 The multi-light-trail scheme for a multicast demand $\langle A;\{B,C,D\};30\text{ Gb/s}\rangle$.

light-tree scheme, the multi-light-trail accommodates the multicast demand by a light-trail and a lightpath for the same two sub-demands as shown in Fig. 3.5. In particular, destination node B receives the signal by tapping the light-trail via $A \rightarrow B \rightarrow C$. The multi-light-trail method consumes also seven FSs and two transmitters as the multi-light-tree scheme does. It achieves spectrum reduction by employing an additional transmitter compared to the light-trail scheme.

3.4 Problem Statement

In this chapter, we focus on the RMSA problem for a single multicast demand denoted by $\langle s_r;\mathbf{F}_r;t_r\rangle$, requesting a data transmission from the source s_r to the set of destinations $\mathbf{F}_r$ at the bit rate t_r. Let ω_m^r denote the number of FSs to be assigned to serve the multicast demand r for the required bit rate given that MS m is utilized. By definition, we have $\omega_m^r = \lceil t_r/\mathcal{C}_m \rceil$ as presented in [8], where $\lceil x \rceil$ is the smallest integer that is greater than or equal to x. For instance, based on the values of MSs in Table 3.1, an FS modulated by QPSK has a capacity $\mathcal{C}_{\text{QPSK}} = 25$ Gb/s and a transparent reach $\tau_{\text{QPSK}} = 2{,}000$ km. We can observe from Table 3.1 that, for an

example multicast connection requesting $t_r = 45$ Gb/s and a transmission distance of 1,800 km, the number of required FSs given that QPSK is utilized is two, i.e., $\omega^r_{\text{QPSK}} = 2$. Here, the highest-order MS that can be assigned to this particular connection is QPSK since $\tau_{\text{QPSK}} > 1,800$ km but $\tau_{\text{8QAM}} < 1,800$ km.

Based on the network model described above, we further make the following assumptions. We assume that the EON does not support spectrum conversion. Thus, the spectrum continuity constraint must be satisfied. To support distance-adaptive spectrum resource allocation, all transponders are central frequency tunable and also MS tunable. For simplicity, in this thesis we do not consider the use of regenerators. We assume that every SD pair has at least one path, of which the transmission distance is within the transparent reach of the lowest-order MS considered, e.g., 4,000 km for BPSK as in Table 3.1.

In this chapter, we aim to compare the performances of the five provision schemes, namely, lightpath, light-tree, multi-light-tree, light-trail, and multi-light-trail, for a single multicast demand by investigating their resource usage. Given the above-mentioned network model and the multicast demand, the objective is to minimize the total amount of consumed spectrum, i.e., the sum of the spectrum in all the links allocated to a demand, in the context of EONs. We also consider both network cases with and without the consideration of the distance-adaptive transmission where the benefit of distance-adaptive spectrum allocation is evaluated.

3.5 MILP Formulations

We evaluate the five schemes by comparing the total spectrum usage in provisioning the demand. We provide three MILP formulations for the lightpath, multi-light-tree, and multi-light-trail provisioning schemes, aiming to minimize the total number of utilized spectrum in terms of FSs. In particular, for the multi-light-tree and multi-light-trail cases, the problem is formulated as a multi-objective problem to

also find the minimized number of used transmitters after the total spectrum usage is optimized. Note that the formulations for the multi-light-tree, and multi-light-trail methods can also be applied to the light-tree and light-trail approaches by varying the inputs, respectively.

In the following, we present the formulations for a set of multicast demands, i.e., **R**. However, the formulation is applicable to the single demand case where the set contains only one element.

3.5.1 Lightpath-Based MILP

Variables

$P^r_{d,ij}$ Binary; equals one if the path to destination d, $d \in \mathbf{F}_r$, of multicast demand r, traverses fiber link (i,j), $(i,j) \in \mathbf{L}$; zero, otherwise.

D^r_d Real; denotes the distance of the path from source s_r to destination d of multicast demand r.

$K^r_{d,m}$ Binary; equals one if MS $m, m \in \mathbf{M}$, is assigned to the lightpath from source s_r to destination d of multicast demand r; zero, otherwise.

$B^{r,d}_{ij,m}$ Binary; equals one if MS $m, m \in \mathbf{M}$, is assigned to the lightpath from source s_r to destination d of multicast demand r and this lightpath traverses link ij; zero, otherwise, i.e., $B^{r,d}_{ij,m} = P^r_{d,ij} \cdot K^r_{d,m}$. This is a nonlinear equation but is linearized as we show later.

N^r_{ij} denotes the number of FSs in link ij required by multicast demand r, $N^r_{ij} \geq 0$.

W^r_d Integer; denotes the number of FSs required by the lightpath from source s_r to destination d of multicast demand r. Note that the FSs include the

spectral bandwidth used to carry the data and a guard band following the bandwidth in order to avoid interference with possible signals that follow.

S_d^r Integer; denotes the start index of the FSs required by the lightpath from source s_r to destination d of multicast demand r, $S_d^r \geq 1$.

E_d^r Integer; denotes the end index of the FSs required by the lightpath from source s_r to destination d of multicast demand r, $E_d^r \geq 1$.

$A_{d,ij}^r$ Integer; denotes a lower bound of the number of FSs in link (i, j) used by the lightpath from source s_r to destination d of multicast demand r, $A_{d,ij}^r \geq 0$.

$X_{r_2,d_2}^{r_1,d_1}$ Binary; equals to one if the path from source s_{r_1} to destination d_1 of multicast demand r_1 and the path from source s_{r_2} to destination d_2 of multicast demand r_2 share common link(s).

$O_{r_2,d_2}^{r_1,d_1}$ Binary; equals to zero if the indices of the FSs assigned to the lightpath from source s_{r_1} to destination d_1 of multicast demand r_1 is greater than the indices of the FSs assigned to the lightpath from source s_{r_2} to destination d_2 of multicast demand r_2 when the two lightpaths share common link(s), i.e., $X_{r_2,d_2}^{r_1,d_1} = 1$.

Objective

$$\textbf{min} \sum_{r \in \mathbf{R}} \sum_{(i,j) \in \mathbf{L}} N_{ij}^r \tag{3.1}$$

Objective (3.1) is to minimize the total number of FSs that are used to accommodate the given multicast demand.

Constraints

We divide the constraints into four groups, namely, *path computation*, *modulation determination*, *FS usage in links*, and *spectrum allocation*. The first group of constraints guarantees flow conservation where a path is found for each SD pair of a multicast demand. The second group ensures that an MS is assigned to the lightpath of each SD pair so that the distance of the lightpath does not exceed the maximum reach of the signal using the MS. The third constraint group ensures that the sum of the numbers of FSs used by all lightpaths is calculated. The fourth group ensures that the three constraints, namely, spectrum continuity, contiguity, and non-overlapping, are met.

1) Path Computation

$$\sum_{(i,j)\in\mathbf{L}} P^r_{d,ij} = \begin{cases} 1, & i = s_r \text{ or } j = d, \\ 0, & j = s_r \text{ or } i = d, \end{cases} \quad \forall r \in \mathbf{R}, d \in \mathbf{F}_r \tag{3.2}$$

$$\sum_{(i,x)\in\mathbf{L}} P^r_{d,ix} = \sum_{(x,j)\in\mathbf{L}} P^r_{d,xj}, \quad \forall r \in \mathbf{R}, d \in \mathbf{F}_r, x \in \mathbf{V} \setminus \{s_r, d\}. \tag{3.3}$$

Constraints (3.2) and (3.3) ensures flow conservation, where there are one egress link and one ingress link at the source node and the destination node, respectively, while for each intermediate node, the number of egress links equals to the number of ingress links. In this way, a path can be found for each SD pair of a multicast demand.

2) Modulation Determination

$$D^r_d = \sum_{(i,j)\in\mathbf{L}} \ell_{ij} \cdot P^r_{d,ij}, \quad \forall r \in \mathbf{R}, d \in \mathbf{F}_r \tag{3.4}$$

$$\sum_{m\in\mathbf{M}} K^r_{d,m} = 1, \quad \forall r \in \mathbf{R}, d \in \mathbf{F}_r \tag{3.5}$$

$$\tau_m^r - D_d^r \geq \Delta \cdot \left(K_{d,m}^r - 1\right), \quad \forall r \in \mathbf{R}, d \in \mathbf{F}_r, m \in \mathbf{M}. \tag{3.6}$$

Constraint (3.4) guarantees that the distance of a path is the sum of the length of the links traversed by the path. Constraint (3.5) ensures that one of the MSs considered is assigned to the lightpath. Constraint (3.6) guarantees that the transmission distance of the lightpath of each SD pair is within the transparent reach of the assigned MS.

3) FS Usage in Links

$$N_{ij}^r = \sum_{d \in \mathbf{F}_r} \sum_{m \in \mathbf{M}} B_{ij,m}^{r,d} \cdot (\omega_m^r + g), \quad \forall r \in \mathbf{R}, (i,j) \in \mathbf{L} \tag{3.7}$$

$$B_{ij,m}^{r,d} \leq P_{d,ij}^r, \quad \forall r \in \mathbf{R}, d \in \mathbf{F}_r, (i,j) \in \mathbf{L}, m \in \mathbf{M} \tag{3.8}$$

$$B_{ij,m}^{r,d} \leq K_{d,m}^r, \quad \forall r \in \mathbf{R}, d \in \mathbf{F}_r, (i,j) \in \mathbf{L}, m \in \mathbf{M} \tag{3.9}$$

$$B_{ij,m}^{r,d} \geq P_{d,ij}^r + K_{d,m}^r - 1, \quad \forall r \in \mathbf{R}, d \in \mathbf{F}_r, (i,j) \in \mathbf{L}, m \in \mathbf{M}. \tag{3.10}$$

Constraint (3.7) guarantees that the number of FS used in a link is the sum of the numbers of FS required by the lightpaths of all SD pairs that traverse the link. The calculation procedure of equation (3.7) is provided as follows.

$$\begin{aligned} N_{ij}^r &= \sum_{d \in \mathbf{F}_r} P_{d,ij}^r \cdot \sum_{m \in \mathbf{M}} K_{d,m}^r \cdot (\omega_m^r + g) \\ &= \sum_{d \in \mathbf{F}_r} \sum_{m \in \mathbf{M}} P_{d,ij}^r \cdot K_{d,m}^r \cdot (\omega_m^r + g) \\ &= \sum_{d \in \mathbf{F}_r} \sum_{m \in \mathbf{M}} B_{ij,m}^{r,d} \cdot (\omega_m^r + g), \quad \forall r \in \mathbf{R}, (i,j) \in \mathbf{L} \end{aligned}$$

where $B^{r,d}_{ij,m} = P^r_{d,ij} \cdot K^r_{d,m}$ is derived and is a non-linear equation involving only an multiplication of two binary variables. We replace this non-linear equation by the three linear constraints (3.8), (3.9), and (3.10).

4) Spectrum Allocation

$$W^r_d = \sum_{m \in \mathbf{M}} K^r_{d,m} \cdot (\omega^r_m + g), \quad \forall r \in \mathbf{R}, d \in \mathbf{F}_r \tag{3.11}$$

$$E^r_d = S^r_d + W^r_d - 1, \quad \forall r \in \mathbf{R}, d \in \mathbf{F}_r \tag{3.12}$$

$$\begin{aligned} &X^{r_2,d_2}_{r_1,d_1} + X^{r_1,d_1}_{r_2,d_2} \geq 2 \cdot \left(P^{r_1}_{d_1,ij} + P^{r_2}_{d_2,ij} - 1 \right), \\ &\forall r_1, r_2 \in \mathbf{R}, d_1 \in \mathbf{F}_{r_1}, d_2 \in \mathbf{F}_{r_2}, (i,j) \in \mathbf{L} : r_1 \neq r_2 \text{ or } d_1 \neq d_2 \end{aligned} \tag{3.13}$$

$$\begin{aligned} &O^{r_1,d_1}_{r_2,d_2} + O^{r_2,d_2}_{r_1,d_1} = 1, \\ &\forall r_1, r_2 \in \mathbf{R}, d_1 \in \mathbf{F}_{r_1}, d_2 \in \mathbf{F}_{r_2} : r_1 \neq r_2 \text{ or } d_1 \neq d_2 \end{aligned} \tag{3.14}$$

$$\begin{aligned} &E^{r_2}_{d_2} - S^{r_1}_{d_1} \leq \Delta \cdot \left(O^{r_1,d_1}_{r_2,d_2} + 1 - X^{r_1,d_1}_{r_2,d_2} \right) - 1, \\ &\forall r_1, r_2 \in \mathbf{R}, d_1 \in \mathbf{F}_{r_1}, d_2 \in \mathbf{F}_{r_2} : r_1 \neq r_2 \text{ or } d_1 \neq d_2. \end{aligned} \tag{3.15}$$

Constraint (3.11) ensures that the number of required FSs with regard to the assigned MS is allocated to the lightpath of each SD pair. Constraint (3.12) ensures that the end FS index is equal to the start FS index plus the number of required FSs minus one. These two constraints guarantee spectrum continuity where the lightpath occupies the FSs from the start index to the end index in all the traversed links. Since the occupied FSs are contiguous, the spectrum contiguity constraint is also satisfied.

Constraints (3.13), (3.14), and (3.15) ensure the spectrum non-overlapping constraint where if two lightpaths share common link(s), the start FS index of one lightpath should be greater than the end FS index of the other. Here, the two lightpaths may be for the same multicast demand or different ones.

3.5.2 Light-Tree-Based MILP

Different from the lightpath scheme, the multi-light-tree scheme establishes a variable number of light-trees (a lightpath is a special case of a light-tree) for the optimal accommodation of a multicast demand. We introduce two new notations as follows.

Notations

$\mathbf{T}^r$ A set of transmitters that are available for multicast demand r.

α A weighting factor.

If $\mathbf{T}^r$ contains only one element, this light-tree-based MILP is for the light-tree scheme which uses only one light-tree for a multicast. When the input of $\mathbf{T}^r$ contains more elements, multiple light-trees can be used for a multicast, and this MILP applies to the multi-light-tree scheme.

Variables

$\mathbb{G}^r_{k,d}$ Binary; equals one if destination d, $d \in \mathbf{F}_r$, is covered by the light-tree using transmitter k of multicast demand r; zero, otherwise.

$\mathbb{U}^r_k$ Binary; equals one if transmitter k is used to support multicast demand r.

$\mathbb{H}^r_k$ Real; denotes a distance that is longer than or equal to the longest distance among all the paths included in the light-tree using transmitter k of multicast demand r.

$\mathbb{K}^r_{k,m}$ Binary; equals one if MS m, $m \in \mathbf{M}$, is assigned to the light-tree using transmitter k of multicast demand r; zero, otherwise.

$\mathbb{L}^r_{k,ij}$ Binary; equals one if link ij, $ij \in \mathbf{L}$, is assigned to the light-tree using transmitter k of multicast demand r; zero, otherwise.

$\mathbb{B}^{r,k}_{ij,m}$ Binary; equals one if MS m, $m \in \mathbf{M}$, is assigned to the light-tree sourcing from transmitter k of multicast demand r and this light-tree covers link ij; zero, otherwise.

$\mathbb{W}^r_k$ Integer; denotes the number of FSs required by the light-tree using transmitter k of multicast demand r, $\mathbb{W}^r_k \geq 0$.

$\mathbb{S}^r_k$ Integer; denotes the start index of the FSs required by the light-tree using transmitter k of multicast demand r, $\mathbb{S}^r_k \geq 1$.

$\mathbb{E}^r_k$ Integer; denotes the end index of the FSs required by the light-tree using transmitter k of multicast demand r; $\mathbb{E}^r_k \geq 1$.

$\mathbb{X}^{r_1,k_1}_{r_2,k_2}$ Binary; equals to one if the light-tree using transmitter k_1 of multicast demand r_1 and the light-tree using transmitter k_2 of multicast demand r_2 share common link(s).

$\mathbb{O}^{r_1,k_1}_{r_2,k_2}$ Binary; equals to zero if the indices of the FSs assigned to the light-tree using transmitter k_1 of multicast demand r_1 is greater than the indices of the FSs assigned to the light-tree using transmitter k_2 of multicast demand r_2 when the two light-trees share common link(s), i.e., $\mathbb{X}^{r_1,k_1}_{r_2,k_2} = 1$.

Objective

$$\textbf{min} \sum_{r \in \mathbf{R}} \sum_{(i,j) \in \mathbf{L}} N^r_{ij} + \alpha \cdot \sum_{r \in \mathbf{R}} \sum_{k \in \mathbf{T}^r} \mathbb{U}^r_k \tag{3.16}$$

In the light-tree-based MILP, we consider a multi-objective formulation where the total number of used FSs and the number of used transmitters is minimized. The

minimization of the used FSs takes a higher priority to make a fair comparison with the previous scheme by setting α to be a small fraction.

Constraints

Similar to the lightpath scheme, we also divide the constraints into five groups, namely, *tree grouping*, *tree construction*, *modulation determination*, *FS usage in links*, *spectrum allocation*. The first group ensures that for a given multicast, a destination receives the signal from only one tree. The second group is to guarantee that a tree structure for a multicast demand is constructed. The third group is to ensure that an MS is assigned to the light-tree to meet the requirement that the maximum distance from the source to the destinations does not exceed the transparent reach of the signal with the MS. The fourth group is to ensure that the number of FSs used in a link is the sum of the FSs used by all light-trees. The fifth group is to guarantee the three constraints in spectrum allocation.

1) Tree Grouping

$$\sum_{k \in \mathbf{T}^r} \mathbb{G}^r_{k,d} = 1, \quad \forall r \in \mathbf{R}, d \in \mathbf{F}_r \tag{3.17}$$

$$\mathbb{U}^r_k \geq \mathbb{G}^r_{k,d}, \quad \forall r \in \mathbf{R}, k \in \mathbf{T}^r, d \in \mathbf{F}_r \tag{3.18}$$

$$\mathbb{U}^r_k \leq \sum_{d \in \mathbf{F}_r} \mathbb{G}^r_{k,d}, \quad \forall r \in \mathbf{R}, k \in \mathbf{T}^r. \tag{3.19}$$

Constraint (3.17) ensures that a destination node receives the signal from the light-tree of one transmitter at the source node for a multicast demand. Constraints (3.18) and (3.19) ensure that the transmitter is used if there is a destination receiving signals from its light-tree.

2) Tree Construction

$$\mathbb{L}^r_{k,ij} \geq P^r_{d,ij} + \mathbb{G}^r_{k,d} - 1, \quad \forall r \in \mathbf{R}, k \in \mathbf{T}^r, d \in \mathbf{F}_r, (i,j) \in \mathbf{L} \tag{3.20}$$

$$\sum_{i \in \mathbf{V}:(i,j) \in \mathbf{L}} \mathbb{L}^r_{k,ij} \leq 1, \quad \forall r \in \mathbf{R}, k \in \mathbf{T}^r, j \in \mathbf{V}. \tag{3.21}$$

We reuse constraints (3.2) and (3.3) in the lightpath scheme to compute a path for each SD pair. Constraint (3.20) guarantees that every link of a path to a destination which receives signals from a transmitter is included in the light-tree. Constraint (3.21) ensures that a tree structure is formed by the paths by forcing a node in a tree to have only one parent node.

3) Modulation Determination

$$\sum_{m \in \mathbf{M}} \mathbb{K}^r_{k,m} = \mathbb{U}^r_k, \quad \forall r \in \mathbf{R}, k \in \mathbf{T}^r, d \in \mathbf{F}_r \tag{3.22}$$

$$\mathbb{H}^r_k + \Delta \geq D^r_d + \Delta \cdot \mathbb{G}^r_{k,d}, \quad \forall r \in \mathbf{R}, k \in \mathbf{T}^r, d \in \mathbf{F}_r \tag{3.23}$$

$$\tau^r_m - \mathbb{H}^r_k \geq \Delta \cdot \left(\mathbb{K}^r_{k,m} - 1\right), \quad \forall r \in \mathbf{R}, m \in \mathbf{M}, k \in \mathbf{T}^r. \tag{3.24}$$

Constraint (3.22) ensures that one MS is assigned to a light-tree if the associated transmitter is utilized. Constraint (3.4) in the lightpath method and constraints (3.23) and (3.24) ensure that the longest distance among the paths from the source to the destinations of a light-tree does not exceed the maximum reach of the assigned MS.

4) FS Usage in Links

$$N^r_{ij} = \sum_{k \in \mathbf{T}^r} \sum_{m \in \mathbf{M}} \mathbb{B}^{r,k}_{ij,m} \cdot (\omega^r_m + g), \quad \forall r \in \mathbf{R}, (i,j) \in \mathbf{L} \tag{3.25}$$

$$\mathbb{B}^{r,k}_{ij,m} \leq \mathbb{L}^{r}_{k,ij}, \quad \forall r \in \mathbf{R}, k \in \mathbf{T}^r, (i,j) \in \mathbf{L}, m \in \mathbf{M} \tag{3.26}$$

$$\mathbb{B}^{r,k}_{ij,m} \leq \mathbb{K}^{r}_{k,m}, \quad \forall r \in \mathbf{R}, k \in \mathbf{T}^r, (i,j) \in \mathbf{L}, m \in \mathbf{M} \tag{3.27}$$

$$\mathbb{B}^{r,k}_{ij,m} \geq \mathbb{K}^{r}_{k,m} + \mathbb{L}^{r}_{k,ij} - 1, \quad \forall r \in \mathbf{R}, k \in \mathbf{T}^r, (i,j) \in \mathbf{L}, m \in \mathbf{M}. \tag{3.28}$$

Constraint (3.25) ensures that the FSs in a link used by a multicast demand is the sum of the FSs used in the light-trees that include the link. We present the calculation procedure as follows.

$$\begin{aligned} N^{r}_{ij} &= \sum_{k \in \mathbf{T}^r} \mathbb{L}^{r}_{k,ij} \cdot \sum_{m \in \mathbf{M}} \mathbb{K}^{r}_{d,m} \cdot (\omega^{r}_{m} + g) \\ &= \sum_{k \in \mathbf{T}^r} \sum_{m \in \mathbf{M}} \mathbb{L}^{r}_{k,ij} \cdot \mathbb{K}^{r}_{d,m} \cdot (\omega^{r}_{m} + g) \\ &= \sum_{k \in \mathbf{T}^r} \sum_{m \in \mathbf{M}} \mathbb{B}^{r,k}_{ij,m} \cdot (\omega^{r}_{m} + g), \quad \forall r \in \mathbf{R}, (i,j) \in \mathbf{L} \end{aligned}$$

where $\mathbb{B}^{r,k}_{ij,m} = \mathbb{L}^{r}_{k,ij} \cdot \mathbb{K}^{r}_{k,m}$, which is a non-linear equation. Similar to the previous MILP, we also linearize this equation by constraints (3.26), (3.27), and (3.28).

5) Spectrum Allocation

$$\mathbb{W}^{r}_{k} = \sum_{m \in \mathbf{M}} \mathbb{K}^{r}_{k,m} \cdot (\omega^{r}_{m} + g), \quad \forall r \in \mathbf{R}, k \in \mathbf{T}^r \tag{3.29}$$

$$\mathbb{E}^{r}_{k} = \mathbb{S}^{r}_{k} + \mathbb{W}^{r}_{k} - 1, \quad \forall r \in \mathbf{R}, k \in \mathbf{T}^r \tag{3.30}$$

$$\begin{aligned} &\mathbb{X}^{r_2,k_2}_{r_1,k_1} + \mathbb{X}^{r_1,k_1}_{r_2,k_2} \geq 2 \cdot \left(\mathbb{L}^{r_1}_{k_1,ij} + \mathbb{L}^{r_2}_{k_2,ij} - 1 \right), \\ &\forall r_1, r_2 \in \mathbf{R}, k_1 \in \mathbf{T}^{r_1}, k_2 \in \mathbf{T}^{r_2}, (i,j) \in \mathbf{L} : r_1 \neq r_2 \text{ or } k_1 \neq k_2 \end{aligned} \tag{3.31}$$

$$\begin{aligned}&\mathbb{O}_{r_2,k_2}^{r_1,k_1}+\mathbb{O}_{r_1,k_1}^{r_2,k_2}=1,\\&\qquad\forall r_1,r_2\in\mathbf{R},k_1\in\mathbf{T}^{r_1},k_2\in\mathbf{T}^{r_2}:r_1\neq r_2 \text{ or } k_1\neq k_2\end{aligned}\tag{3.32}$$

$$\begin{aligned}&\mathbb{E}_{k_2}^{r_2}-\mathbb{S}_{k_1}^{r_1}\leq\Delta\cdot\left(\mathbb{O}_{r_2,k_2}^{r_1,k_1}+3-\mathbb{U}_{k_1}^{r_1}-\mathbb{U}_{k_2}^{r_2}-\mathbb{X}_{r_2,k_2}^{r_1,k_1}\right)-1,\\&\qquad\forall r_1,r_2\in\mathbf{R},k_1\in\mathbf{T}^{r_1},k_2\in\mathbf{T}^{r_2}:r_1\neq r_2 \text{ or } k_1\neq k_2.\end{aligned}\tag{3.33}$$

Constraint (3.29) ensures that the number of FSs corresponding to the assigned MS is allocated to a light-tree. Constraint (3.30) ensures that the end FS index is equal to the start FS index plus the number of the allocated FSs minus one. Similar to the lightpath scheme, constraints (3.29) and (3.30) ensure the spectrum continuity and the spectrum contiguity. Constraints (3.31), (3.32), and (3.33) guarantee that the spectrum non-overlapping constraint is satisfied. If two light-trees share common link(s), the start index of the FSs used by one light-tree is greater than the end index of FSs used by the other. This applies to both cases where the two light-trees are for the same multicast demand and different ones.

3.5.3 Light-Trail-Based MILP

We reuse some variables and constraints in the light-tree-based MILP by replacing "light-tree" by "light-trail" in the definitions of the notations and variables, and the descriptions of the constraints. The MILP presented here applies to both the light-trail and multi-light-trail schemes by adjust the input of $\mathbf{T}^r$ in the same way as discussed in the previous MILP. Also, two new variables and some new constraints are introduced as follows.

Variables

$\mathbb{F}^r_{k,ij}$ Integer; denotes the number of flows of light-trail k via link ij, $ij \in \mathbf{L}$, of multicast demand r; $0 \leq \mathbb{F}^r_{k,ij} \leq |\mathbf{F}_r|$. In other words, it equals the number of destinations receiving the signal of light-trail k transmitted via link ij.

$\mathbb{D}^r_k$ Real; denotes the length of light-trail k of multicast r; $\mathbb{D}^r_k \geq 0$.

Objective

The objective is the same as the one presented for the light-tree-based scheme, i.e., objective (3.16).

Constraints

The constraints can also be divided into six groups, namely, *flow conservation*, *trail construction*, *modulation determination*, *trail grouping*, *FS usage in links*, and *spectrum allocation*. The first group ensures flow conservation for a multicast. The second group ensures a trail structure for routing the flows. The modulation determination group guarantees that the distance of a light-trail does not exceed the transparent reach of the assigned modulation. For the fourth group, we reuse the constraints (3.17), (3.18), and (3.19) to ensure that each destination of a multicast is covered by a light-trail. The fifth group ensures that for each link, the FS usage is the sum of the FSs assigned to the light-trail(s), where we reuse the constraints (3.25), (3.26), (3.27), and (3.28). Finally, the sixth group ensures the spectrum continuity, contiguity, and non-overlapping constraints for light-trails in the spectrum allocation, where we utilize the constraints (3.29), (3.30), (3.31), (3.32), and (3.33).

1) Flow Conservation

$$\sum_{k \in \mathbf{T}^r} \left(\sum_{(s_r,j) \in \mathbf{L}} \mathbb{F}^r_{k,s_r j} - \sum_{(i,s_r) \in \mathbf{L}} \mathbb{F}^r_{k,i s_r} \right) = |\mathbf{F}_r|, \quad \forall r \in \mathbf{R} \tag{3.34}$$

$$\sum_{(s_r,j)\in\mathbf{L}} \mathbb{F}^r_{k,s_rj} - \sum_{(i,s_r)\in\mathbf{L}} \mathbb{F}^r_{k,is_r} = \sum_{d\in\mathbf{F}_r} \mathbb{G}^r_{k,d}, \quad \forall r \in \mathbf{R}, k \in \mathbf{T}^r \tag{3.35}$$

$$\sum_{(x,j)\in\mathbf{L}} \mathbb{F}^r_{k,xj} = \sum_{(i,x)\in\mathbf{L}} \mathbb{F}^r_{k,ix}, \quad \forall r \in \mathbf{R}, k \in \mathbf{T}^r, x \in \mathbf{V} \setminus \mathbf{F}_r : x \neq s_r \tag{3.36}$$

$$\mathbb{G}^r_{k,x} + \sum_{(x,j)\in\mathbf{L}} \mathbb{F}^r_{k,xj} = \sum_{(i,x)\in\mathbf{L}} \mathbb{F}^r_{k,ix}, \quad \forall r \in \mathbf{R}, k \in \mathbf{T}^r, x \in \mathbf{F}_r. \tag{3.37}$$

Constraints (3.34), (3.35), (3.36), and (3.37) guarantees commodity flow conservation of a multicast. Constraint (3.34) ensures that the number of egress flows via all transmitters at the source equals to the number of destinations of a multicast. Constraints (3.35) ensures that for each light-trail, the number of egress flows at the source equals to the number of ingress flows plus the number of destinations receiving the signal. Constraint (3.36) guarantees that for each light-trail, the number of ingress flows at an intermediate node, i.e., neither the source or a destination, is equal to the number of egress flows. Constraint (3.37) ensures that for every light-trail, the number of ingress flows at a destination is equal to the number of egress flows plus one, if the destination receives the signal of the light-trail, otherwise the two numbers are equal.

2) Trail Construction

$$|\mathbf{F}_r| \cdot \mathbb{L}^r_{k,ij} \geq \mathbb{F}^r_{k,ij}, \quad \forall r \in \mathbf{R}, k \in \mathbf{T}^r, (i,j) \in \mathbf{L} \tag{3.38}$$

$$\mathbb{L}^r_{k,ij} \leq \mathbb{F}^r_{k,ij}, \quad \forall r \in \mathbf{R}, k \in \mathbf{T}^r, (i,j) \in \mathbf{L} \tag{3.39}$$

$$\sum_{(s_r,j)\in\mathbf{L}} \mathbb{L}^r_{k,s_rj} = \mathbb{U}^r_k + \sum_{(i,s_r)\in\mathbf{L}} \mathbb{L}^r_{k,is_r}, \quad \forall r \in \mathbf{R}, k \in \mathbf{T}^r \tag{3.40}$$

$$\sum_{(x,j)\in\mathbf{L}} \mathbb{L}^r_{k,xj} = \sum_{(i,x)\in\mathbf{L}} \mathbb{L}^r_{k,ix}, \quad \forall r \in \mathbf{R}, k \in \mathbf{T}^r, x \in \mathbf{V} \setminus \mathbf{F}_r : x \neq s_r \tag{3.41}$$

$$\sum_{(d,j)\in\mathbf{L}} \mathbb{L}^r_{k,dj} \leq \sum_{(i,d)\in\mathbf{L}} \mathbb{L}^r_{k,id}, \quad \forall r \in \mathbf{R}, k \in \mathbf{T}^r, d \in \mathbf{F}_r \tag{3.42}$$

$$\mathbb{U}^r_k + \sum_{d\in\mathbf{F}_r} \sum_{(d,j)\in\mathbf{L}} \mathbb{L}^r_{k,dj} = \sum_{d\in\mathbf{F}_r} \sum_{(i,d)\in\mathbf{L}} \mathbb{L}^r_{k,id}, \quad \forall r \in \mathbf{R}, k \in \mathbf{T}^r, d \in \mathbf{F}_r. \tag{3.43}$$

Constraints (3.38), (3.39), (3.40), (3.41), (3.42), and (3.43) guarantee that a trail is constructed. Constraints (3.38) and (3.39) ensure that a link belongs to a light-trail if the link is used to carry the signal. Constraint (3.40) ensures that if a light-trail is active or utilized, the number of egress links at the source equals to the number of ingress links plus one, otherwise, the two numbers are the same. Constraint (3.41) guarantees that the numbers of ingress and egress links are equal at an intermediate node. Constraint (3.42) ensures that the number of ingress links at a destination is greater than or equal to the number of egress links. Constraint (3.43) guarantees that if a light-tree is active, the trail ends at one of the destinations where the number of ingress links equals to the number of egress link plus one.

3) Modulation Determination

$$\mathbb{D}^r_k = \sum_{(i,j)\in\mathbf{L}} \left(\ell_{ij} \cdot \mathbb{L}^r_{k,ij}\right), \quad \forall r \in \mathbf{R}, k \in \mathbf{T}^r \tag{3.44}$$

$$\tau^r_m - \mathbb{D}^r_k \geq \Delta \cdot \left(\mathbb{K}^r_{k,m} - 1\right), \quad \forall r \in \mathbf{R}, m \in \mathbf{M}, k \in \mathbf{T}^r. \tag{3.45}$$

Constraints (3.44), (3.22), and (3.45) guarantees that an MS is assigned to an active light-trail with a transmission distance bounded by the transparent reach. Constraint (3.44) guarantees that the distance of a trail is the sum of the lengths of the links that belong to the trail. We reuse the constraint (3.22) to guarantee that an

Table 3.2 MILP Problem Sizes

	Number of Variables	Number of Constraints
Lightpath-Based	$O\begin{pmatrix}\|\mathbf{R}\|\|\bar{\mathbf{F}}\|\|\mathbf{L}\|\|\mathbf{M}\| \\ +\|\mathbf{R}\|^2\|\bar{\mathbf{F}}\|^2\end{pmatrix}$	$O\begin{pmatrix}\|\mathbf{R}\|\|\bar{\mathbf{F}}\|\|\mathbf{L}\|\|\mathbf{M}\| \\ +\|\mathbf{R}\|^2\|\bar{\mathbf{F}}\|^2\|\mathbf{L}\|\end{pmatrix}$
Light-Tree-Based	$O\begin{pmatrix}\|\mathbf{R}\|\|\mathbf{L}\|(\|\bar{\mathbf{F}}\|+\|\bar{\mathbf{T}}\|\|\mathbf{M}\|) \\ +\|\mathbf{R}\|^2\|\bar{\mathbf{T}}\|^2\end{pmatrix}$	$O\begin{pmatrix}\|\mathbf{R}\|\|\bar{\mathbf{T}}\|\|\mathbf{L}\|\left(\|\mathbf{M}\|+\|\bar{\mathbf{F}}\|\right) \\ +\|\mathbf{R}\|^2\|\bar{\mathbf{T}}\|^2\|\mathbf{L}\|\end{pmatrix}$
Light-Trail-Based	$O\begin{pmatrix}\|\mathbf{R}\|\|\mathbf{L}\|(\|\bar{\mathbf{F}}\|+\|\bar{\mathbf{T}}\|\|\mathbf{M}\|) \\ +\|\mathbf{R}\|^2\|\bar{\mathbf{T}}\|^2\end{pmatrix}$	$O\begin{pmatrix}\|\mathbf{R}\|\|\bar{\mathbf{T}}\|\|\mathbf{L}\|\|\mathbf{M}\| \\ +\|\mathbf{R}\|^2\|\bar{\mathbf{T}}\|^2\|\mathbf{L}\|\end{pmatrix}$

MS is assigned to a light-trail if it is active. Constraint (3.45) ensures that the trail distance cannot exceed the transparent reach of the assigned MS.

3.5.4 MILP Problem Sizes

We present the problem sizes of the three MILP formulations in terms of dominant numbers of variables and constraints as shown in Table 3.2. The notations used in the table, namely, $|\mathbf{R}|$, $|\mathbf{L}|$, $|\mathbf{M}|$, $|\bar{\mathbf{F}}|$, and $|\bar{\mathbf{T}}|$, are the numbers of demands, network links, considered MSs, and the average numbers of destinations and transmitters available per demand, respectively.

3.6 Numerical Results

We have presented the MILP formulations for the five provisioning schemes, namely, lightpath, light-tree, multi-light-tree, light-trail, and multi-light-trail. We aim to compare the schemes by the total spectrum usage for provisioning a single multicast demand, although the presented MILPs can be applied for the case of multiple demands. Since we examine the minimum total spectrum consumption, we consider networks with unlimited capacity, the spectrum continuity and contiguity constraints are relaxed in this chapter as they do not affect the optimal results. However these constraints will be utilized in the following chapter.

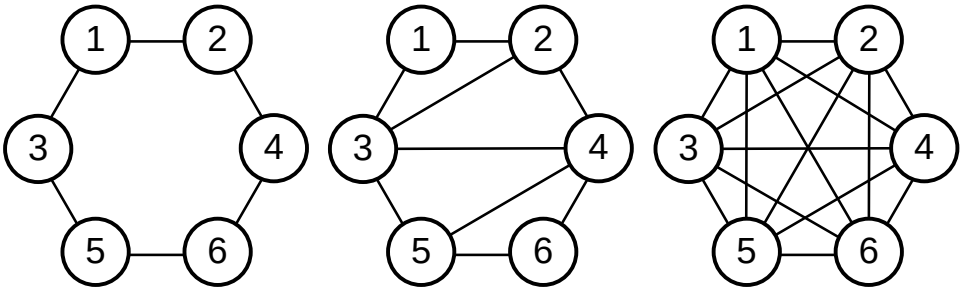

(a) (b) (c)

Fig. 3.6 Six-node networks: (a) N6S6; (b) N6S9; (c) N6S15.

Table 3.3 Link Lengths of the Six-Node Networks

Link	Length [km]	Link	Length [km]	Link	Length [km]
(1,2)	780	(5,6)	780	(3,6)	1450
(2,1)	780	(6,5)	780	(6,3)	1450
(1,3)	780	(1,4)	1450	(4,5)	1450
(3,1)	780	(4,1)	1450	(5,4)	1450
(2,4)	780	(1,5)	1450	(6,1)	2050
(4,2)	780	(5,1)	1450	(1,6)	2050
(3,5)	780	(2,3)	1450	(2,5)	2050
(5,3)	780	(3,2)	1450	(5,2)	2050
(6,4)	780	(2,6)	1450	(3,4)	2050
(4,6)	780	(6,2)	1450	(4,3)	2050

3.6.1 Test Conditions

We consider the three six-node networks as shown in Fig. 3.6, namely, six-link (N6S6) network, nine-link (N6S9) network, 15-link (N6S15) network. The link lengths of the six-node networks can be found in Table 3.3. We also consider two realistic networks that are used in many publications, namely, 11-node 26-link COST239 network [6] and 24-node 43-link USNET [7] as shown in Fig. 3.7. The numbers beside the links in the figure are the link lengths in kilometers. We consider a single multicast demand. Without loss of generality, the source and destinations of a demand are selected randomly. We investigate the impact of different multicast session sizes, i.e., numbers of destinations on the performance comparison. For each size, 100 experiments are conducted for randomly generated demands. We obtain a

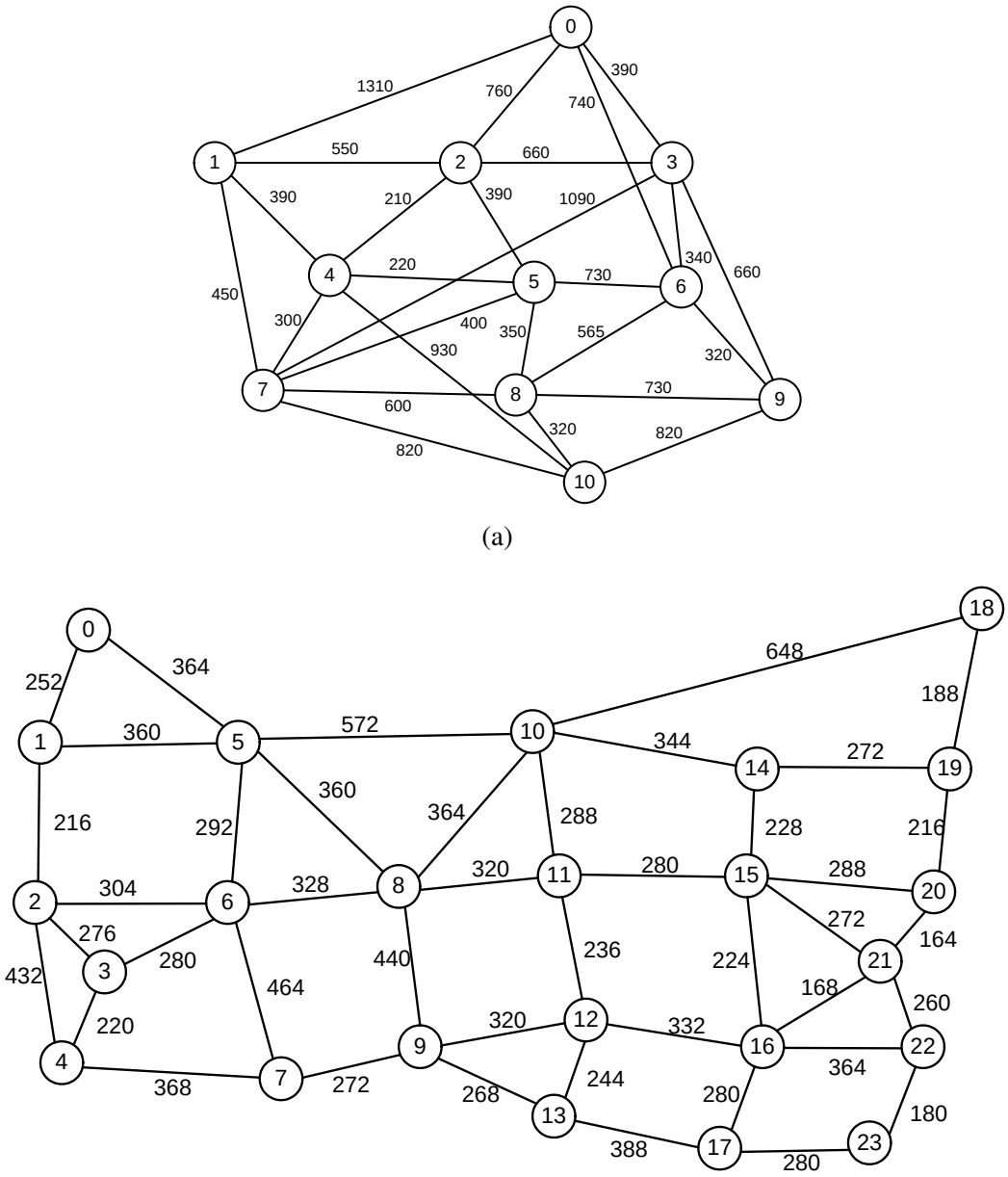

(a)

(b)

Fig. 3.7 Real-size networks: (a) COST239 [6]; (b) USNET [7].

value for each experiment and take the average of the values as the result. Assume that all the demands request a bit rate of 100 Gb/s. For the case of distance-adaptive resource allocation, we consider three MSs, and as shown in Table 3.4 each demand has spectrum requirements of eight, four, and three FSs with transparent reaches of 4,000 km, 2,000 km, 1,000 km when it is modulated by BPSK, QPSK, and 8QAM,

Table 3.4 The Requirements of FSs and Transparent Reach for a 100-Gb/s Signal Using Different MSs

Bit Rate	Modulation Level	MS	Number of Required FSs	Transparent Reach [km]
100 Gb/s	1	BPSK	8	4,000
	2	QPSK	4	2,000
	3	8QAM	3	1,000

respectively. We also consider a case with no distance-adaptive spectrum allocation which means that demands requesting for the same data rate require the same amount of spectrum. For this case, only one modulation is available for the demands, i.e., BPSK, for all the considered networks. Also, to guarantee the quality of transmission, the distances of the connections are limited by 4,000 km due to the modulation used. The optimal results are provided by a commercial solver, i.e., Gurobi [145], solving the MILPs.

3.6.2 Network Cases with Distance-Adaptive Transmission

The N6S6 Network

The performances of the five provisioning schemes are compared for the N6S6 network as shown in Fig. 3.8. We compare their spectrum usage, transmitter usage, and utilized modulation levels.

Figure 3.8a shows the comparison of total spectrum usage among the five schemes. We can see in the figure, with the increase of the multicast session size, i.e., the number of destinations, the total spectrum usage goes up for all cases. On average, the light-trail and lightpath schemes present the highest spectrum usage, the light-tree follows, and the multi-light-trail and multi-light-tree approaches use the least spectrum. Compared to the lightpath scheme, the light-trail uses 6.2% more spectrum while the light-tree achieves about 16% spectrum savings. By employing additional transmitters, the multi-light-trail and multi-light-tree schemes reduce the

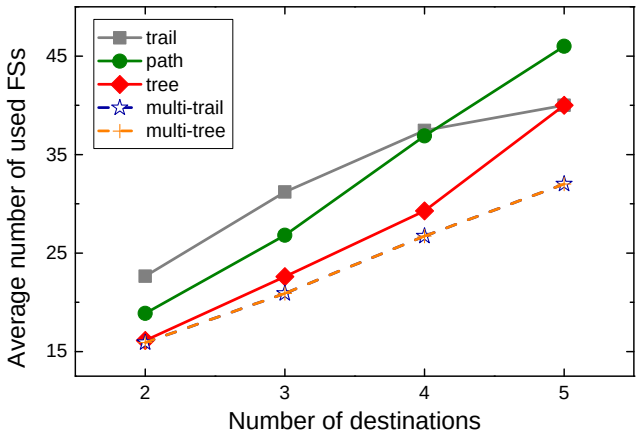

(a)

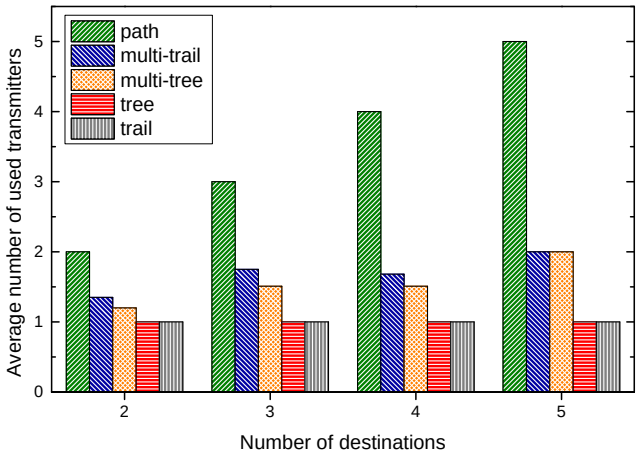

(b)

Fig. 3.8 Resource usage of the five schemes for the N6S6 network in terms of: (a) used FSs; (b) used transmitters.

spectrum consumption by around 28% and 9.4% compared to the light-trail and light-tree schemes, respectively. Moreover, when the multicast session grows bigger, the multi-light-tree scheme achieves increased percentage of reduction of consumed spectrum compared to the light-tree, while the multi-light-trail scheme shows a decrease of percentage of reduction compared to the light-trail method. This is because for the light-tree, the level of used MS decreases as covering more destination extends the transmission distance, while the light-trail has a higher possibility that it contains cycles for the case of small multicast session sizes due to the ring topology of the network.

For the lightpath and light-trail methods, when the multicast session size is small, the former outperforms the latter, while for the case of broadcast, the latter is better than the former in terms of spectrum usage. This is because when the multicast size is large, the lightpath scheme suffers from extensive overlap among the paths leading to considerable spectrum usage, while for small multicast sizes, a single light-trail covering all the destinations usually contains cycles leading to additional spectrum allocation and also extended distance and therefore excessive spectrum usage as discussed in Section 3.3.4. However, this is not the case for a light-tree. In a light-tree, the signal copies are distributed to multiple egress links without cycles, and also the bandwidth of the tree trunk is shared by destinations presenting benefits over the light-trail.

Both the multi-light-tree and multi-light-trail schemes use the same amount of spectrum achieving a 24% reduction over the lightpath scheme. There are two reasons to explain this. One is that as discussed in Section 3.3.4, for any light-trail associated with a multicast connection in a network that contains multicast-incapable nodes, there is an equivalent light-tree in the corresponding MC network so that a multi-light-trail solution does not consume less spectrum than the corresponding multi-light-tree scheme. The other reason is that omitting the transmitter usage, for any light-tree in a multi-light-tree solution in an MC network of this ring topology, there is an equivalent light-trail-based solution with possibly multiple light-trails in the corresponding multicast-incapable network of the same topology. In the ring network, a light-tree has two cases. One case is to traverse its nodes via a clockwise/counterclockwise path where the intermediate node, if it is a destination, performs light splitting to drop a signal copy; the other case is to split its signal at the source into two copies transmitted via the clockwise and counterclockwise paths, respectively. For the former case, the light-trail using the same path can also be used to support the transmission, while the intermediate destination nodes, if existed, tap the signal for local use. For the latter case, two light-trails along the two paths are

Table 3.5 Average Level of Used Modulation by the Five Schemes in the N6S6 Network

Multicast Session Size	Lightpath	Multi-Light-Trail	Multi-Light-Tree	Light-Tree	Light-Trail
2	2.175	1.74	1.74	1.64	1.23
3	2.216667	1.855	1.855	1.45	1
4	2.2125	1.68	1.68	1.17	1
5	2.2	1.5	1.5	1	1

used to support the transmission. These also make the light-trail especially suitable for ring networks [146]. In this regard, the multi-light-trail method will achieve the same spectrum consumption as the multi-light-tree at the cost of employing more transmitters.

As shown in Fig. 3.8b, for transmitter usage, the light-trail and light-tree methods use only one transmitter, while the lightpath scheme uses the most transmitters, which equal to the number of destinations of a multicast. The multi-light-tree and multi-light-trail approaches have a moderate usage of transmitters, with the latter having a slightly higher usage than the former. This is because in this ring network, the multi-light-tree scheme may use a single light-tree that splits signal at the source and transmit the signal copies via two directions, clockwise and counterclockwise while the multi-light-trail scheme will need two light-trails for this case.

Table 3.5 also presents the average level of modulation used by the schemes. The lightpath scheme uses the highest level modulations, the multi-light-trail and multi-light-tree rank second, and then the light-tree scheme, while the light-trail using the lowest-level modulation.This can be explained by the fact that the lightpaths use short paths to reach their destinations, while a light-trail transmits the signal via a trail to cover all the destinations resulting in a long distance, hence low-level modulation usage. Compared to the light-trail, the light-tree has a shorter transmission distance. Also, the multi-light-trail and multi-light-tree schemes use multiple transmitters as denoted in Fig. 3.8b and each covers part of the destinations with a short distance.

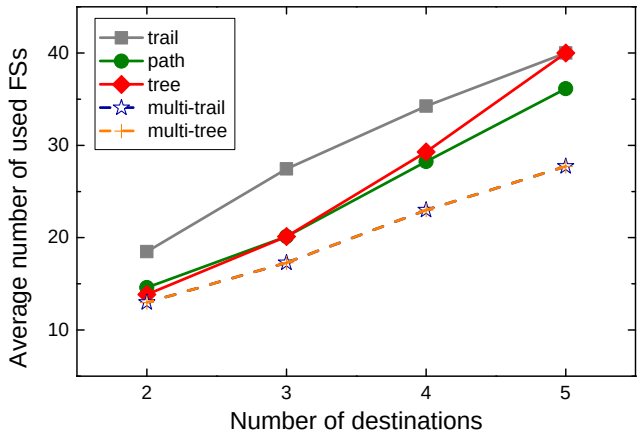

(a)

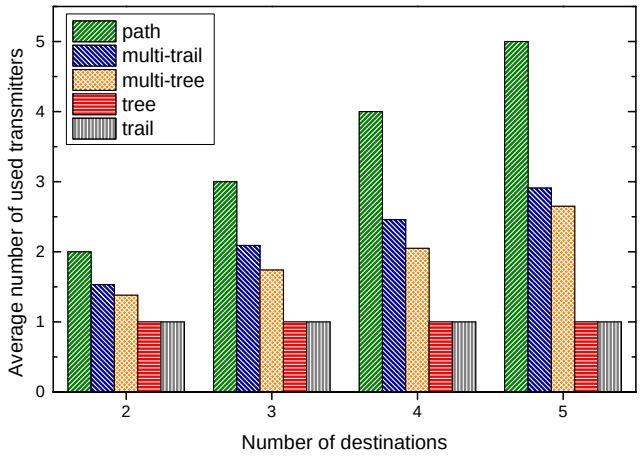

(b)

Fig. 3.9 Resource usage of the five schemes for the N6S9 network in terms of: (a) used FSs; (b) used transmitters.

The N6S9 Network

Figure 3.9 shows the comparison of the five provisioning schemes for the N6S9 network. As shown in Fig. 3.9a, on average, the light-trail approach has the highest spectrum usage, the light-tree and lightpath schemes follow, while the multi-light-trail and multi-light-tree approaches use the least spectrum. Compared to the lightpath scheme, the light-trail scheme consumes about 24% more spectrum, while the light-tree scheme consumed 2.3% more spectrum. This is because the modulation used in the light-trail and light-tree schemes is low, resulting in excessive spectrum

Table 3.6 Average Level of Used Modulation by the Five Schemes in the N6S9 Network

Multicast Session Size	Lightpath	Multi-Light-Trail	Multi-Light-Tree	Light-Tree	Light-Trail
2	2.175	1.875	1.875	1.64	1.23
3	2.216667	1.94	1.925	1.45	1
4	2.2125	1.940833	1.895	1.17	1
5	2.2	1.825	1.825	1	1

usage. Furthermore, the lightpaths can reach their destinations in fewer hops for the N6S9 network which is denser than the N6S6. Compared to the light-trail and light-tree schemes, the multi-light-trail and multi-light-tree schemes achieve 33% and 18% reductions of spectrum consumption at the cost of higher transmitter usage, respectively, resulting in about a 17% reduction as compared to the lightpath method. Different from the N6S6 network, the percentage reduction achieved by the multi-light-trail scheme over the light-trail is more stable over the multicast session size in the N6S9 network, since the present network is denser than the N6S6 network and the possibility of light-trails containing cycles decreases.

The N6S9 network has similar observations of transmitter usages as shown in Fig. 3.9b to the N6S6 network. Compared to the N6S6 network, the multi-light-trail and multi-light-tree schemes use more transmitters in the N6S9 network because of its higher network density. The modulation usage is shown in Table 3.6. The multi-light-trail scheme uses a higher modulation level than the multi-light-tree as it uses more transmitters in this denser network.

The N6S15 Network

We also show the comparison of the five provisioning schemes for the fully-mesh N6S15 network in Fig. 3.10. We can see in Fig. 3.10a that the light-trail scheme shows the highest spectrum consumption, and then the light-tree, while the light-path, multi-light-trail and multi-light-tree approaches have the least spectrum usage.

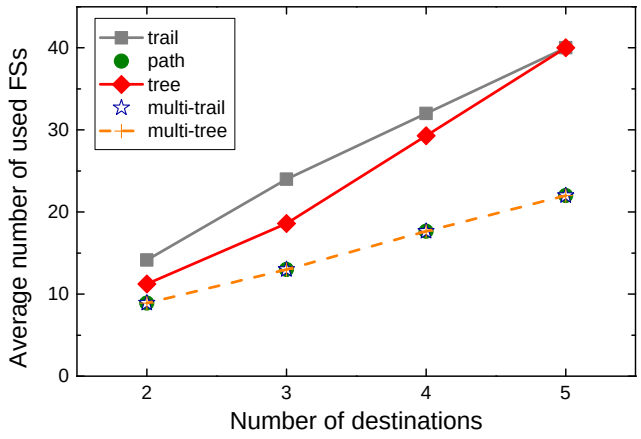

(a)

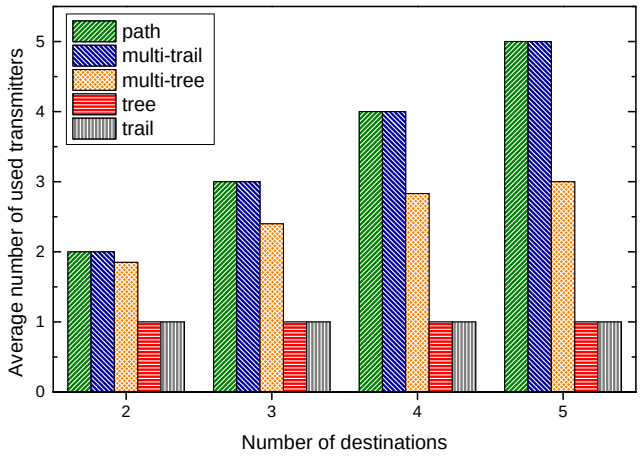

(b)

Fig. 3.10 Resource usage of the five schemes for the N6S15 network in terms of: (a) used FSs; (b) used transmitters.

Compared to the lightpath scheme, on average, the light-trail and light-tree schemes utilize 77% and 54% more spectrum, respectively, while the multi-light-trail and multi-light-tree methods have the same spectrum usage as the lightpath scheme. This is due to the completeness of the network, the lightpaths reach the destinations by only one hop.

For the transmitter usage as shown in Fig. 3.10b, we can see that the multi-light-trail scheme uses the same number of transmitters as the lightpath scheme. This means that the multi-light-trail method provides solutions which are a special case containing only lightpaths from the source to their destinations. However, the multi-

Table 3.7 Average Level of Used Modulation by the Five Schemes in the N6S15 Network

Multicast Session Size	Lightpath	Multi-Light-Trail	Multi-Light-Tree	Light-Tree	Light-Trail
2	2.175	2.175	2.175	1.64	1.23
3	2.216667	2.216667	2.185	1.45	1
4	2.2125	2.2125	2.085	1.17	1
5	2.2	2.2	2	1	1

light-tree approach still has a moderate transmitter usage thanks to the multicasting capability. Table 3.7 shows the comparison of the modulation used, the N6S15 network showing observations similar to the one found for the N6S9 network. The difference is that for the present N6S15 network, the multi-light-trail scheme has the same modulation usage as the lightpath scheme as both schemes provide the same solution.

The COST239 Network

Figure 3.11 compares the resource usage of the five provisioning schemes for the COST239 network. The comparison of the total spectrum usage is as shown in Fig. 3.11a. Note that we do not present the results for some cases because of their long running times due to the high computation complexity of the MILP or because of the infeasibility that their transmission distances exceed the reaches of the MSs. The light-trail scheme consumes the most spectrum, followed by the lightpath scheme, then the light-tree and multi-light-trail schemes, while the multi-light-tree approach achieves the least spectrum usage. Compared to the lightpath scheme, the light-trail scheme consumes 33% more spectrum averaged over the multicast sizes two, four, and six due to significant low level of modulation used as shown in Table 3.8, while the light-tree scheme achieves 24% reduction of spectrum consumption. The percentage of spectrum savings of the multi-light-tree scheme is small, i.e., 7.8%, over the light-tree scheme as the multi-light-tree has low transmitter usage as shown

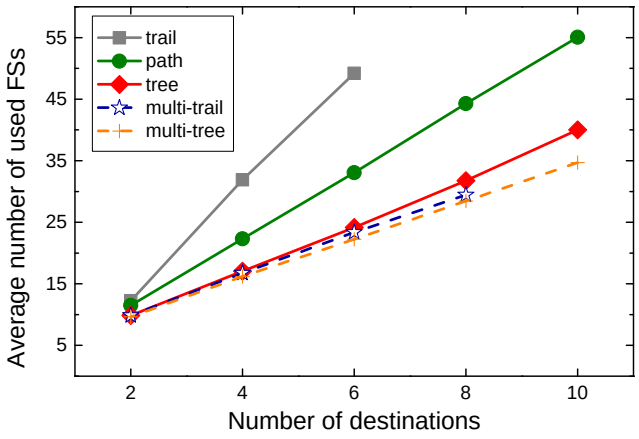

(a)

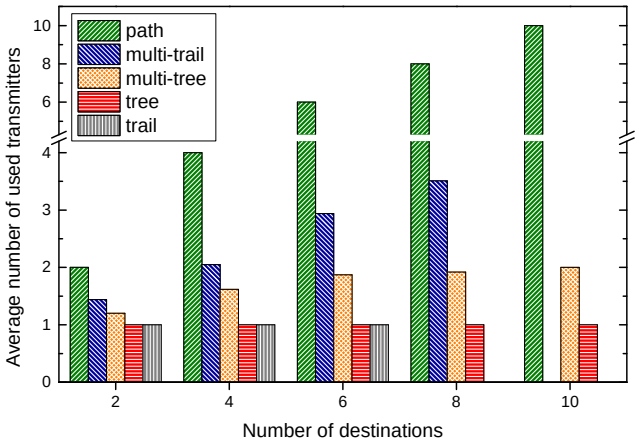

(b)

Fig. 3.11 Resource usage of the five schemes for the COST239 network in terms of: (a) used FSs; (b) used transmitters.

in Fig. 3.11b. This is because most of the paths to the destinations use the same modulation and these paths are supported by only one transmitter. Compared to the light-trail scheme, the multi-light-trail scheme saves 40% spectrum averaged over the three cases of the multicast session sizes. This is achieved by employing more transmitters and the usage of a relatively high level MS as shown in Fig. 3.11b and Table 3.8, respectively.

Table 3.8 Average Level of Used Modulation by the Five Schemes in the COST239 Network

Multicast Session Size	Lightpath	Multi-Light-Trail	Multi-Light-Tree	Light-Tree	Light-Trail
2	2.59	2.55	2.47	2.38	2.09
4	2.6425	2.398333	2.48	2.2	1.27
6	2.615	2.443	2.495	2.09	1
8	2.62	2.438	2.49	2.03	infeasible
10	2.618	-	2.5	2	infeasible

The USNET Network

For the USNET network, we also compare the approaches as shown in Fig. 3.12. We provide results of the light-trail scheme only for multicast session sizes up to five since the distance exceeds the transparent reaches of the MSs considered. Also, we do not present some of the results of the multi-light-trail and multi-light-tree schemes as these experiments required over 10 hours of computation. As shown in Fig. 3.12a, the light-trail scheme has the highest spectrum consumption, then the lightpath, and the multi-light-trail, light-tree and multi-light-tree schemes use the least spectrum. Compared to the lightpath scheme, the light-tree scheme achieves on average 47% reduction of spectrum consumption. Also, we see in the figure that the light-tree scheme performs better than the multi-light-trail scheme, and achieves performance close to that of the multi-light-tree scheme. This can be explained by the fact that a light-tree for a multicast provides considerable spectrum sharing among the transmissions to the destinations in sparse networks like the USNET network. The transmitter usage and level of modulation used are presented in Fig. 3.12b and Table 3.9, respectively.

Running Time

We also provide the running times of the MILP algorithms as shown in Tables 3.10 and 3.11 for the COST239 and USNET networks, respectively. Here the running

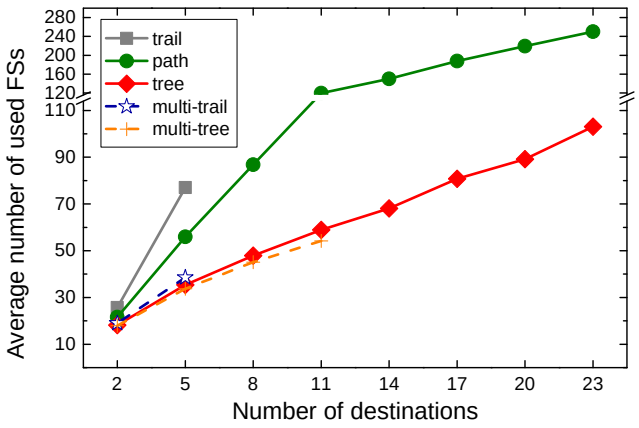

(a)

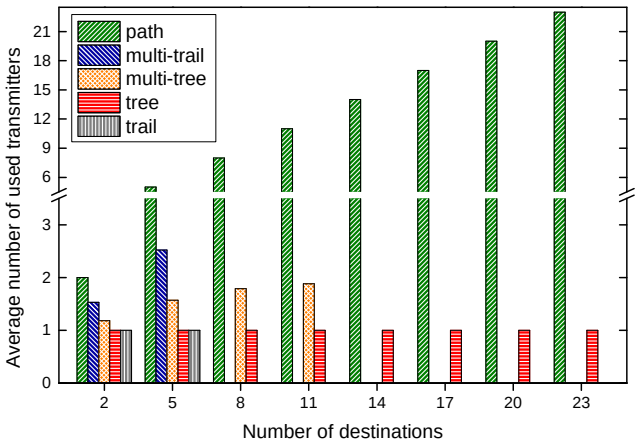

(b)

Fig. 3.12 Resource usage of the five schemes for the USNET network in terms of: (a) used FSs; (b) used transmitters.

time returned by the parameter "_solve_time" in [147] includes both system and user CPU seconds. For the lightpath, light-tree and light-trail schemes, the MILP is solved in seconds. Please note that for the light-trail scheme, some of the running time values are not shown due to the infeasibility where the transmission distance of a single light-trail covering all the destinations exceeds the transparent reaches of all considered MSs. Compared to the former three methods, the multi-light-trail and multi-light-tree schemes require significantly more time due to the increased computational complexity by allowing variable transmitter usage.

Table 3.9 Average Level of Used Modulation by the Five Schemes in the USNET network

Multicast Session Size	Lightpath	Multi-Light-Trail	Multi-Light-Tree	Light-Tree	Light-Trail
2	2.565	2.43	2.415	2.32	1.95
5	2.568	2.361667	2.325	2.02	1.04
8	2.5925	-	2.365	1.97	infeasible
11	2.59	-	2.375	1.92	infeasible
14	2.585	-	-	1.91	infeasible
17	2.582352941	-	-	1.87	infeasible
20	2.594	-	-	1.9	infeasible
23	2.580869565	-	-	1.88	infeasible

Table 3.10 Comparison of Running Times in Units of Seconds by the Five Schemes in the COST239 Network

Multicast Session Size	Lightpath	Multi-Light-Trail	Multi-Light-Tree	Light-Tree	Light-Trail
2	0.10	1.61	2.34	0.07	0.24
4	0.17	10.03	15.65	0.15	0.69
6	0.22	74.44	72.19	0.19	0.65
8	0.24	233.13	598.78	0.15	-
10	0.29	-	3990.84	0.15	-

Table 3.11 Comparison of Running Times in Units of Seconds by the Five Schemes in the USNET Network

Multicast Session Size	Lightpath	Multi-Light-Trail	Multi-Light-Tree	Light-Tree	Light-Trail
2	0.26	3.60	2.39	0.52	0.60
5	0.23	493.09	53.80	0.51	1.20
8	0.34	-	1070.21	0.61	-
11	0.56	-	7208.87	0.69	-
14	0.73	-	-	0.58	-
17	0.96	-	-	0.57	-
20	1.30	-	-	0.56	-
23	1.49	-	-	0.61	-

Table 3.12 Comparison of the Five Schemes for Provisioning a Multicast Demand

	Transmitter Usage	Modulation Level Usage	Spectrum Usage
Lightpath	High	High	Medium (dense network)/ High (sparse network)
Light-Tree	Low	Low	High (dense network)/ Medium (sparse network)
Multi-Light-Tree	Medium	Medium	Lowest
Light-Trail	Low	Low	Highest
Multi-Light-Trail	Medium	Medium	Low

We summarize the comparison of the five schemes for the provision of a single multicast demand in EONs considering distance-adaptive spectrum allocation as shown in Table 3.12. For the transmitter usage, the lightpath scheme always has the highest usage, the light-tree and light-trail schemes use only one transmitter achieving the least usage, and the multi-light-trail and multi-light-tree schemes have a medium transmitter usage. For the modulation usage, the lightpath scheme uses modulation of the highest-level, the multi-light-tree and multi-light-trail methods follow, and the light-tree method uses the lowest-level modulation. Moreover, for the spectrum usage, the multi-light-tree scheme always achieves the lowest spectrum consumption for all the considered network cases, while the multi-light-trail method uses slightly more spectrum. Compared to the light-tree scheme, the lightpath approach achieves reduced spectrum consumption when the network is densely connected, however, for sparse networks, the light-tree scheme outperforms the lightpath. Moreover, the light-trail scheme consumes the most spectrum due to the utilization of low-level modulation for a long trail covering all destinations.

3.6.3 Network Cases without Distance-Adaptive Transmission

We also compare the five schemes when no distance-adaptive spectrum allocation is used. We assume that all network cases use a fixed MS, i.e., BPSK, for all connections with a limitation of 4,000 km on the transmission distances. Fig. 3.13, 3.14, 3.15,

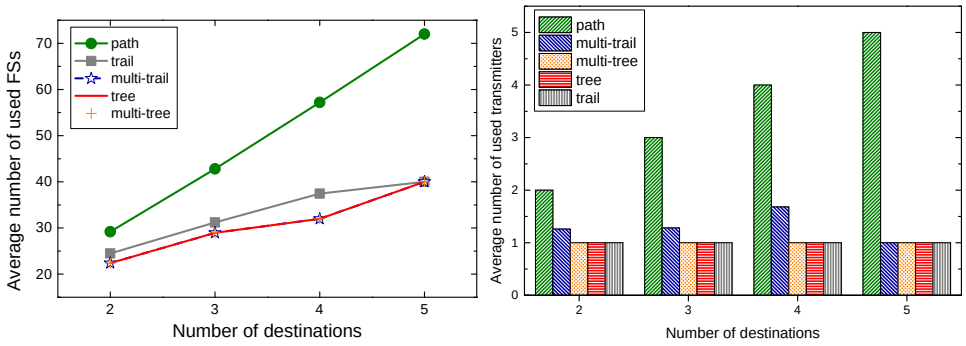

(a) (b)

Fig. 3.13 Resource usage of the five schemes for the N6S6 network without distance-adaptive transmission in terms of: (a) used FSs; (b) used transmitters.

and 3.16 show the spectrum and transmitter usages of the five schemes for the various network cases except the USNET network as the problem size is too large.

For the spectrum usage, the lightpath scheme has the highest spectrum consumption, while the light-tree and multi-light-tree schemes use the least spectrum, and are slightly better than the light-trail and multi-light-trail schemes. For all network cases, the multi-light-tree scheme actually uses a single light-tree for a multicast as the light-tree scheme does since it consumes only one transmitter. However, for the spectrum usage, the multi-light-trail scheme performs marginally worse than the multi-light-tree scheme and has a slightly higher transmitter usage. Also, for all network cases, the lightpath scheme consumes significantly more spectrum than all the other schemes, which is different from the network cases considering distance-adaptive transmission.

For the transmitter usage, the light-tree, multi-light-tree and light-trail methods use only one transmitter, the multi-light-trail scheme has a slightly higher transmitter usage, while the lightpath scheme consumes the most transmitters, the number of which is equal to the number of destinations of the provisioned multicast.

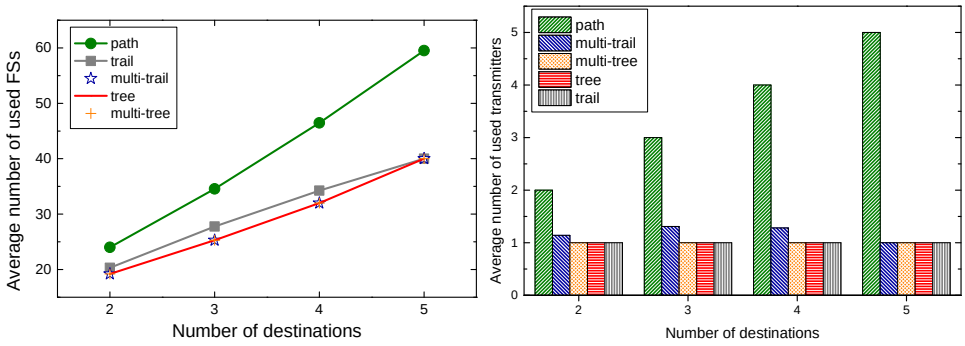

(a) (b)

Fig. 3.14 Resource usage of the five schemes for the N6S9 network without distance-adaptive transmission in terms of: (a) used FSs; (b) used transmitters.

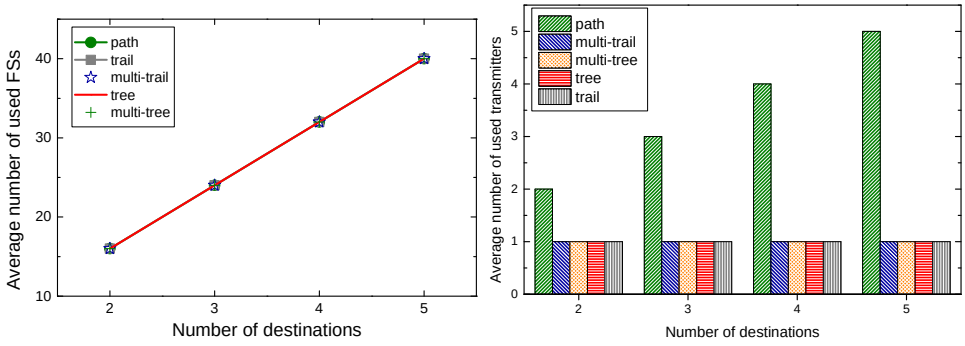

(a) (b)

Fig. 3.15 Resource usage of the five schemes for the N6S15 network without distance-adaptive transmission in terms of: (a) used FSs; (b) used transmitters.

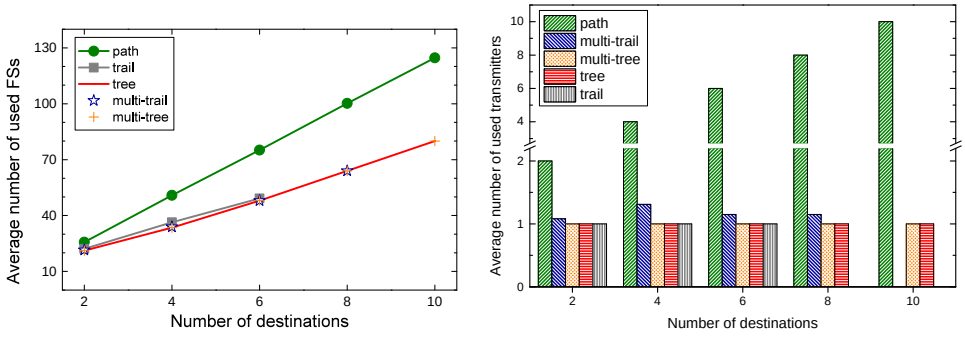

(a) (b)

Fig. 3.16 Resource usage of the five schemes for the COST239 network without distance-adaptive transmission in terms of: (a) used FSs; (b) used transmitters.

Table 3.13 Spectrum Savings of Distance-Adaptive Spectrum Allocation for a Multicast Demand†

	N6S6	N6S9	N6S15	COST239
Lightpath	36.1%	39.9%	45.0%	55.8%
Light-Tree	14.6%	14.2%	15.2%	50.5%
Multi-Light-Tree	23.3%	30.7%	45.0%	54.4%
Light-Trail	1.9%	2.3%	2.9%	-
Multi-Light-Trail	23.3%	30.7%	45.0%	-

† Based on the optimum presented in the previous figures

3.6.4 Benefit of Distance-Adaptive Spectrum Allocation

We also evaluate the benefit of distance-adaptive spectrum allocation for multicast demands. We summarize the spectrum savings of the network cases with distance-adaptive spectrum allocation over those without it as shown in Table 3.13. Comparing the three six-node networks, with the increase of network density, higher percentages of spectrum savings by the distance-adaptive spectrum allocation are observed for the lightpath, multi-light-tree, and multi-light-trail schemes than for the light-tree and light-trail methods where the saving percentages do not change significantly. This is due to the modulations used by the light-tree and light-trail methods are of low level so as to cover all the destinations of a multicast. Furthermore, some of the SD pairs with short distances still need to use the spectrum-inefficient modulation leading to excessive spectrum usage. Moreover, the saving percentages of the light-tree and light-trail approaches are significantly smaller than the other three since the modulation used (as shown in the previous tables) is closer to the one used for the case without distance-adaptive resource allocation. An exception is the COST239 network for the light-tree scheme which achieves significant spectrum savings. This

is because we use BPSK for the case considering no distance-adaptive spectrum allocation in order to allow comparison with the light-trail approach which entails very long distances, but the light-tree can use more spectrally efficient modulation, e.g., QPSK, for the multicast with a level greater than or equal to 2 as presented in Table 3.8.

3.7 Summary

We compared the five schemes, namely, lightpath, light-tree, multi-light-tree, light-trail, and multi-light-trail, to provision a single demand in the context of EONs with and without considering distance-adaptive transmission. Spectrum savings brought by the distance-adaptive spectrum allocation have been seen for all network cases. In particular, the savings are significant for the lightpath, multi-light-tree, and multi-light-trail schemes, and further go up as the network density increases.

When considering the distance-adaptive transmission, the multi-light-tree scheme has the lowest spectrum usage, followed by the multi-light-trail approach, then the lightpath and light-tree schemes, while the light-trail scheme consumes the most spectrum. For the lightpath and the light-tree schemes, when the network is densely connected, the light-tree scheme has a higher spectrum usage, while for sparse network cases, the lightpath method consumes more spectrum. For the transmitter usage, the lightpath scheme has the highest requirement, the light-tree and the light-trail have the lowest usage. The multi-light-tree and multi-light-trail schemes have both moderate usage of transmitters, the latter having a requirement slightly higher than the former.

Chapter 4

Light-Tree-Based EON Design

The previous chapter compared the optimal performances of existing approaches that can be used to provision multicast services. MILP formulations were developed to derive the optimal solutions. The light-tree-based solutions provide better spectrum efficiency than the others. In this chapter, we focus on designing EONs for multicast services by light-trees under the assumption that the network nodes are MC. The previous chapter presented numerical results when minimizing the total spectrum usage for a single demand. In this chapter, we adapt the MILP for the objective of minimizing the spectrum requirement in the entire network for multiple demands. Due to the intractability of MILP for large problems, we also propose an efficient and scalable heuristic algorithm, and compare its performance to that of existing algorithms. Numerical results show that our heuristic approach outperforms the existing ones. The proposed methods have many applications. It not only applies to backbone networks but also to other networks, e.g., inter-datacenter networks, where the database synchronization requires significant multicast, copying massive data in one datacenter to other datacenters. Also, since unicast and broadcast are two special cases of multicast, the proposed methods can also be applied for the unicast and broadcast traffic. A detailed problem statement is presented next.

4.1 Problem Description

We consider the same network model as Chapter 3. We also assume that the network nodes are MC and do not have spectrum conversion capability, which implies that the requirement of spectrum continuity should be met. The distance-adaptive transmission is also considered. Given a set of multicast demands, the objective is to minimize the maximum spectrum requirement among the links such that all the demands are accommodated.

4.2 MILP Formulation

We adapt the light-tree-based MILP presented in Chapter 3 to the new objective with additional variables and constraints which are presented next.

Extra Variables

$\mathbb{A}^r_{k,ij}$ Integer; denotes a number that is greater than or equal to the number of FSs in link (i, j) used by the light-tree using transmitter k of multicast demand r; $\mathbb{A}^r_{k,ij} \geq 0$.

C Integer; denotes the maximum number of the FSs required in the entire network.

Objective

$$\textbf{min } C \tag{4.1}$$

The objective (4.1) is to minimize the maximum number of FSs required in network links so as to accommodate the given multicast demand.

Constraints

$$C \geq \mathbb{E}_k^r, \quad \forall r \in \mathbf{R}, k \in \mathbf{T}^r \tag{4.2}$$

$$\mathbb{A}_{k,ij}^r \geq \mathbb{W}_k^r - \Delta \cdot (1 - \mathbb{L}_{k,ij}^r), \quad \forall r \in \mathbf{R}, k \in \mathbf{T}^r, (i,j) \in \mathbf{L} \tag{4.3}$$

$$C \geq \sum_{r \in \mathbf{R}} \sum_{k \in \mathbf{T}^r} \mathbb{A}_{k,ij}^r, \quad \forall (i,j) \in \mathbf{L}. \tag{4.4}$$

Constraint (4.2) ensures that the maximum index of FSs required should be greater than or equal to the end index of FSs assigned. Constraints (4.3) and (4.4) are redundancy constraints for faster solutions.

The complete set of constraints for the problem investigated in this chapter are the constraints (3.17), (3.18), (3.19), (3.2), (3.3), (3.20), (3.21), (3.22), (3.4), (3.23), (3.24), (3.29), (3.30), (3.31), (3.32), (3.33), (4.2), (4.3), (4.4).

MILP Problem Size

We calculate the size of the MILP problem by the dominant numbers of variables and constraints. The dominant number of variables is $O\left(|\mathbf{R}||\mathbf{L}|(|\bar{\mathbf{F}}| + |\bar{\mathbf{T}}||\mathbf{M}|) + |\mathbf{R}|^2|\bar{\mathbf{T}}|^2\right)$, and the dominant number of constraints is $O\left(|\mathbf{R}||\bar{\mathbf{T}}||\mathbf{L}|(|\mathbf{M}| + |\bar{\mathbf{F}}| + |\mathbf{R}||\bar{\mathbf{T}}|)\right)$, where $|\mathbf{R}|$, $|\mathbf{L}|$, $|\mathbf{M}|$, $|\bar{\mathbf{F}}|$, and $|\bar{\mathbf{T}}|$ are the numbers of demands, network links, MSs considered, and the average numbers of destinations and transmitters available per demand, respectively.

4.3 Heuristic Algorithm

In principle, MILPs can be solved for small networks. However, solving MILPs is known to be computationally prohibitive for real-size networks, therefore we provide an efficient heuristic algorithm that is scalable to large instances. As in our MILP

formulation, we also consider distance-adaptive spectrum allocation in the heuristic approach. The main idea is to attempt assigning an MS as high-level as possible so as to allocate few spectral resources to a demand and finding a tree with the fewest links where the maximum distance from the source to destinations along the tree does not exceed the transparent reach of the attempted MS. The reasons are as follows. The higher-level MS is assigned to a connection, the fewer FSs are required in each traversed link. Also, having a higher-level MS corresponds to having a shorter transparent reach, which generally in turn limits the number of links in the tree. In this way, the number of links in the tree is minimized, and the number of FSs required in each of these links is minimized, hence each multicast demand is accommodated with minimum spectrum resources.

We believe that the problem of finding a minimum-cost tree connecting a subset of the nodes with a bound on the distances of the paths between the source to the destinations is NP-complete since a special case of the problem with a bound set at infinity is proven NP-complete [148]. Thus, in what follows we present a multicast routing heuristic algorithm that finds a tree with near-optimal cost.

4.3.1 Multicast Routing Scheme

Our aim is to find a minimum-cost tree subject to the transparent reach constraint where the longest distance from the source to the destinations along the tree is within the transparent reach of the assigned MS. This is achieved in part by an algorithm that we call *distance-constrained minimum-cost anycast path* algorithm that finds a minimum-cost path from a source to one of the destinations within a given distance. In this way, we can implement Minimum-cost Path Heuristic (MPH) [149] as shown next in order to obtain a minimum-cost tree by repeatedly resetting to zero the cost of the links traversed by paths that have already been found and finding a minimum-cost path among the remaining destinations until a path is obtained for each SD pair.

Algorithm 1 Distance-Constrained Minimum-Cost Anycast Path

Input: A graph $G = (\mathbf{V}, \mathbf{L})$, a multicast session $r = \langle s_r; \mathbf{F}_r; t_r \rangle$, and a distance τ;
Output: **null** or a minimum-cost path from the source to one of the destinations, where its distance does not exceed τ.

Create $|\mathbf{V}|$ sets of subgraphs, i.e., $\mathcal{G}_c$, $c = 0, 1, \ldots, |\mathbf{V}| - 1$, where the subgraphs in $\mathcal{G}_c$ have a cost of c;
Create a subgraph g with a node s_r, reset its cost $g.c$ to 0, and distance $g.t$ to 0, set its end node $g.d$ to s_r, and its set of traversed links $g.\Gamma$ to $\emptyset$, and add it in $\mathcal{G}_0$;
while $\mathbf{F}_r \neq \emptyset$ and $\mathcal{G} \neq \emptyset$, where $\mathcal{G} \leftarrow \bigcup_{c=0}^{|\mathbf{V}|-1} \mathcal{G}_c$, **do**
  Remove the first element g_1 which has firstly a minimum cost and secondly a minimum distance from $\mathcal{G}$;
  if the end node of g_1, i.e., $g_1.d \in \mathbf{F}_r$, **then**
    return g_1;
  end if
  for all v in the neighboring node set of node $g_1.d$, **do**
    if v is not in g_1, and link $(g_1.d, v)$, denoted by $\bar{l}$, $\bar{l} \in \mathbf{L}$, **then**
      Create a subgraph g' and set $g'.\Gamma \leftarrow g_1.\Gamma \cup \{\bar{l}\}$;
      Set $g'.c \leftarrow g_1.c + \bar{l}.c$, $g'.t \leftarrow g_1.t + \bar{l}.t$, where $l.c$ and $l.t$ are the cost and distance of link l, respectively;
      Set $g'.d \leftarrow v$, $c' \leftarrow g'.c$;
      if the distance of g', $g'.t \leq \tau$, **then**
        if there is already a subgraph g_y terminated at v, $g_y.c = c'$, and $g'.t < g_y.t$, **then**
          Replace g_y with g';
          Delete g_y from $\mathcal{G}_{c'}$, and insert g' into $\mathcal{G}_{c'}$ in an increasing order of the distance;
        else if there is no subgraph of cost c', **then**
          Record g' for v of cost c' and insert g' into $\mathcal{G}_{c'}$ in an increasing order of the distance;
        end if
      end if
    end if
  end for
end while
return **null**;

Moreover, such an algorithm can be applied to route anycast (one-to-one-of-many) traffic in EONs with a bound on the path distance.

The distance-constrained minimum-cost anycast path algorithm is based on the breadth-first search algorithm, and its pseudocode is provided by Algorithm 1. Since in our case, the link cost is either zero or one, the cost of a path P_i from a given

Algorithm 2 DCMCT

Input: A graph $G = (\mathbf{V}, \mathbf{L})$, a multicast session $r = \langle s_r; \mathbf{F}_r; t_r \rangle$, and a distance τ;
Output: **null** or a minimum-cost tree $\mathcal{T}$ connecting the source to the destinations, where the path distances do not exceed τ.

1: Create a subgraph $\mathcal{G}$;
2: **for all** link l in $\mathcal{P}$, **do**
3: Set the cost of link l to 1, i.e., $l.c \leftarrow 1$;
4: **end for**
5: **while** $|\mathbf{F}_r| \neq 0$, **do**
6: Call Algorithm 1 with inputs of G, $\langle s_r; \mathbf{F}_r; t_r \rangle$, and τ to obtain a path $\mathcal{P}$;
7: **if** $\mathcal{P} \neq$ **null**, **then**
8: Add $\mathcal{P}$ to $\mathcal{G}$;
9: Remove the destination of $\mathcal{P}$ from $\mathbf{F}_r$;
10: **for all** link l in $\mathcal{P}$, **do**
11: $l.c \leftarrow 0$;
12: **end for**
13: **else**
14: **return null**;
15: **end if**
16: **end while**
17: Run shortest path tree algorithm on the subgraph $\mathcal{G}$ to obtain a tree $\mathcal{T}$ that connects the source to the destinations;

source, s_r, to node i is the sum of the costs of the links traversed by P_i. Thus, the path cost is a non-negative integer and is smaller than or equal to $|\mathbf{V}| - 1$, where $|\mathbf{V}|$ is the number of the network nodes. For a given path cost, it is possible that no path with that given cost can be found from s_r to node i. It is also possible that there is at least one shortest-distance path of that given cost, where we randomly select one of these shortest paths for possible consideration. Thus, for a given cost value, out of $|\mathbf{V}|$ possible cost values, each node has at most one selected shortest-distance path from s_r. Consequently, in total, each node has up to $|\mathbf{V}|$ selected shortest-distance paths. Each of these paths is considered at most once (see Line 4 in Algorithm 1), and we need to consider at most $|\mathbf{V}|^2$ paths until we find a minimum-cost path from s_r to one of the destinations within a given distance. In this case, the condition/expression of the **while** loop in Line 3 is checked at most $|\mathbf{V}|^2$ times. Within the **while** loop, once a shortest-distance path from s_r to node n of a certain cost is considered, we

scan the nodes adjacent to n for the **for** loop in Line 8, so the number of the adjacent nodes is at most $|\mathbf{V}|-1$, which implies at most $|\mathbf{V}|-1$ potential paths. Then, within the **for** loop, for each node v among the adjacent nodes, we compare its distance of the newly found path, P'_v, to the distance of the path, P_v (if there is one recorded at node v), with the same cost, and delete P_v from a list of (up to $|\mathbf{V}|$) paths with the same cost if the list contains P_v and insert the path with the shorter distance into the list in an increasing order of the distance. To sum up, the **while** loop exits within $|\mathbf{V}|^2$ times. Within the **while** loop, the **for** loop exits within $|\mathbf{V}|$ times. Within the **for** loop, the insertion of a path has a complexity of $|\mathbf{V}|$. Thus, Algorithm 1 has a complexity of $O(|\mathbf{V}|^4)$.

Based on Algorithm 1, we obtain a near-optimal tree in a similar way that MPH does. We present the pseudocode in Algorithm 2. Firstly, we initialize the cost of the links in $\mathbf{L}$ to one. Secondly, we repeatedly call Algorithm 1 to find a path P_d in G from the source to the destination d, and reset to zero the cost of the links traversed by P_d, until a path is found for each SD pair. Then, to guarantee that a tree is obtained by the found paths, we use Dijkstra's algorithm to find a shortest-path tree in the subgraph consisting of all links in the paths. In this case, the longest path among the paths to all the destinations along the tree should have a distance no larger than the longest path among the previously obtained paths for all SD pairs.

Algorithm 2 calls Dijkstra's algorithm once and Algorithm 1 for a total of $|\mathbf{F}_r|$ times, where $|\mathbf{F}_r|$ is the number of destinations of the multicast session. The former can be achieved at a complexity of $O(|\mathbf{V}|^2)$, and the latter has a complexity of $O(|\mathbf{V}|^4)$. Thus, Algorithm 2 has a complexity of $O(|\mathbf{V}|^4|\mathbf{F}_r|)$.

4.3.2 Heuristic Algorithm for Provisioning a Single Demand

To provision a multicast demand, we give a heuristic algorithm based on the usage of SWP [66]. The reason is that compared to two-step algorithms, such SWP-based

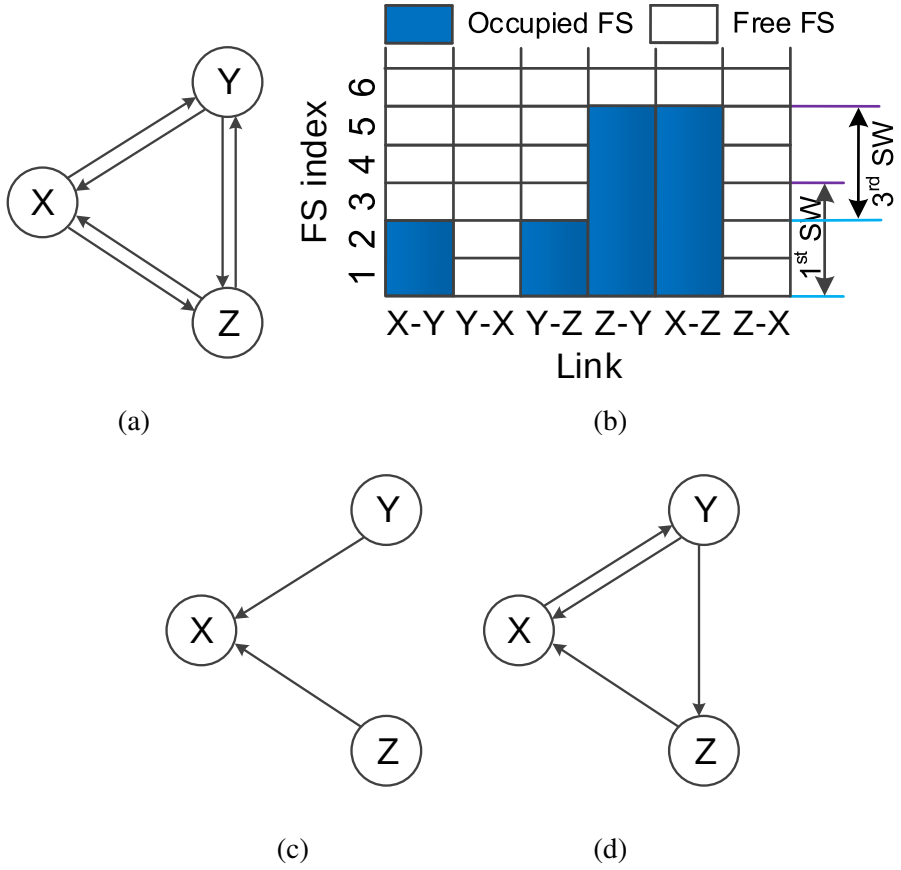

Fig. 4.1 Illustration for the concepts of SW and SWP: (a) an example network graph; (b) FSs usage; (c) a graph on the first SWP for finding a tree for a demand requesting for 3 FSs; (d) a graph of the third SWP for finding a tree for the same demand.

algorithms have been demonstrated to achieve better performance for joint routing and the availability of spectrum resources [150]. Before presenting the algorithm, we introduce the concepts of SW and SWP proposed in [66]. An SW in a fiber link is a window of spectrum containing a certain number of contiguous FSs. The availability of an SW is subject to the availability of the FSs contained in it. If any FS within an SW cannot be used by other connections because of the limitation of the spectrum non-overlapping constraint, the SW is unavailable; otherwise, it is available. Then, an SWP is a plane of virtual graph corresponding to an SW. The virtual graph contains all the nodes of the original graph and the links, in each of which, the SW is available.

Figure 4.1 illustrates the concepts of SW and SWP. The original graph and the usage of FSs in each fiber link are shown in Figs. 4.1a and 4.1b, respectively. Assume that a demand, namely, D, arrives and requests three FSs. To accommodate it, an SW should contain three FSs. In each fiber link, there are several possible such SWs, e.g., the first SW, second SW, and third SW occupying FSs 1 to 3, 2 to 4, and 3 to 5, respectively. The first SW corresponds to the first SWP. If the first SW in a link is available, the link should be in the first SWP, and vice versa. In Figs. 4.1c and 4.1d, we provide two graphs of the first and the third SWPs that can be used to find a tree for such a demand.

Such an SWP scheme provides a simple, but efficient, way to satisfy the three constraints in the spectrum assignment. Spectrum continuity is guaranteed since the graph of an SWP contains links with the same available FSs. Spectrum contiguity is met since each SW of the links of the SWP corresponds to a number of contiguous FSs. We also ensure spectrum non-overlapping by removing links from the graph of the SWP. The FSs in these links are utilized by other connections and cannot be reused.

To reduce the number of SWPs to be considered for accommodating a demand, we introduce the concept of an *SWP starting-FS list*, which is a list of start FS indices of the SWPs considered for allocating future demands. Each time after a multicast demand is served, the SWP starting at FS $n+1$ following the end FS n of the latest served multicast connection is usually different from other SWPs. We store the former FS index, i.e., $n+1$, in an increasing order in the SWP starting-FS list. Initially, the list contains an FS index, i.e., 1. Any SWP starting at an FS between the FSs of i-th and $(i+1)$-th elements of the SWP starting-FS list will have a subset of links that are available in the SWP starting at the FS of i-th element given the SW size, i.e., the number of FSs an SW contains. For the example of Fig. 4.1b, the SWP starting-FS list includes only FSs 1, 3, and 6. If for example, we consider possible demands requesting a number of contiguous FSs, a possible SWP starting at FS 2

Algorithm 3 Provisioning a demand with DCMCT and First Fit Spectrum Allocation

Input: A network graph $G = (\mathbf{V}, \mathbf{L})$, a multicast demand $r = \langle s_r; \mathbf{F}_r; t_r \rangle$, a set $\mathbf{M}_r$ of feasible MSs and their corresponding transparent reaches for r, the maximum number Ω among the FS indexes in a link, and an SWP starting-FS list;
Output: MC-RMSA for accommodating r.

while r has not been accommodated, **do**
  for all MS m in $\mathbf{M}_r$ from the highest to the lowest modulation level, **do**
    Obtain the number, i.e., ω_m^r, of required FSs for r and the transparent reach τ_m assuming that MS m is utilized;
    for all FS index α, $\alpha + \omega_m^r - 1 \leq \Omega$, from lowest to highest in the SWP starting-FS list, **do**
      Obtain an SWP whose SW starts from this FS index α and ends at FSs index ε, $\varepsilon = \alpha + \omega_m^r - 1$;
      Obtain the graph, i.e., $G' = (\mathbf{V}', \mathbf{L}')$;
      Call Alogrithm 2 with the inputs of the graph G', a multicast session $\langle s_r; \mathbf{F}_r; t_r \rangle$, and a distance τ_m, to find a tree for r;
      if such a tree is found, **then**
        Accommodate r by allocating the FSs of the present SW in the links of the found tree;
        Insert FSs index $\varepsilon + 1$ into the SWP starting-FS list in an increasing order;
      end if
    end for
  end for
end while

does not need to be considered, either because it is equivalent to the one starting at FS 1, or because it contains a subset of links that are available in the SWP starting at FS 1.

Assuming that a set of feasible MSs is given, for each multicast demand, we try to assign the MSs from the highest to the lowest modulation level. For a given MS, we calculate the number of required FSs. Then, for given FS usage in each fiber link, we scan the SWPs to obtain a graph, denoted by G'. Next, we call a routing scheme to find a tree to route the multicast connection. The details are presented in Algorithm 3. Algorithm 3 serves a single demand, thus can be easily applied for the case of dynamic traffic where demands arrive sequentially at random, then hold network resources for the required service durations, and finally depart.

Since Algorithm 2 has a complexity of $O(|\mathbf{V}|^4|\mathbf{F}_r|)$, Algorithm 3 calls it at most $|\mathbf{M}|\Omega$ times, where $|\mathbf{M}|$ and Ω are the numbers of considered MSs and FSs in each fiber link, respectively. Thus, Algorithm 3 has a complexity of $O(|\mathbf{V}|^4|\mathbf{F}_r||\mathbf{M}|\Omega)$.

4.3.3 Provisioning of Multiple Demands

Assume that we can find a tree for every multicast session, e.g., by running Dijkstra's algorithm for a shortest path tree, in the original graph. The distances of the paths to all destinations are within the transparent reach of the lowest-level MS considered, e.g., 4,000 km for BPSK.

Based on the assumption above and on the heuristic algorithm for provisioning a multicast demand, we present a greedy algorithm that increases the spectrum resources required in each fiber link in a greedy way when currently available resources in the network are not sufficient to accommodate it. The greedy algorithm includes three steps, namely, *initialization*, *order-operation of the multicast demands*, and *connection setup one by one*. We also introduce a *multi-iteration process* [66] to improve performance.

1) Initialization

To serve a multicast demand, given a set of MSs, we find the feasible MSs that the multicast could utilize and a tree that includes the fewest links for the feasible highest-level MS. Firstly, we obtain a shortest path tree $\mathcal{T}_1$ by running Dijkstra's algorithm for the multicast. Then, we can obtain the longest distance among all paths, and therefore obtain the highest-level MS m that $\mathcal{T}_1$ can utilize. For the same MS m, we also find a tree $\mathcal{T}_2$ by Algorithm 2. We select the tree $\mathcal{T}_1$ or $\mathcal{T}_2$ that involves fewer links and record it as the *candidate tree*. Accordingly, we obtain a set of feasible MSs that are not of higher-level than m.

2) Order Operation of the Demands

The order in which the demands are served also affects the result. In this case, we consider three ordering methods. The first one is to arrange the demands in the decreasing order of a certain metric, e.g., the ordering method used in [128]. The second and third ordering methods are the ones we demonstrated for unicast demands in [66]. The second one is to randomly shuffle the demands to obtain a randomly ordered demand sequence where the demands are accommodated following the obtained sequence. Extending the second method, the third one prioritizes the accommodations of the demands with the highest spectrum requirement by the candidate tree. In other words, it groups the demands with the same spectrum requirement by the candidate tree, while within each group, the demands are ordered as in the obtained sequence. The demand groups are then accommodated in the decreasing order of the spectrum requirements.

3) Connection Setup One by One

We first reset the number of FSs in each fiber link of the network to zero. If the demand cannot be accommodated under the current network resources, we add one FS in each fiber link, and run Algorithm 3 on the newly available SWPs. This procedure is repeated until the demand is accommodated, or the number of added FSs reaches the number n of FSs required by this multicast demand assuming that the highest-level feasible MS is used. If the procedure stops because of the latter, we do not use Algorithm 3, instead we accommodate the demand by allocating the n newly added FSs in the links of the candidate tree obtained in the initialization step.

After all the demands are served, we can obtain the number of required FSs in each link and thus the required spectrum in units of GHz.

4) Multi-Iteration Process

Since the performance of the proposed greedy algorithm is dependent on the order in which the demands are served, we adopt a multi-iteration process to further improve the performance. A result can be obtained for each sequence of demands served via the greedy algorithm. In multi-iteration process, we randomly shuffle a set of the demands multiple times, obtain multiple demand sequences (thus multiple results), and select the best one as the final result. In this way, the quality of the result for the multi-iteration process is dependent on the number of distinct sequences of the demands. The larger the number of demand sequences, a better result can be achieved but at the cost of a longer computational time.

4.4 Numerical Results

In this section, we present numerical results for the MC-RMSA problem in EONs. We compare the performance of the proposed heuristic algorithm to the optimal solution obtained by the MILP and other existing heuristic algorithms. We also look into the influence of the multi-iteration process on the performance of the heuristic algorithm.

4.4.1 Test Conditions

We consider the following three test networks: (1) a six-node nine-link (n6s9) network as shown in Fig. 4.2, (2) the 11-node 26-link COST239 network, and (3) the 24-node 43-link USNET network. The latter two are shown in Fig. 3.7 of Chapter 3 and are widely used in literature. The proposed approach can also apply to larger networks, e.g., with hundreds of nodes, considering its polynomial-time complexity. The bandwidth of an FS in each fiber is 12.5 GHz. We consider three MSs, namely, BPSK, QPSK, and 8QAM. The MSs and the corresponding transparent reaches are

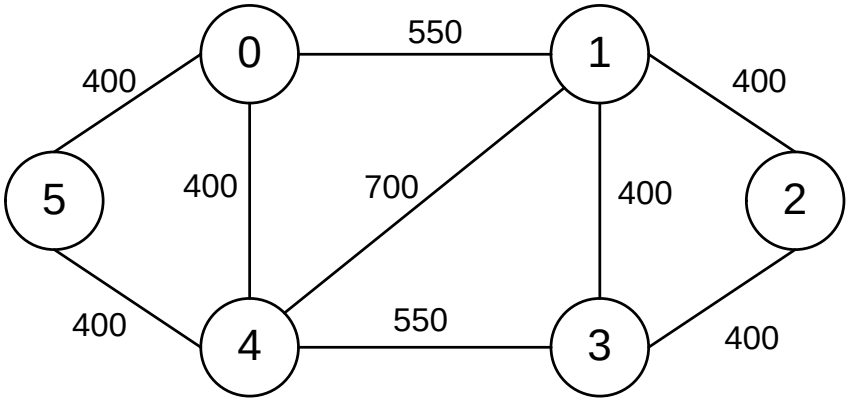

Fig. 4.2 A six-node nine-link (n6s9) network.

shown in Table 3.1. We consider 10 sets of multicast demands. Because of the known computational limitations of the MILP formulation, we only consider 15 multicast demands per set for the n6s9 network, and compare the performance of the algorithm with the optimal MILP solution. For the other two larger networks, we consider that each set contains 50 multicast demands, and compare the performance of the proposed heuristic algorithm with the heuristic proposed in [128]. The multicast sessions are obtained by randomly shuffling the set of network nodes. The bit rate values of the demands follow a uniform distribution of range (100, 200) Gb/s. We use up to 10,000 random sequences for each set of demands to investigate the impact of the number of random sequences on the performance of the algorithm. We also look into the relationship between the required spectrum and the number of destinations, where we assume that the demands of each set have the same number of destinations.

We compare the existing heuristic algorithm proposed in [128] called AFA, which is based on precalculated trees. We use the same procedure to obtain the candidate trees as in [128]. We precalculate up to 20 shortest paths for each SD pair and derive up to 10000 candidate trees using the paths for each demand. As the selection of the candidate trees has a strong impact on the performance of AFA, we also use the algorithm proposed in [129] and select the candidate trees with the best choices demonstrated in the same paper. Specifically, among all the possible trees

that are constructed by the paths, the trees are ranked in a non-decreasing order of the highest-level modulations, fewest links, and shortest total lengths with the highest, medium, and lowest priorities, respectively. The top-ranking trees are selected as candidates.

For AFA, we consider the ordering method proposed in [128]. The ordering method considered in this chapter contains three sequences in the decreasing orders of the three metrics, namely, the bit rate, the number of FSs required by the first candidate tree, and the multiplication of the former two. The minimum among the values produced by the three sequences is selected as the result of this ordering method. Since the demands we consider for each set have the same destination count, the sequence in [128] involving the multiplication of the receiver number and a metric is the same as the one we use in this chapter involving that metric. Also, as AFA was proposed for its key ability that the accommodations of the demands are adaptively ordered, we do not consider the random demand sequences for AFA. For the proposed heuristic algorithms, we consider the aforementioned three ordering methods. For the two cases of random ordering, to further improve the solution quality, we use a multi-iteration process. For the multi-iteration process, it is important to know the right number of demand sequences to be used. If this number is too large, it adversely affects the running time, while if it is too small, accuracy is compromised. It is therefore important to investigate the impact of this number on the performance of the algorithm.

Henceforth, the following notations, names and abbreviations will be used. We use "MILP" to stand for the MILP approach. For the proposed heuristic algorithm, we use a prefix, i.e., "DCMCT," to denote the algorithm that uses Algorithm 3 with DCMCT as the routing scheme in the greedy algorithm. We also use the shortest path tree algorithm to replace DCMCT in the greedy algorithm, and denote it by "SPT." We use several suffixes to denote the type of ordering of the demands used in the algorithm. For instance, suffix "_DO" denotes that the Decreasing Order

mentioned above is adopted. The remaining suffixes in this paper are used to denote a multi-iteration process with a certain number of considered random sequences, e.g., "_1k" for 1,000 randomly shuffled sequences. In this way, we can obtain the short name of a greedy algorithm by combining the prefix and a suffix. For example, "DCMCT_100" refers to a greedy algorithm that employs Algorithm 3 with DCMCT under 100 random sequences for each set of demands. For the existing algorithm presented in [128] based on candidate trees, we denote it by "AFA(p,t)_DO" where p denotes the maximum number of paths considered for each pair of nodes and the top-ranked t trees among those constructed by the paths are considered candidates for each multicast demand.

The heuristic algorithms are implemented using the Java environment on Eclipse 4.6.3, while we use a commercial optimization software, i.e., AMPL/Gurobi 7.0 [145], to solve the MILP problem. Our test platform is a Lenovo M900 running Microsoft Windows 10 Enterprise (64-bit), which is equipped with 64-GB RAM and an Intel(R) Core(TM) i7-6700 CPU running at 3.4 GHz.

4.4.2 Performance Comparison

1) The Six-Node Network

We investigate the impact of the number of demand sequences on the performance of the proposed heuristic algorithm for the n6s9 network. As the algorithms with the multi-iteration process yield similar observations for the second and third ordering methods, we take the DCMCT algorithm with the second method as an example shown in Fig. 4.3. As the network is of small size, we consider up to 10,000 demand sequences. As we can see in Fig. 4.3, when the number of demand sequences increases, the proposed algorithm presents a better performance requiring less spectrum, and approaching the optimum of MILP. In particular, DCMCT_10k consumes 1.8% more spectrum than the optimum averaging over the five destination

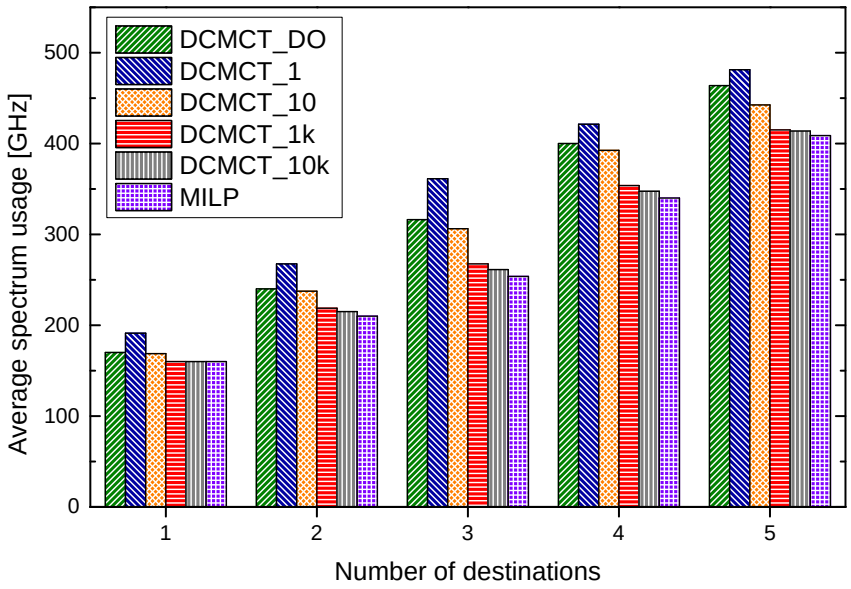

Fig. 4.3 Performance comparison in the n6s9 network.

cases. Moreover, the performance improvement is significant for 1,000 random sequences, and a saturation is seen afterwards. We consider 1,000 random demand sequences sufficient as we obtain a good performance, i.e., a 3% gap to the optimum, and the running time is acceptable, i.e., around 1 second. We also compare the multi-iteration process with decreasing order. We can see that the algorithm with 10 random sequences, i.e., DCMCT_10, outperforms the case with three decreasing ordered sequences, i.e., DCMCT_DO. These demonstrate the benefit of the multi-iteration process.

Figure 4.4 shows the performance comparison among the heuristic and optimal algorithms in the n6s9 network. As the network is of small size, we consider up to 20 paths for each node pair and maximally 1,000 candidate trees for the AFA algorithm. When the number of destinations increases, the spectrum requirement increases for all algorithms. Among the heuristic algorithms, DCMCT_DO and AFA(20,1k)_DO requires the most spectrum, DCMCT_1k_DO follows, and DCMCT_1k performs the best. In particular, AFA(20,1k)_DO consumes 14% more spectrum compared to the optimum given by MILP, and marginally outperforms DCMCT_DO by 0.7% on average. Compared to DCMCT_DO, DCMCT_1k_DO and DCMCT_1k reduce

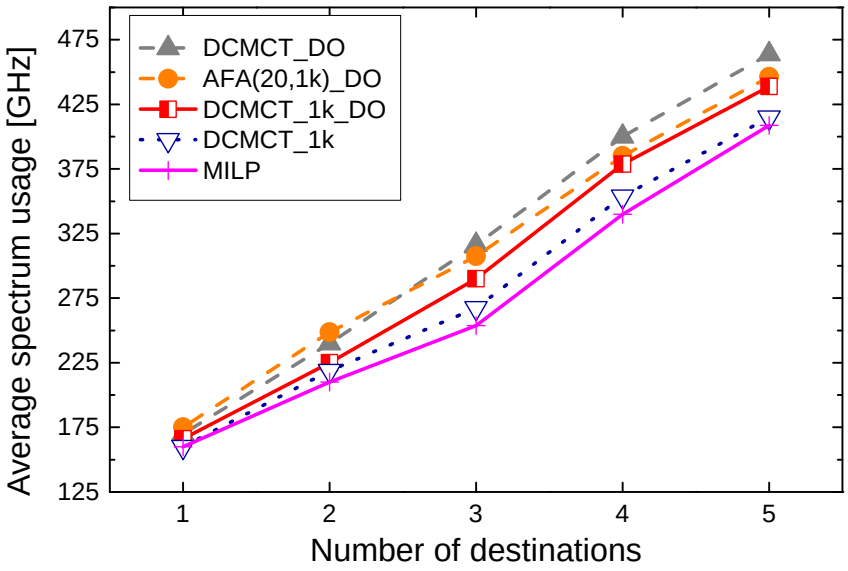

Fig. 4.4 Comparison of spectrum requirements in the n6s9 network.

the spectrum consumption by over 5% and 10%, respectively. In particular, for DCMCT_1k, the usage of 1,000 random demand sequences also brings it a sufficiently good performance with a gap of about 3% to the MILP optimum. As discussed previously, the performance can further be improved when more such sequences are considered. These demonstrate the benefit of using the multi-iteration process. Moreover, compared to DCMCT_1k_DO, DCMCT_1k presents a better performance for the following three reasons. (i) The demand sequences with near-optimal performance may not be ordered explicitly, for example, not likely in the decreasing orders as used in DCMCT_1k_DO. (ii) DCMCT_1k has the ability to explore possibly all demand sequences as it shuffle the whole set of demands randomly. (iii) Last but not least, since both the n6s9 network and the number of considered demands are small, 1,000 random demand sequences may contain those that are able to provide the optimal or near-optimal performance.

2) The COST239 Network

We also investigate the impact of the number of candidate trees on the performance of the AFA algorithm. As shown in Fig. 4.5, we consider up to 20 shortest paths

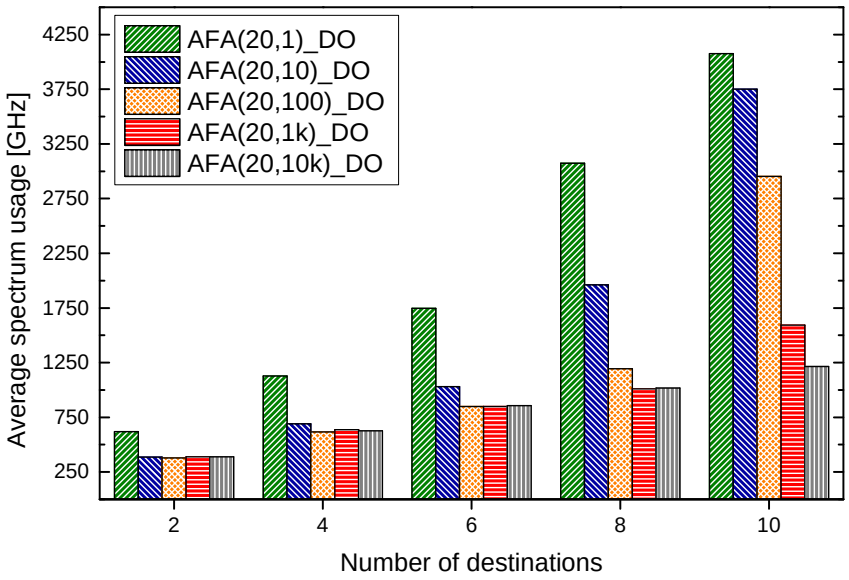

Fig. 4.5 The impact of the number of candidate trees on the performance of the AFA algorithm in the COST239 network.

for each node pair and 10,000 candidate trees for each multicast in the COST239 network. As we can see in the figure, with the increase of the number of considered candidate trees, the performance of the algorithm improves at the beginning by yielding a lower requirement of spectrum, and finally becomes stable with a small fluctuation. This is because having more choices of candidate solutions for each multicast helps reuse the network resources, but the accommodation of a demand might adversely affect that of the future demand, making the algorithm performance vary slightly. Moreover, multicast with a larger session size requires more candidate trees to obtain sufficiently good performance. For instance, for multicast with no more than six destinations, the performance is good enough within 100 candidate trees, while for those with eight destinations, it requires 1,000 trees. This can be explained as follows. When the multicast session size is large, the multicast tree spans many links making it hard to reuse the spectrum. For desirable performance, the accessibility to more trees is required.

Figure 4.6 shows the running times of the AFA algorithm in the COST239 network. Please note that the running time includes the times of the generation of

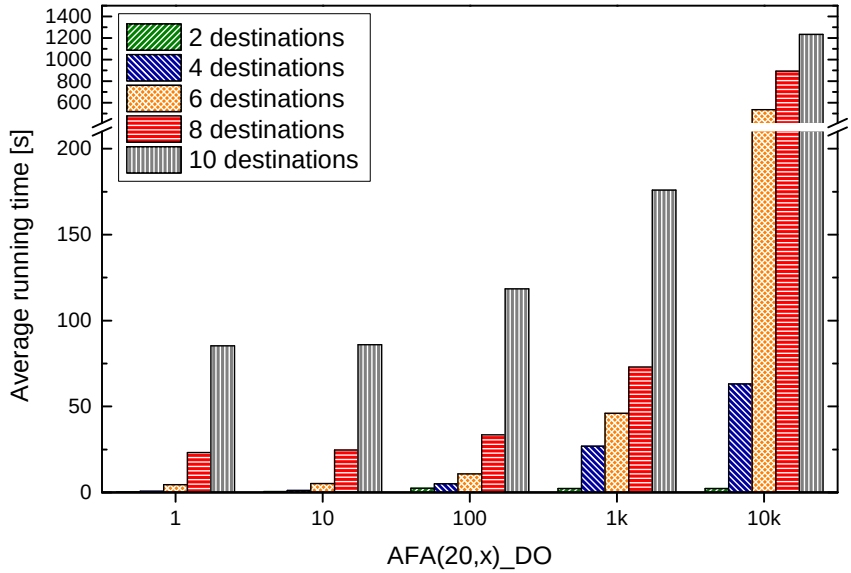

Fig. 4.6 Running time of the AFA algorithm in the COST239 network.

k-shortest paths and the calculation of candidate trees. The x axis is the number of candidate trees considered for the AFA algorithm. We can see that the running times increase when the value x increases. Also, for every value of x, we see a significant increase of the running time when the multicast session size increases. The reasons are twofold. The number of possible trees constructed by the k-shortest paths increases exponentially over the multicast session size, and the complexity is $O(\mathcal{K}^{\mathcal{D}})$, where $\mathcal{K}$ is the number of shortest paths between two nodes and $\mathcal{D}$ is the number of destinations of the multicast. The other reason is that with the increased number of destinations, it takes the AFA algorithm more time to search for a qualified tree to accommodate the demand to meet the strengthening constraints, e.g., spectrum continuity.

We also present the running times of the proposed heuristic algorithms. Since these algorithms behave similarly in terms of their running times, we discuss one of them as an example. In Table 4.1, we provide the running times of DCMCT_n, where n is the number of considered random demand sequences. The running time grows linearly with the increase in the number of random sequences. For instance, when the multicast session size is 2, DCMCT_100 consumes 0.92 sec-

Table 4.1 The Running Times of the Heuristic Algorithms in Units of Seconds

Multicast Size	DCMCT_n (n: Number of Considered Sequences)						AFA(20,1k)_DO
	1	100	1k	2k	6k	10k	
2	0.01	**0.92**	8.58	16.98	50.39	83.72	2.21
4	0.01	1.47	**14.65**	29.19	87.42	145.64	26.90
6	0.02	1.97	19.78	**39.53**	118.41	196.98	46.09
8	0.03	2.47	24.78	**49.60**	148.72	247.88	72.87
10	0.03	2.87	28.55	57.12	**171.25**	285.43	175.85

ond, while DCMCT_10k with 100 times the number of sequences considered in DCMCT_100 requires 83.72 seconds, which is approximate 100 times the running time of DCMCT_100.

Next, we compare the spectrum requirements of the algorithms under the condition that they have the well-matched running times. As shown in Table 4.1, we provide the running times of AFA(20,1k)_DO. We use the spectrum requirement obtained by AFA(20,1k)_DO, and take its running times as the upper bound of the running times allowed for the DCMCT algorithm. As shown in the table, for each case of the multicast size, the value in bold does not exceed the running time of AFA(20,1k)_DO. By these values in bold, we can roughly obtain the number of random demand sequences so that the running time does not exceed that of AFA(20,1k)_DO. Then we check back the spectrum requirements of the DCMCT algorithm with the obtained numbers. For example, when the multicast size is two, the running time of AFA(20,1k)_DO is 2.21 seconds. According to the table, we find that the DCMCT algorithm that does not exceed the running time is 100 and we then take the spectrum requirement by DCMCT_100 to compare with that by AFA(20,1k)_DO. We name the DCMCT algorithm under the second and third ordering methods with bounded running times by DCMCT_x and DCMCT_y_DO, respectively.

Figure 4.7 shows the performance comparison of the spectrum requirements among the algorithms with bounded running times for the COST239 network. We

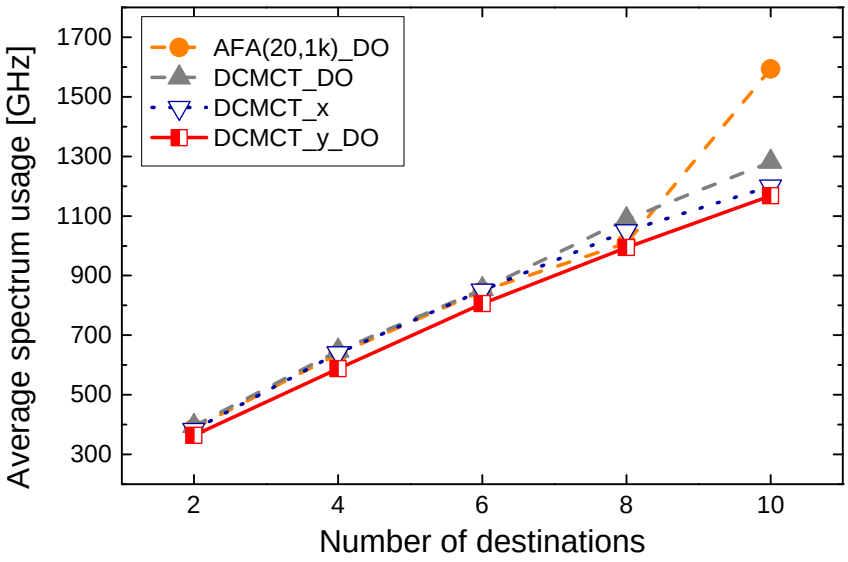

Fig. 4.7 Comparison of spectrum requirements in the COST239 network.

see that, for all the destination cases, DCMCT_y_DO always yields the best performance. By averaging over all the five cases of considered session sizes, DCMCT_x follows and then DCMCT_DO, while AFA(20,1k)_DO shows the worst performance. Specifically, DCMCT_DO, DCMCT_x and DCMCT_y_DO achieve reductions of the spectrum requirements by about 1.5%, 4.3%, and 9.5% when compared to AFA(20,1k)_DO, respectively. Even DCMCT_DO, where only three demand sequences are considered, with an average running time of only tens of milliseconds outperforms AFA(20,1k)_DO. This is attributed to the ability to possibly find any tree that can be used to accommodate a demand by the DCMCT algorithm. Also, we see the improvement brought by the multi-iteration process when comparing DCMCT_x (or DCMCT_y_DO) to DCMCT_DO. Moreover, in the COST239 network we observe that DCMCT_y_DO outperforms DCMCT_x, which is different from what we observed in the n6s9 network. This can be explained as follows. Since we consider sets containing more demands and a relatively large network, the number of demand sequences considered is very limited compared to the number of all possible sequences (given as the factorial of the number of demands). This makes

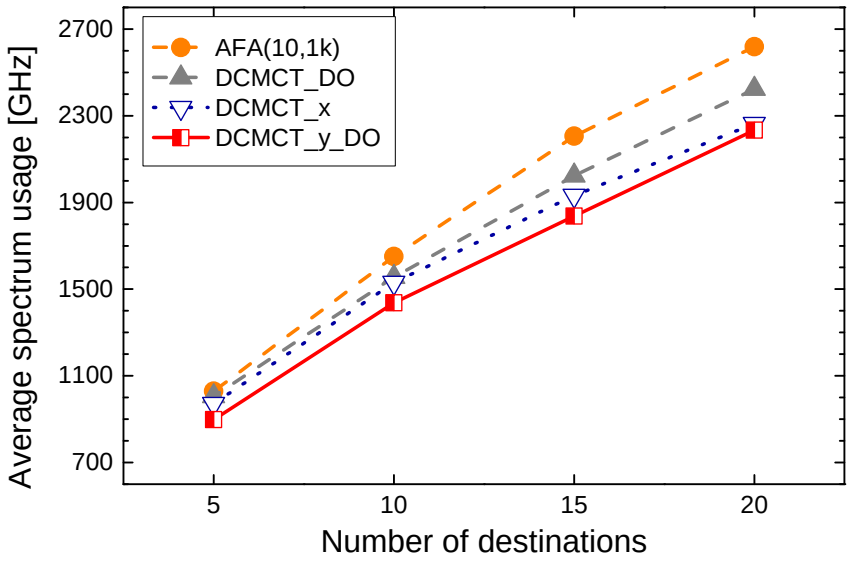

Fig. 4.8 Comparison of spectrum requirements in the USNET network.

it hard to hit the sequences that yield the optimal or near-optimal results, so that the ordering methods may help the multi-iteration process achieve better performance.

3) The USNET Network

Similarly, in Fig. 4.8 we compare the performance of the AFA and the proposed DCMCT algorithms in the USNET network with limited running times. Due to the rapid growth of the time used to calculate candidate trees for the AFA algorithm over the multicast session size, without loss of generality, we consider 10 shortest paths for each node pair and construct up to 1,000 candidate trees for each of the given demands in the USNET network which is larger than the previous two. For the DCMCT algorithm, we consider up to 10,000 random sequences for each experiment. As we can see in the figure, DCMCT_y_DO has the lowest spectrum requirement, DCMCT_x follows, and then DCMCT_DO, while AFA(10,1k) requires the most spectrum. In particular, for every multicast session size, the DCMCT algorithm with any of the three ordering methods outperforms AFA(10,1k). In particular, compared to AFA(10,1k) that consumes several tens up to thousands of seconds, DCMCT_DO with some hundreds of milliseconds still achieves 6% reduction of the spectrum

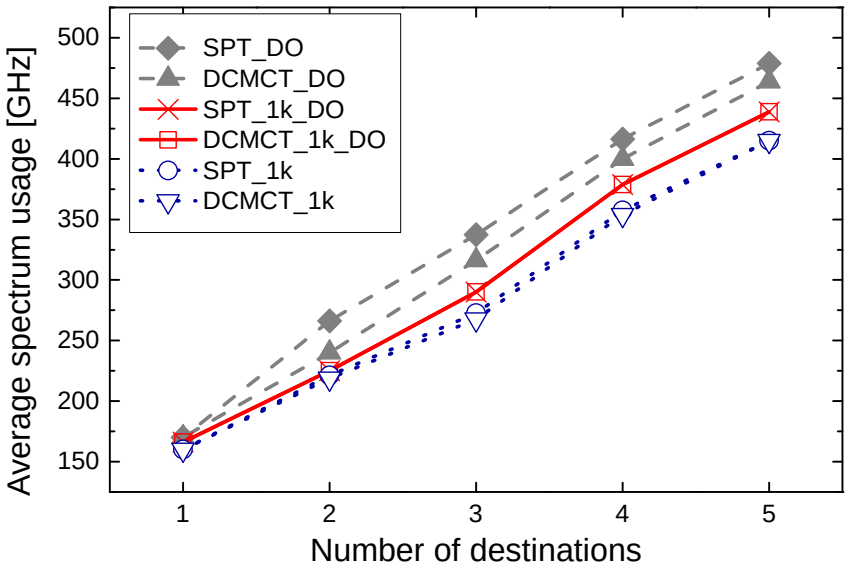

Fig. 4.9 Performance comparison between DCMCT and SPT in the n6s9 network.

requirement. This can be attributed to the ability of the DCMCT algorithm to access to additional tree solutions. Moreover, with the help of the multi-iteration process, the spectrum requirement reductions achieved by DCMCT_x and DCMCT_y_DO over AFA(10,1k) become more significant, i.e., by 10% and 14%, respectively.

4) Comparison Between DCMCT and SPT

We also consider the use of the SPT algorithm that finds the shortest path trees for multicast sessions in Algorithm 3 to replace the proposed DCMCT that aims for the minimum cost trees. We assume the same ordering methods, the same multi-iteration process and the same number of random sequences, and compare their performance in the three networks.

Figure 4.9 shows the comparison in the n6s9 network. The "DO," i.e., the first ordering scheme, provides the worst performance, while the "1k," i.e., the second ordering method, performs the best, and the "1k_DO," i.e., the third ordering approach, presents a moderate performance when compared to the previous two. Also, for each of the three ordering methods, the DCMCT algorithm presents a performance equal to or better than the SPT algorithm. This is because the DCMCT

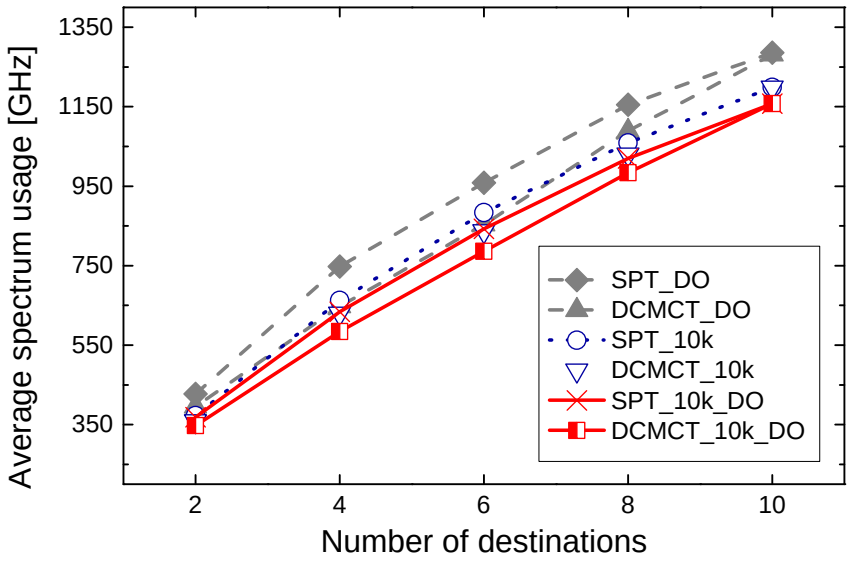

Fig. 4.10 Performance comparison between DCMCT and SPT in the COST239 network.

algorithm attempts to minimize the cost of the obtained tree directly while the SPT tries to achieve the same goal via an indirect way by minimizing the shortest distances between SD pairs. For the case of the "DO," the DCMCT algorithm requires 4.6% less spectrum than the SPT. Moreover, as for the DCMCT algorithm, the multi-iteration process also helps improve the performance of the SPT algorithm when we compare SPT_1k or SPT_1k_DO to SPT_DO.

In Fig. 4.10, we also compare the performance of the DCMCT and SPT algorithms in the COST239 network. The COST239 network presents observations similar to the n6s9 network. An exception is that in the COST239 network, both algorithms with "10k_DO" perform the best and outperform the two with "10k" while the two algorithms with the latter ordering method outperforms those with the former in the n6s9 network.

The performance comparison between the DCMCT and SPT algorithms in the USNET network is presented in Fig. 4.11. The observations in the USNET network are consistent to that in the COST239 network. Specifically, DCMCT_DO, DCMCT_10k, and DCMCT_10k_DO achieve reduction of the spectrum requirement

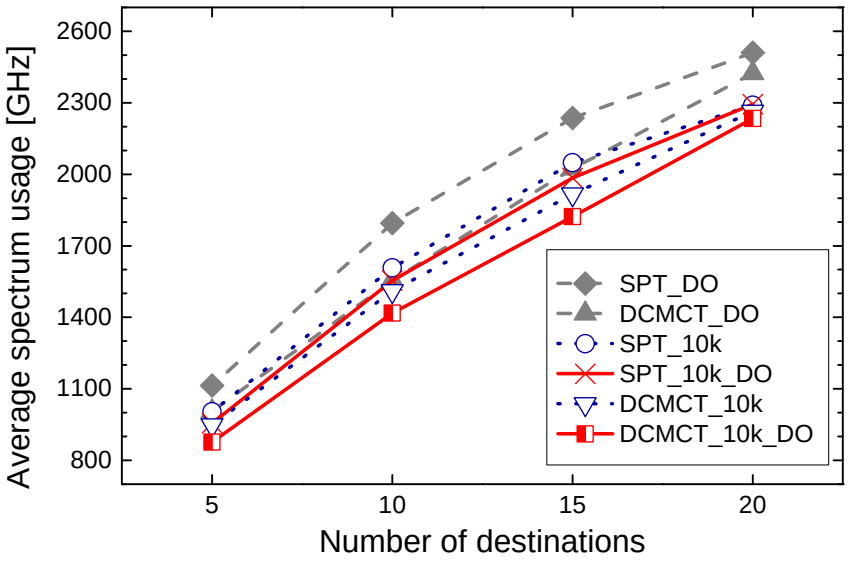

Fig. 4.11 Performance comparison between DCMCT and SPT in the USNET network.

by 9%, 4.8% and 7% over SPT_DO, SPT_10k, and SPT_10k_DO, respectively, with even DCMCT_10k outperforming the best of the SPT approaches, i.e., SPT_10k_DO. These demonstrate the benefit of DCMCT algorithm over the SPT.

4.5 Summary

In this chapter, we have investigated the routing and spectrum assignment problem in EONs. We provided a MILP formulation to solve small-size problems while for large instances we proposed an efficient heuristic algorithm. We analyzed the complexity of the proposed algorithm and proved that it is polynomial in time. To demonstrate the effectiveness of the proposed algorithm, we compared it to the state-of-the-art and the shortest-path tree algorithms. We also considered ordering methods that affect the performance of the algorithms. Numerical results show that for various cases, the proposed algorithm achieves a performance close to the optimum and outperforms the other heuristic algorithms.

Chapter 5

Provisioning Multicast in EONs with Shared Protection

In the previous chapter, we presented and compared the five schemes for provisioning multicast demands in EONs, and demonstrated the efficiency of light-tree-based schemes. In this chapter, we present a shared protection scheme for light-trees against any link failure in EONs.

5.1 Introduction

As surveyed in the previous chapters, extensive studies have focused on using light-trees for the provision of multicast services in optical networks since multicasting in the optical layer has been demonstrated to be more energy- and spectrum-efficient than IP multicasting [106].

Protection is considered an important attribute of optical networks. The occurrence of a single link failure in optical networks could result in severe service disruption. This is especially true when a trunk of the multicast tree fails, in which case multiple destinations are affected and cannot receive data from the source. Therefore, adequate protection should be preplanned in optical networks so that

they can continue operating under failures. Also, protection in the optical layer is beneficial in many aspects, e.g., simpler operations than that in higher layers and therefore faster recovery speed [74].

5.1.1 Related Work

In the previous chapter, we have already presented related work on provisioning multicast demands using light-tree technology. Here we focus on reviewing protection schemes proposed for optical networks.

Literature on multicast survivability in WDM optical networks can be classified into five categories: (1) tree-based [151–154], (2) segment-based [148, 155–157], (3) path-based [148, 158], (4) ring-based [159, 160], and (5) p-cycle-based [161–163] protection.

In tree-based protection, a backup tree protects the primary tree that supports the connection under normal operations. However, when a link in the primary tree fails, a backup tree takes over and serves the connection. Médard *et al.* [151] proposed algorithms to find two arc-disjoint trees. Singhal and Mukherjee [152] developed ILP models to minimize the total cost of all multicast sessions, one model considers wavelength continuity constraint; and the other model also considers the limited splitting degree and the splitter-bank size. Long and Kamal [153] proposed to protect each segment of the primary tree by a backup tree, i.e., for a given primary tree, there is a set of backup trees, one of which is invoked to take over the connection when a segment in the primary tree fails. This is different from the previous approach where an arc-disjoint tree is used to protect the primary tree from any single-link failure. Constantinou and Ellinas [154] proposed the Steiner Node Heuristic (SNH) algorithm; it uses Minimum Path Heuristic (MPH) [149] to obtain a tree, and then iteratively updates this subgraph by including one more node and related links, and employs MPH to find a tree in the sub-graph until no tree can be found at a lower

cost. To make connections survivable, the algorithm first utilizes the SNH to find the primary tree, and then removes the links of the primary tree, again employing SNH to find an arc-disjoint backup counterpart. The authors compared the proposed algorithm with the pruned Prim's heuristic [164] and MPH.

For segment-based protection, the concept of a segment is similar to that of a path. A segment starts from a segment node and ends at a downstream one. However, the definitions of a segment node, i.e., the end node of a segment, are not unified. In [148], a segment node could be the source, a destination (leaf), or a splitting node. Singhal *et al.* [148] proposed two heuristic algorithms for segment-disjoint protection: One finds the primary tree first, then identifies the segments of the tree, and finds disjoint counterparts as backup. The other, after identifying the segments, abandons the segments of the primary tree, and finds a pair of link-disjoint paths for two end nodes of each segment. Panayiotou *et al.* [155, 156] limited the definition of a segment node so that only the source and destinations are segment nodes, and proposed a level protection heuristic. It first finds the primary tree using Steiner tree heuristic [165], and then hierarchically orders the level of segment nodes; it finds a tree that starts from level i-th segment node spanning all $(i+1)$-th level segment nodes for a segment of level $(i, i+1)$ and does not traverse directed links used in the primary segments that are closer to the source. Such protection can handle multiple failures in segments at the same level. Constantinou *et al.* [157] proposed a directed-graph multicast protection heuristic based on Suurballe's algorithm [166] to find the minimum sum cost of disjoint path-pair for each SD pair. Each time after a path-pair is found for an SD pair, it adds again those SD pairs that were added before the current SD pair.

For path-based protection, the primary multicast tree is protected on an SD pair basis, i.e., a multicast session is considered as multiple SD pairs, and the primary path for each SD pair is protected by a link-disjoint backup path. Singhal *et al.* [148] proposed an ILP model for static traffic and a heuristic based on Suurballe's algorithm.

Simulation results demonstrate its good blocking performance. Furthermore, Singhal and Mukherjee [158] considered cross-sharing and self-sharing protection schemes that help reduce resource consumption. Network coding has been considered in provisioning multicast connections with 1+1 dedicated protection [167].

For ring-based protection, Leelarusmee *et al.* [159] proposed two protection techniques. One is one ring for all multicast sessions that allows the sharing of channel capacity among multiple demands, while this is not allowed for the other technique, i.e., one ring for one multicast session. Rahman and Ellinas [160] investigated the 1+1 dedicated ring-based protection of multicast connections.

Applications of the *p*-cycle protection scheme [64] to WDM optical networks have also been extensively studied e.g., [161–163].

In addition to the work on WDM optical networks, there are few studies on multicast protection or survivability in EONs [122, 168]. In [122], the authors used multiple lightpaths to provision a multicast connection and proposed a dedicated path protection scheme. Our approach in this chapter is based on shared protection that is more spectrally efficient than dedicated protection [148]. The reference [168] considered shared protection for multicast connections but did not consider distance-adaptive spectrum resource allocation, which is our focus in the present chapter. The preliminary work of this chapter was presented in [169].

5.1.2 Organization

The remainder of this chapter is organized as follows. In Section 5.2, we provide a detailed description of the problem considered in this chapter. The MILP formulation is presented in Section 5.3, and the heuristic algorithm is presented in Section 5.4. Numerical results and discussions are provided in Section 5.5. Section 5.6 summarizes the chapter.

5.2 MC-RMSA with Shared Protection

In this section, we present the shared protection scheme used for protecting multiple multicast sessions in EONs. This is then followed by the statement of the MC-RMSA problem with shared protection.

5.2.1 Shared Protection

A light-tree for a multicast session is a unidirectional connection where an optical signal is transmitted from a given source to multiple destinations. Under normal operations where no failure occurs, such a tree is called a primary tree, which can be viewed as a set of primary paths between the source and each destination. A primary link is a link in the primary tree. One protection scheme to protect a light-tree has each of its primary paths protected via a link-disjoint backup path. The backup paths for the corresponding SD pairs can share spectrum resources in their common link(s). The advantages of such path-based protection have been recognized in [148].

To protect a light-tree, there are two mutually exclusive cases in the protection scheme. One case is that the backup path of any SD pair shares no common link with the primary tree. The other case is that at least one of the backup paths shares common link(s) with the primary tree. However, any common link must be a link in the primary paths of other SD pairs since, for each SD pair, the backup path and the primary path are link-disjoint; this is known as self-sharing protection [158]. Thus, a light-tree can be protected as long as for each SD pair of the multicast session (i) a backup path is link-disjoint from its primary path, and (ii) we reserve spectrum resources in the backup-only links that are not in the primary tree but in the backup paths of all SD pairs. These reserved spectrum resources could be utilized when the primary tree fails.

When protecting multiple light-trees, the reserved spectrum resources in the backup-only links can be shared as long as these light-trees do not fail simultaneously. Such a shared protection among multiple light-trees is known as cross-sharing [158].

In this chapter, we consider four types of links that are included for serving a multicast connection, namely, primary-only link, backup-only link, self-sharing link, and cross-sharing link. For a multicast connection, a primary-only link is a link included only in the primary tree. Similarly, a backup-only link is a link included only as backup, while a self-sharing link is a link that is included in both primary and backup paths of different SD pairs. Hence, primary-only, backup-only, and self-sharing links are mutually exclusive. A cross-sharing link is a link that is included in multiple multicast connections only as backup. Thus, a cross-sharing link for multiple multicast connections is a backup-only link in each of these multicast connections, while a backup-only link may not be a cross-sharing link.

Figure 5.1 illustrates the shared protection scheme that we consider in this chapter based on these basic concepts. For the example network of Fig. 5.1a, Figs. 5.1b and 5.1c show the routing case of two multicast sessions, i.e., $M_1 = \langle A; \{B,C\} \rangle$ and $M_2 = \langle B; \{C,D\} \rangle$, respectively. As shown in Fig. 5.1b, the primary tree of M_1 contains links (A,B) and (A,C). The backup path to destination node B and that to destination node C are $A \rightarrow D \rightarrow B$ and $A \rightarrow D \rightarrow C$, respectively. These two backup paths share a common link (A,D), but share no common link with the primary tree. In this case, a link included is either a primary-only link or a backup-only link, and there are no self-sharing links. For M_2, as shown in Fig. 5.1c, the primary tree contains links (B,C) and (B,D). To protect the primary path $B \rightarrow C$ from a single link failure, a link-disjoint backup path $B \rightarrow D \rightarrow C$ is found, which uses the link (B,D) in the primary path $B \rightarrow D$. Similarly, a link-disjoint backup path $B \rightarrow C \rightarrow D$ is found for the primary path $B \rightarrow D$, which uses the link (B,C) in the primary path $B \rightarrow C$. In this case, both (B,C) and (B,D) are self-sharing links. Links (C,D) and (D,C) are backup-only links, where the reserved spectrum resources could be

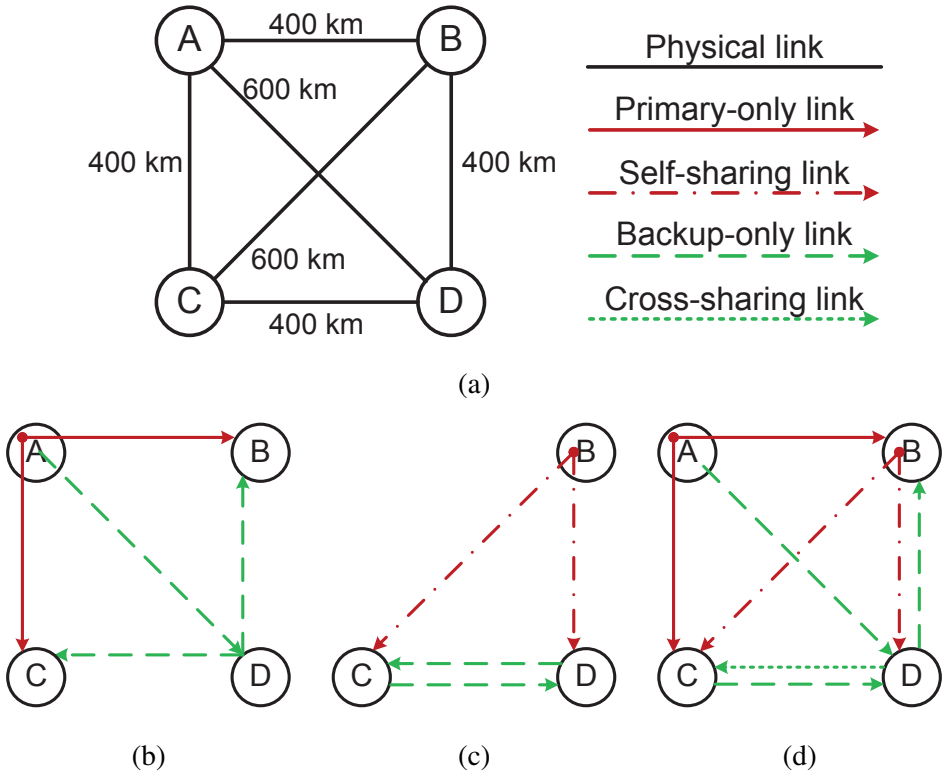

Fig. 5.1 An example of the shared protection scheme: (a) a four-node fully-mesh network; (b) routing for $M_1 = \langle A; \{B,C\} \rangle$; (c) routing for $M_2 = \langle B; \{C,D\} \rangle$; and (d) sharing between M_1 and M_2.

used to protect other multicast connections by cross-sharing. In Fig. 5.1d, link (D,C) is a backup-only link for both M_1 and M_2, so the reserved spectrum resources in the link can be used to protect both multicast connections. This is because their primary connections contain no common links and will not fail simultaneously in case of a single link failure, and therefore there is no competition on utilizing the reserved resources in the cross-sharing link for service restoration.

5.2.2 Problem Statement

In this chapter, we focus on the MC-RMSA problem with shared protection for static traffic, where a set of multicast demands **R** is given. We consider the network model and distance-adaptive transmission described in Chapter 3, under similar assumptions as made in the same chapter. The network nodes are incapable of

spectrum conversion, the transponders are central frequency and MS tunable, and the network is free of regenerators. As we consider to provision multicast services by light-trees, each node is assumed to be multicast-capable based on the splitter-and-delivery switch [143]. An input signal going through such a multicast-capable node can be dropped locally and/or switched to one, many, or all of its output ports. We assume that the power loss of the signal due to the splitting is compensated by amplifiers in the node. We also assume that every SD pair has at least one pair of disjoint paths, where the transmission distance is within the transparent reach of the lowest-level MS considered, e.g., 4,000 km for BPSK as in Table 3.1. This assumption is made for simplicity, and extension to larger networks that involve regenerators is left for future work.

In this case, to implement the shared protection scheme where spectrum resources used in a link of the primary path between an SD pair can be utilized to protect another SD pair within the same multicast session, we consider that the same spectrum resources (modulated by the same MS) are allocated in each link of the primary tree and are reserved in the backup-only links of the multicast connection. Such a consideration also implies faster recovery and transponder savings. Thus, for MS assignment, all primary and backup paths should be taken into account in the transparent reach constraint. For example, for the multicast session M_2 in Fig. 5.1c, the backup paths of the primary paths $B \rightarrow C$ and $B \rightarrow D$ are $B \rightarrow D \rightarrow C$ and $B \rightarrow C \rightarrow D$, respectively. The longest transmission distance among all four paths is 1,000 km, thus the MS assigned to the multicast connection of M_2 should have a transparent reach of no less than 1,000 km.

The objective of the MC-RMSA problem with shared protection is to minimize the maximum spectrum required in the links subject to the condition that all the given multicast demands are accommodated when considering distance-adaptive spectrum allocation. The light-tree of each multicast session is protected on an SD pair basis; the primary path of each SD pair of the multicast connection is protected

by a link-disjoint backup path from any single link failure in both directions. This means that the network can continue to operate when only one link fails at a time.

5.3 MILP Formulation

To solve the MC-RMSA problem with shared protection, we first provide a MILP formulation. Let Δ be a large number. We use a set, $\mathbf{O}$, of operation indicator as follows. To find a primary and a backup paths for each SD pair for protection concern, we set $\mathbf{O} = \{1,2\}$, where the variables with superscripts 1 and 2 are for the primary and backup connection, respectively. We use the general term *routing subgraph* to denote the primary tree and backup paths for all SD pairs used to serve a protected multicast demand. Here for each SD pair, the primary path and the backup path do not share any common link, not even a link in opposite directions.

5.3.1 Variables

$P_{d,ij}^{r,o}$ Binary; equals one if a path to destination d, $d \in \mathbf{F}_r$, of multicast connection r, $r \in \mathbf{R}$, traverses fiber link (i,j), $(i,j) \in \mathbf{L}$, for operation (primary or backup) indicator o, $o \in \mathbf{O}$; zero, otherwise.

X_{ij}^{r} Binary; equals one if fiber link (i,j), $(i,j) \in \mathbf{L}$, is included to serve multicast connection r, $r \in \mathbf{R}$.

Y_{ij}^{r} Binary; equals one if fiber link (i,j), $(i,j) \in \mathbf{L}$, is a primary link of multicast connection r, $r \in \mathbf{R}$.

D_r Real; denotes a distance that is longer than or equal to the longest distance among all the paths included in multicast connection r, $r \in \mathbf{R}$.

N_r Integer; denotes the number of FSs in primary links allocated to multicast connection r, $r \in \mathbf{R}$; $N_r \geq 0$.

K_m^r Binary; equals one if MS $m, m \in \mathbf{M}$, is assigned to multicast connection r, $r \in \mathbf{R}$; zero, otherwise.

S_r Integer; denotes the starting FS index of multicast connection r, $r \in \mathbf{R}$, $S_r \geq 1$.

E_r Integer; denotes the ending FS index of multicast connection r, $r \in \mathbf{R}$, $E_r \geq 1$.

T_{ij}^r Integer; denotes a number that is no smaller than the number of FSs in fiber link (i, j), $(i, j) \in \mathbf{L}$, assigned to multicast connection r, $r \in \mathbf{R}$, $T_{ij}^r \geq 0$.

$H_{r_2}^{r_1}$ Binary; equals one if a fiber link included to serve multicast connection r_1, $r_1 \in \mathbf{R}$, is a primary link of another multicast connection r_2, $r_2 \in \mathbf{R}$, where $r_1 \neq r_2$.

$Z_{r_2}^{r_1}$ Binary; equals zero if the ending FS index E_{r_2} of multicast connection r_2, $r_2 \in \mathbf{R}$, is smaller than the starting FS index S_{r_1} of another multicast connection r_1, $r_1 \in \mathbf{R}$, where $r_1 \neq r_2$, i.e., $S_{r_1} \geq E_{r_2} + 1$.

C Integer; maximum number among the numbers of required FSs in all fiber links.

5.3.2 Objective

$$\textbf{Minimize } \mathcal{G} \cdot C \tag{5.1}$$

The objective is to minimize the maximum spectrum among the required spectrum in all fiber links in the entire network.

5.3.3 Constraints

The constraints can be classified into five groups. The first group of constraints is called *searching and constructing a routing subgraph*, where the constraints ensure

that a pair of link-disjoint paths is found for each SD pair of a multicast connection and that a routing subgraph for the multicast connection is constructed by these paths for all SD pairs. The second group is called *modulation determination*. It consists of constraints ensuring that an MS is assigned to each multicast connection, and the transparent reach constraint is met. The third is the *spectrum assignment* group, where the constraints guarantee that a sufficient number of FSs are assigned to each multicast connection, and that the three constraints, namely, spectrum continuity, spectrum contiguity, and spectrum non-overlapping, are all met. The fourth is a group of *redundancy constraints* for faster solutions. The last group provides a *lower bound* on the number of FSs required in all links.

Searching and Constructing a Routing Subgraph

$$\sum_{(i,j)\in\mathbf{L}} P_{d,ij}^{r,o} = \begin{cases} 1, & i = s_r \text{ or } j = d, \\ 0, & j = s_r \text{ or } i = d, \end{cases} \quad \forall o \in \mathbf{O}, r \in \mathbf{R}, d \in \mathbf{F}_r \tag{5.2}$$

$$\sum_{(i,x)\in\mathbf{L}} P_{d,ix}^{r,o} = \sum_{(x,j)\in\mathbf{L}} P_{d,xj}^{r,o}, \quad \forall o \in \mathbf{O}, r \in \mathbf{R}, d \in \mathbf{F}_r, x \in \mathbf{V} \setminus \{s_r, d\} \tag{5.3}$$

$$\sum_{o\in\mathbf{O}} (P_{d,ij}^{r,o} + P_{d,ji}^{r,o}) \leq 1, \quad \forall r \in \mathbf{R}, d \in \mathbf{F}_r, (i,j) \in \mathbf{L} \tag{5.4}$$

$$\Delta \cdot Y_{ij}^{r} \geq \sum_{d\in\mathbf{F}_r} P_{d,ij}^{r,1}, \quad \forall r \in \mathbf{R}, (i,j) \in \mathbf{L} \tag{5.5}$$

$$\sum_{(i,j)\in\mathbf{L}} Y_{ij}^{r} \leq 1, \quad \forall r \in \mathbf{R}, j \in \mathbf{V} \tag{5.6}$$

$$\Delta \cdot X_{ij}^{r} \geq \sum_{d\in\mathbf{F}_r, o\in\mathbf{O}} P_{d,ij}^{r,o}, \quad \forall r \in \mathbf{R}, (i,j) \in \mathbf{L}. \tag{5.7}$$

Constraints (5.2) and (5.3) guarantee that the flow conservation requirement is met. They are used to search routing paths for all SD pairs of a multicast connection. Constraint (5.4) ensures that the primary and the backup paths for each SD pair of a multicast connection do not share common link(s), not even a link in opposite directions, i.e., they are link-disjoint. However, paths from different SD pairs could share common link(s). Constraint (5.5) ensures that a fiber link included in a primary path is a primary link included for the multicast connection. Constraint (5.6) guarantees that a primary tree is constructed by the primary paths by ensuring that each node in a tree has only one ingress fiber link. Constraint (5.7) ensures that a fiber link included in any path is used to serve the multicast connection.

Modulation Determination

$$\sum_{m \in \mathbf{M}} K_m^r = 1, \quad \forall r \in \mathbf{R} \tag{5.8}$$

$$D_r \geq \sum_{(i,j) \in \mathbf{L}} \ell_{ij} \cdot P_{d,ij}^{r,o}, \quad \forall o \in \mathbf{O}, r \in \mathbf{R}, d \in \mathbf{F}_r \tag{5.9}$$

$$\tau_m - D_r \geq \Delta \cdot (K_m^r - 1), \quad \forall r \in \mathbf{R}, m \in \mathbf{M}. \tag{5.10}$$

Constraint (5.8) ensures that one of the MSs is selected for each multicast connection. Constraints (5.9) and (5.10) guarantee that the transparent reach constraint is met. Constraint (5.9) ensures that a distance used to determine the MS assigned to each multicast connection is no shorter than the longest distance among all paths included in the multicast connection. Constraint (5.10) guarantees that the transparent reach of the selected MS for the multicast connection is no shorter than the longest distance among all paths.

Spectrum Assignment

As the MS is determined from the constraints above, the corresponding number of FSs for the multicast connection can be obtained. Further, spectrum assignment subject to the three constraints is presented as follows.

$$N_r = \sum_{m \in \mathbf{M}} \omega_m^r \cdot K_m^r, \quad \forall r \in \mathbf{R} \tag{5.11}$$

$$E_r = S_r + N_r - 1, \quad \forall r \in \mathbf{R} \tag{5.12}$$

$$H_{r_2}^{r_1} \geq X_{ij}^{r_1} + Y_{ij}^{r_2} - 1, \quad \forall (i,j) \in \mathbf{L}, r_1, r_2 \in \mathbf{R}, r_1 \neq r_2 \tag{5.13}$$

$$Z_{r_2}^{r_1} + Z_{r_1}^{r_2} = 1, \quad \forall r_1, r_2 \in \mathbf{R}, r_1 \neq r_2 \tag{5.14}$$

$$E_{r_2} - S_{r_1} \leq \Delta \cdot (Z_{r_2}^{r_1} + 1 - H_{r_2}^{r_1}) - 1, \quad \forall r_1, r_2 \in \mathbf{R}, r_1 \neq r_2 \tag{5.15}$$

$$E_{r_1} - S_{r_2} \leq \Delta \cdot (Z_{r_1}^{r_2} + 1 - H_{r_2}^{r_1}) - 1, \quad \forall r_1, r_2 \in \mathbf{R}, r_1 \neq r_2. \tag{5.16}$$

Constraint (5.11) ensures that a number of FSs in accordance to the selected MS are assigned to the multicast connection. Constraint (5.12) guarantees that spectrum contiguity constraint is satisfied by assigning a number, calculated by (5.11), of contiguous FSs, from the starting FS index to the ending FS index, to the multicast connection. Constraint (5.13) ensures that two multicast connections are said to share common link(s) if a link in the primary tree of one multicast connection is included to serve the other multicast connection. Constraints (5.14), (5.15), and (5.16) ensure spectrum continuity and spectrum non-overlapping between two multicast

connections. For the former, the same FSs, from the starting FS index to the ending FS index, in its primary links and backup-only links are allocated to and reserved for the multicast connection, respectively. For the latter, if a primary link of a multicast connection is also used (as either primary or backup link) to serve another multicast connection, the indices of the FSs of one multicast connection should be smaller than those of the FSs of the other multicast connection. This is because in shared protection, only the FSs for the primary connection are exclusive, FSs on a backup-only link are not exclusive for the multicast connection and can be cross-shared by other connections also only as backup.

Lower Bound

$$C \geq E_r, \quad \forall r \in \mathbf{R}. \tag{5.17}$$

Constraint (5.17) ensures that the maximum number among the numbers of FSs required in all fiber links is greater than or equal to the maximum number among the ending FS indexes of all multicast connections.

Redundancy Constraint

$$T_{ij}^r \geq \Delta \cdot (Y_{ij}^r - 1) + N_r, \quad \forall r \in \mathbf{R}, (i,j) \in \mathbf{L} \tag{5.18}$$

$$C \geq \sum_{r \in \mathbf{R}} T_{ij}^r, \quad \forall (i,j) \in \mathbf{L}. \tag{5.19}$$

Constraints (5.18) and (5.19) are used as redundancy to reduce the search region for faster solutions. Constraint (5.18) ensures that the number of FSs required in each fiber link is greater than or equal to that of the FSs assigned to the primary connection of each multicast connection. Constraint (5.19) ensures that each fiber link, included as a primary link of the multicast connections, should have at least the sum of the number of FSs assigned to those multicast connections.

5.4 Heuristic Algorithm

In principle, the mathematical formulation of the MC-RMSA problem with shared protection presented in Section 5.3 can be used by a MILP solver to find optimal solutions to the problem. However, MILP is computationally prohibitive for realistically sized networks. In this section, we develop an efficient heuristic algorithm to obtain near optimal solutions.

As with the presentation of the algorithm in Chapter 4, we first describe a routing algorithm that is dedicated to the MC-RMSA problem with shared protection. We then provide an algorithm to serve a single multicast demand. Finally we present another algorithm where multiple multicast demands are accommodated in a greedy manner for a low requirement of spectrum.

5.4.1 Routing for a Protected Tree

Our aim is to find a protected tree that will provide a disjoint path pair for each SD pair of a multicast session subject to the transparent reach constraint. For the MC-RMSA problem with shared protection, based on Algorithm 1, we introduce a routing scheme for survivable routing for the multicast session associated with a multicast demand. The routing scheme, called APPF, finds All Primary Paths First for all the SD pairs and then the corresponding link-disjoint ones as their backups. The spectrum used in a primary link of a connection cannot be shared with other connections. However, in shared protection, for better spectrum efficiency, the spectrum used in a backup-only link can also be shared among multiple multicast connections but only as backup. Thus, the graphs for finding the primary tree and the backup paths that are link-disjoint from their corresponding primary paths could be different; we denote them by $G_p = (\mathbf{V}_p, \mathbf{L}_p)$ and $G_b = (\mathbf{V}_b, \mathbf{L}_b)$, respectively.

In APPF, we start by initializing the cost of the links in $\mathbf{L}_p$ to one. Secondly, we implement MPH by repeatedly calling Algorithm 1 for G_p to find a primary path P_d

from the source to destination d, and resetting to zero the cost of the links traversed by P_d, until a path is found for each SD pair. Then, to guarantee that a primary tree is obtained by the primary paths discovered, we use Dijkstra's algorithm to find a shortest-path tree in a subgraph consisting of all links in the primary paths. In this case, the longest path among the paths to all destinations along the primary tree should have a distance no longer than the longest path among the primary paths for all SD pairs. Thirdly, we arrange the destinations in an increasing order of the number of links in their primary paths of the obtained primary tree. We then reset the cost of each link in $\mathbf{L}_b \setminus \mathbf{L}_p$ to zero, and the cost of each link in the obtained primary tree to zero, and the cost of the remaining links in $\mathbf{L}_b$ to one. In order to find a backup path P'_d that is link-disjoint from P_d for each destination d as ordered, we call Algorithm 1 for $G'_b = (\mathbf{V}_b, \mathbf{L}'_b)$, where $\mathbf{L}'_b$ is obtained by removing from $\mathbf{L}_b$ the links traversed by P_d and also the links in the reversed direction of P_d. Then we reset the cost of the links traversed by P'_d to zero. Finally, we obtain a primary tree with a minimum number of links and the backup paths that are link-disjoint from their corresponding primary paths for all SD pairs.

APPF calls Dijkstra's algorithm once and Algorithm 1 for a total of $2|\mathbf{F}_r|$ times, where $|\mathbf{F}_r|$ is the number of destinations of the multicast session. The former can be achieved at a complexity of $O(|\mathbf{V}|^2)$, and the latter has complexity of $O(|\mathbf{V}|^4)$. Thus, APPF has complexity of $O(|\mathbf{V}|^4|\mathbf{F}_r|)$.

5.4.2 Heuristic Algorithm for Provisioning a Single Demand

The heuristic algorithm for provisioning a multicast demand with shared protection is also based on the utilization of the SWP presented in Chapter 4. Figure 5.2 illustrates the usage of SWP for provisioning multicast with protection. The original graph and the usage of FSs in each fiber link are shown in Figs. 5.2a and 5.2b, respectively. Assume that a new demand, namely, D3, requests three FSs. Then, to accommodate

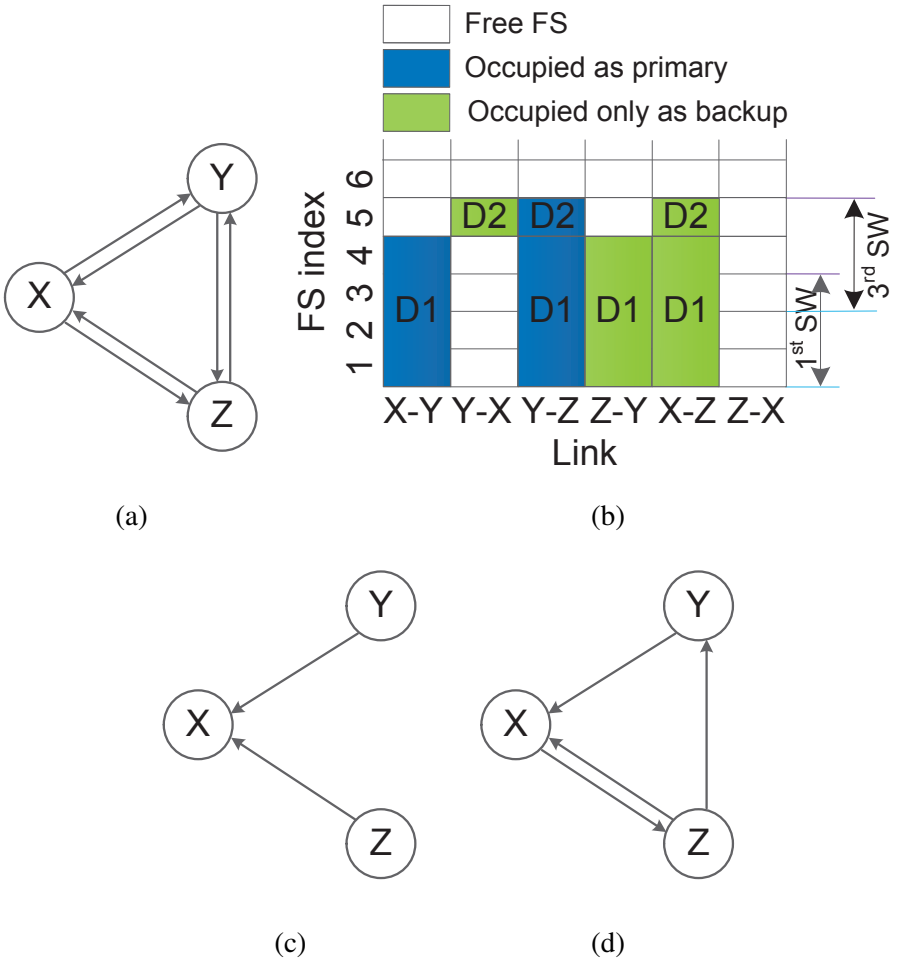

Fig. 5.2 Illustration for the concepts of SW and SWP: (a) an example network graph; (b) FSs usage; (c) a graph G_p on the first SWP for finding a primary tree for a demand requesting for 3 FSs; (d) a graph G_b of the first SWP for finding the backup paths for a demand requesting for 3 FSs.

it, an SW should contain three FSs. In each fiber link, there are several possible such SWs, e.g., the first SW, second SW, and third SW occupying FSs 1 to 3, 2 to 4, and 3 to 5, respectively. The first SW corresponds to the first SWP. If the first SW in a link is available, the link should be in the first SWP. A primary tree provisioned for a multicast connection cannot reuse the spectrum resources that are either allocated to or reserved for other connections, while backup-only spectrum resources can be shared among multiple connections but only as backup. In Figs. 5.2c and 5.2d, for the first SWP we provide a graph used for finding a primary tree and a graph for finding

Algorithm 4 Provisioning a demand with APPF

Input: A network graph $G = (\mathbf{V}, \mathbf{L})$, a multicast demand $r = \langle s_r; \mathbf{F}_r; t_r \rangle$, a set $\mathbf{M}_r$ of feasible MSs and their corresponding transparent reaches for r, the maximum number Ω among the FS indexes in a link, and an SWP starting-FS list;
Output: MC-RMSA for accommodating r.

while r has not been accommodated, **do**
  for all MS m in $\mathbf{M}_r$ from the highest to the lowest modulation level, **do**
    Obtain the number, i.e., ω_m^r, of required FSs for r and the transparent reach τ_m assuming that MS m is utilized;
    for all FS index α, $\alpha + \omega_m^r - 1 \leq \Omega$, from lowest to highest in the SWP starting-FS list, **do**
      Obtain an SWP whose SW starts from this FS index α and ends at FS index ε, $\varepsilon = \alpha + \omega_m^r - 1$;
      Obtain two graphs, namely, $G_p = (\mathbf{V}_p, \mathbf{L}_p)$ and $G_b = (\mathbf{V}_b, \mathbf{L}_b)$;
      Call APPF with the inputs of the two graphs, a multicast session $\langle s_r; \mathbf{F}_r; t_r \rangle$, and a distance τ_m, to find a routing subgraph for r;
      if such a routing subgraph is found, **then**
        Accommodate r by allocating and reserving the FSs of the present SW in its primary links and backup-only links, respectively;
        Insert FS index $\varepsilon + 1$ into the SWP starting-FS list in an increasing order;
      end if
    end for
  end for
end while

the backup paths, respectively. The latter graph contains two more backup-only links, namely, links (X,Z) and (Z,Y), than the former graph.

Assuming that a set of feasible MSs is given, for each multicast demand, we try to assign the MSs from the highest to the lowest modulation level. For a given MS, we calculate the number of required FSs. Then, given FS usage in each fiber link, we scan the SWPs to obtain two graphs, denoted by G_p and G_b, which are used to find the primary tree and the backup paths, respectively. After that, we call a routing scheme to find a pair of primary and backup paths for each SD pair of the multicast connection. The details are presented in Algorithm 4.

Since the complexity of APPF is $O(|\mathbf{V}|^4|\mathbf{F}_r|)$, Algorithm 4 calls it at most $|\mathbf{M}|\Omega$ times, where $|\mathbf{M}|$ and Ω are the numbers of considered MSs and FSs in each fiber link. Thus, Algorithm 4 has a complexity of $O(|\mathbf{V}|^4|\mathbf{F}_r||\mathbf{M}|\Omega)$.

5.4.3 Provisioning of Multiple Demands

Firstly, we assume that we can find a routing subgraph for every multicast session. This is done by running Dijkstra's algorithm to first find a shortest path tree in the original graph and then running Dijkstra's algorithm again for each SD pair to find a shortest path in a modified graph by removing the links traversed by the path in the tree of both directions. The distances of the paths to all destinations are within the transparent reach of the lowest-level MS considered, e.g., 4,000 km for BPSK.

Then, to serve a multicast demand, given a set of MSs, we find a set of feasible MSs it can utilize and a routing subgraph that includes the fewest links for the feasible highest-level MS. Firstly, we obtain a routing subgraph $\mathfrak{R}_1$ by running Dijkstra's algorithm to find a shortest path tree for the multicast, and for each SD pair a shortest path that is link-disjoint from the path in the tree. Then, we can obtain the longest distance among all paths, and therefore obtain the highest-level MS m_1 that $\mathfrak{R}_1$ can utilize. We also try the given MSs from the highest to the lowest level until a routing subgraph $\mathfrak{R}_2$ can be found by APPF. Similarly, we can obtain the highest-level MS m_2 that $\mathfrak{R}_2$ can utilize. After that, we select the higher-level MS, denoted by m, between m_1 and m_2, and record the corresponding routing subgraph as a *candidate routing subgraph*. If m_1 and m_2 are the same, we set $m = m_1$ and we record as a candidate routing subgraph the routing subgraph that has fewer primary links (first consideration) and fewer total links (secondary consideration). Accordingly, we obtain a set of feasible MSs that are not of higher-level than m.

Thirdly, after the set of feasible MSs is found for a multicast demand, we call Algorithm 4 that attempts to allocate the demand with the residual resources in the

network. If the allocation is not successful, we repeatedly add one FS in each fiber and attempt Algorithm 4 on the newly available SWPs. When the number of added FSs is enough for the highest-level feasible MS, the demand is then accommodated by its candidate routing subgraph obtained beforehand with the spectrum of the added FSs.

As the order that the demands are served affects the result, we consider two ordering methods. Similar to the traffic-volume-decreasing order in [66], one method is to arrange the requested multicast connections in decreasing order of the number of required FSs assuming that the highest-level feasible MS is assigned to each demand. The other is to randomly shuffle the demands to obtain a random sequence of demands. The requested multicast connections are sequentially served as follows. For the latter one, we consider the multi-iteration process discussed in Chapter 4 to further improve the performance of the algorithm as we observe in the same chapter.

5.5 Numerical Results

In this section, we present numerical results for the MC-RMSA problem with shared protection. We compare the performance of the proposed heuristic algorithm with the optimum obtained by solving the MILP formulation. We investigate the impact of the number of demand sequences on the performance of the heuristic algorithms. Moreover, we simulate a more straightforward approach where arriving demands are served one by one.

5.5.1 Optimization for Static Multicast Traffic

1) Test Conditions

We consider the following three test networks: (1) the six-node n6s9 network as shown in Fig. 4.2, (2) the 11-node COST239 network, and (3) the 24-node USNET

network as shown in Figs. 3.7a and 3.7b, respectively. The bandwidth of an FS in each fiber is 12.5 GHz. We consider three MSs, namely, BPSK, QPSK, and 8QAM. The MSs and the corresponding transparent reaches are set as shown in Table 3.1. We consider 10 sets of multicast demands. Because of the known computational limitations of the MILP formulation, we only assume that each set contains 10 multicast demands for the n6s9 network, and compare the performance of the algorithm with the optimal MILP solution. We use a commercial optimization software, i.e., AMPL/Gurobi 6.5.1 [145], to solve the MILP problem. For the other two larger networks, each set contains 50 multicast demands, and we compare the performance of the proposed heuristic algorithm with different ordering methods. The multicast sessions of the considered demands are obtained by randomly shuffling the set of network nodes. The bit rate values of the demands follow a uniform distribution of range (100, 200) Gb/s. We use up to 10,000 random sequences for each set of demands, and investigate the number of random sequences on the performance of the algorithm as in the previous chapter. We also look into the relationship between the required spectrum and the number of destinations.

Henceforth, the following notations, names and abbreviations are used. We use "MILP" to stand for the MILP approach. For the heuristic algorithm, we use a prefix, i.e., "APPF_G," to denote the algorithm that uses Algorithm 4 with APPF as the routing scheme in the Greedy algorithm. We also use several suffixes to denote the type of ordering of the demands used in the algorithm. For instance, the suffix "_DO" is used when the set of demands is arranged in a Decreasing Order mentioned above. The remaining suffixes in this paper are used to denote a multi-iteration process with a certain number of considered random sequences, e.g., "_1000" for 1,000 randomly shuffled sequences. In this way, we can obtain the short name of a greedy algorithm by combining the prefix and a suffix. For example, "APPF_G_100" is the short name of a greedy algorithm that employs Algorithm 4 with APPF considering 100 random sequences for each set of demands.

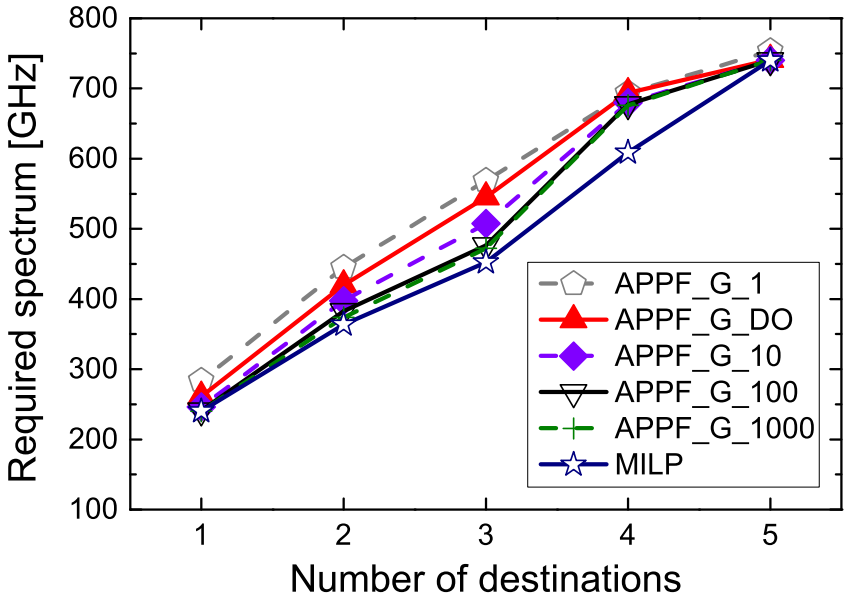

Fig. 5.3 Performance comparison for the n6s9 network (10 demands).

2) Numerical Results and Performance Comparison

For the n6s9 network, we compare the performance of the proposed heuristic algorithm with the optimal MILP algorithm. As shown in Fig. 5.3, with the increase of the number of destinations, the amount of required spectrum steadily increases. The heuristic algorithm, APPF_G_DO, which is based on ordering the demands in a decreasing order of their FS requirements, requires on average 11.8% more spectrum than the optimum. For the multi-iteration methods, the one with one random sequence performs the worst among all approaches. The one with 100 random sequences, i.e., APPF_G_100, has a significant improvement over APPF_G_1, and outperforms APPF_G_DO. Also, APPF_G_100 achieves performance close to MILP, and consumes on average 4.4% more spectrum than the optimum. This demonstrates the benefit of the multi-iteration process. Additional (but not so significant) improvement is achieved by increasing the number of the random sequences to 1,000. Thus, 100 random sequences are considered sufficient to achieve near optimum for the n6s9 network with 10 demands. For the broadcast case, the multi-iteration process does not help much. The heuristic approaches achieve optimum and near optimum

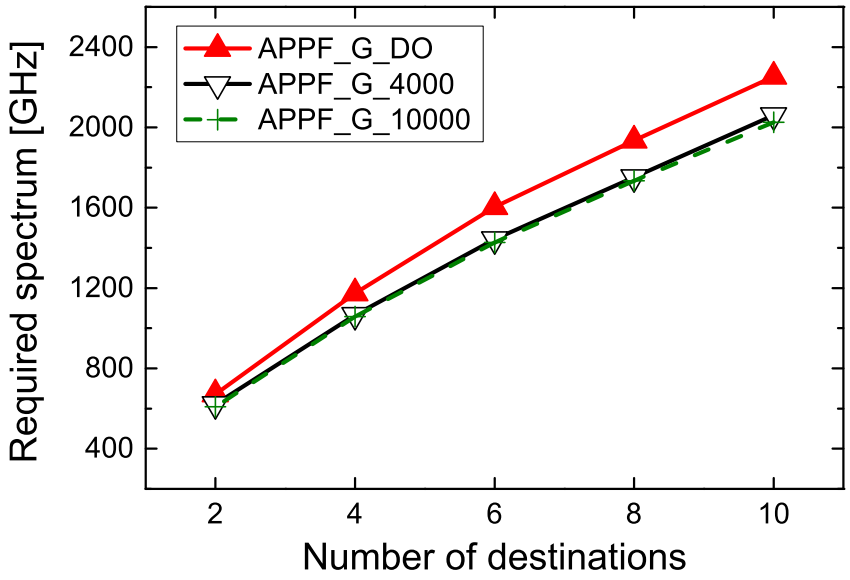

Fig. 5.4 Performance comparison for the COST239 network (50 demands).

since the average nodal degree, i.e., 3, is low, and the probability of accommodating two or more multicast connections that cross-share backup spectrum resources is therefore low.

For the COST239 network, the performance comparison is shown in Fig. 5.4. Similarly, the required spectrum increases steadily as the number of destinations increases. Since we have more demands than in the previous case, for multi-iteration processes, we increase the number of considered random sequences to look into the impact of the number of demand sequences on performance. The heuristic approach with 4,000 random sequences, i.e., APPF_G_4000, saves on average around 9% spectrum compared to the one with a single decreasingly ordered sequence, i.e., APPF_G_DO. We also observe when comparing APPF_G_10000 to APPF_G_4000, only marginal improvement is obtained for two-and-one-half times the number of random sequences considered. Thus, 4,000 random sequences are considered sufficient for 50 demands. For the remaining USNET network, we also consider 4,000 random sequences for 50 demands. Moreover, for the case of broadcast, the COST239 network achieves more benefits in this multi-iteration process than the n6s9 network. The reason is that COST239 has a relatively high nodal degree,

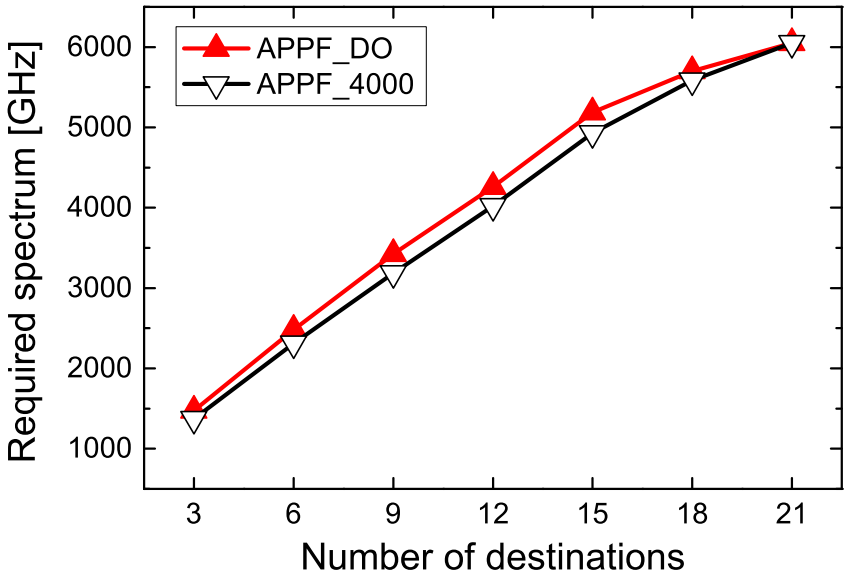

Fig. 5.5 Performance comparison for the USNET network (50 demands).

i.e., 4.7, than n6s9, and thus there is a higher possibility of finding a solution with spectrum resource sharing.

We also consider 50 demands for the USNET network as shown in Fig. 5.5. The number of destinations increases, the amount of required spectrum climbs. Also, for the ordering methods of the demands, an approach considering 4000 random sequences, i.e., APPF_G_4000, saves on average 4.8% spectrum compared to APPF_G_DO. Similar to the case in the n6s9 network, such a multi-iteration process does not improve much when there are many destinations in a multicast session, e.g., 18, as the average nodal degree of USNET is also low, i.e., 3.6.

5.5.2 Markov-Chain Simulation for Dynamic Multicast Traffic with Limited Holding Times

In Section 5.5.1, we assumed that the holding times of the multicast traffic are unlimited and proposed a heuristic approach to the problem. In this section, we adapt this proposed approach to a scenario involving dynamic traffic with limited holding times and show that the performance is good also for such a dynamic scenario.

So far we have considered a static model to minimize the maximum spectrum among the required spectrum in all links for accommodating a given set of unordered demands. Here, we model the network as a dynamic system where multicast demands are admitted and complete their service stochastically over time. In particular, we consider a finite set of multicast demands, each of which can be either *active* or *inactive* at any point in time. We use the term *arrival* to designate a multicast demand attempting to obtain service in the network. An arrival can be either admitted or blocked. If an arrival is admitted, the state of the multicast demand associated with that arrival will change its state from inactive to active, and it will stay active for a period of time (holding time) which is exponentially distributed with mean $1/\mu$. Then, it completes its service and becomes inactive again. A multicast demand will stay inactive for an exponential amount of time with mean $1/\lambda$ until it attempts to enter the system to generate an arrival. Our network has a capacity limitation defined by a finite number of FSs. If a multicast demand arrives and there are no sufficient FSs to accommodate the demand, this new arrival will be blocked. A common performance measure for such a dynamic system is the blocking probability, defined as the ratio of the number of blocked arrivals of multicast demands to the total number of arrivals. Let $\rho = \lambda/\mu$ be a measure of traffic load in our dynamic system.

1) Simulation Conditions

We use the USNET network as a test network, and consider a set of 50 randomly generated demands. The number of demand destinations follows a uniform distribution from one (unicast) to 23 (broadcast). The bit rates also follow a uniform distribution with range (100, 200) Gb/s. For these settings, a static optimization problem, considering that the demands are given unordered, is to minimize the maximum number among the numbers of required FSs in all links under the condition that all multicast

demands are accommodated. For such a static problem, we employ APPF_G_4000 to obtain the nearly optimal number $\mathcal{F}$ of FSs required in each link. Then, in the dynamic case, simulated by a Markov chain simulation, we assume that there are $\mathcal{F}$ FSs in each link for the network being considered. In such a network, the demands can always be accommodated by the solution of APPF_G_4000, and multiple arrivals of a demand are accommodated with exactly the same spectrum and routing subgraph. Thus, we have no blocking for the approach based on APPF_G_4000 with $\mathcal{F}$ FSs in each link. However, for a more straightforward method in dynamic systems, where demands are served one by one, the blocking probability can be significant. Accommodating a demand based on the available network resources upon the arrival will generate different solutions for different returns of the demand. Under this straightforward approach, we use Algorithm 4 with the APPF routing scheme to attempt admitting each arrival of the demands. We consider a range of scenarios from light to heavy traffic load. For each traffic load scenarios, we conduct 11 simulation experiments, each considering one million arrivals for the given demands, and take the average over the 11 results with a confidence interval of 95% as the final result.

2) Simulation Results

The blocking performance is shown in Fig. 5.6, where we provide the error bars though the upper and lower bounds are quite close. As we can see, the straightforward approach for dynamic systems, denoted as "Straightforward" in the figure, has losses. The blocking probability increases with increasing ρ. Specifically, when the traffic load is light $\rho = 1$, the blocking probability is low, 1.209×10^{-4}. However, it rises dramatically to about 42% when $\rho = 10$, and a further increase of blocking probability can be observed for a larger ρ, i.e., heavier traffic load. In contrast, our approach, denoted as "APPF_G_4000" in the figure, does not have service blocking at all for any ρ. This is because the APPF_G_4000 approach minimizes the

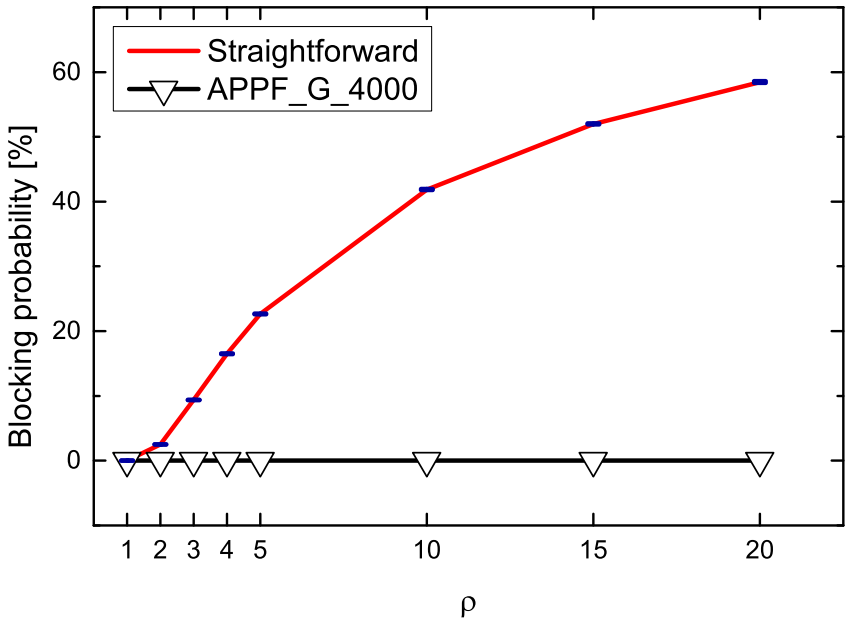

Fig. 5.6 Blocking probability comparison between the straightforward and our solutions versus ρ for the USNET network (50 demands).

maximum spectrum among the required spectrum in all links subject to the condition that all the given demands are accommodated. For a network where each fiber link is equipped with the minimized maximum required spectrum, each time a call arrives, the demand can always be served using the solution based on APPF_G_4000, and there will be no blocking.

5.6 Summary

We have considered multicast-capable routing, modulation and spectrum assignment for an elastic all-optical network with shared protection. For such a network, we have provided a MILP formulation, and developed a new polynomial time heuristic algorithm for a range of cases. Because the serving order of the demands affects the result, we have considered two cases: One is where the demands are arranged in a sequence in decreasing order of their FSs requirements, and the other is to randomly shuffle the demands and obtain a randomly ordered demand sequence. Numerical results show that the heuristic algorithm achieves close performance to

the optimal MILP solution. The heuristic algorithm based on shuffling the demands outperforms the one with specifically ordered demands. We provided complexity analysis to prove that the heuristic algorithm has polynomial time complexity. We considered various cases to demonstrate the scalability of the heuristic algorithm, and the improvement in the quality of the result that can be achieved by considering more demand sequences at the cost of longer running time. In this way, we now have a solution where a tradeoff exists between the performance and the running time. The above-mentioned heuristic approach is based on the assumption that the holding times of multicast traffic are unlimited. Then, we adapted this proposed approach to dynamic traffic with limited holding times and compared it to a more straightforward method using a Markov-chain simulation, where multicast demands are admitted and complete their service stochastically over time. Results show the good performance of the proposed approach also in the dynamic traffic where the straightforward method leads to significant losses under heavy traffic load while our heuristic approach has no losses.

Chapter 6

Conclusions

In this thesis, we considered the provision of multicast services in the context of EONs involving distance-adaptive transmission. We first compared the existing schemes to provision a single multicast demand, then we considered the network design problem of accommodating multiple multicast demands, and finally we introduced protection in the network design.

There are three technologies, namely, lightpath, light-tree, and light-trail, which can be used to accommodate multicast demands. To investigate their effectiveness in provisioning multicast services, we conducted a comparative study of the five schemes, namely, lightpath, light-tree, multi-light-tree, light-trail, and multi-light-trail. We considered distance-adaptive transmission in EONs. We compared their spectrum and transmitter usage. From the perspective of spectrum usage, the multi-light-tree has the lowest requirement among the five schemes. The light-tree scheme is not an efficient solution for densely connected networks; neither the lightpath approach nor the light-trail scheme is efficient for spare networks. From the aspect of transmitter usage, the lightpath scheme always has the highest requirement of transmitters while the light-trail and light-tree schemes have the lowest, while the remaining two schemes lying in-between. We also evaluate the benefit of using distance-adaptive transmission. For all the schemes, spectrum savings are observed.

Moreover, with increased network density, the benefit become more significant. In particular, considerable savings are seen for the lightpath, multi-light-tree and multi-light-trail schemes.

We then focused on the light-tree scheme, where each multicast is provisioned by a light-tree, and addressed the problem of accommodating multiple multicast demands in EONs with distance-adaptive transmission. We provided an MILP formulation and proposed an efficient heuristic algorithm for real-size problems. We investigated the sequence in which the demands are accommodated as it affects the performance of the heuristics, and proposed a couple of ordering strategies for good solutions. Moreover, to demonstrate the effectiveness of the proposed algorithm, we compared it to the existing approaches.

Survivability is an import attribute of optical networks. To enable the network to continue to operate under any single link failure, we further considered protecting the light-trees that are used to provision multicast services in EONs. Between the dedicated and shared protection strategies, in this thesis we focused on the latter for its high spectral efficiency as the backup resources can be shared to protect multiple demands under the condition that their primary connections do not fail simultaneously. For a single multicast, in addition to the case that the backup path from the source to a destination is link-disjoint from all the primary paths in the light-tree, the protection scheme considered in this thesis allows the backup path to share common links with the primary paths to other destinations. This increases spectrum efficiency.

In the comparison made in this thesis we observed that the multi-light-tree approach is more spectrally efficient than the light-tree scheme as the former is more flexible in provisioning a multicast than the latter but at the cost of a few more transceivers. This enhanced flexibility increases the complexity of the problem, and makes protection for the multicast provisioned by the multi-light-tree scheme even more challenging yet interesting for higher spectrum efficiency. The light-trail

technology may also be applied in some specific situations such as EONs with a ring structure, as it adapts to the network with a more cost-effective node architecture. Survivability can be considered in the design; these have not yet been studied and can be considered in future work.

References

[1] Cisco, "Cisco visual networking index: Forecast and methodology, 2015–2020," 2016. [Online]. Available: http://www.cisco.com/c/en/us/solutions/collateral/service-provider/visual-networking-index-vni/complete-white-paper-c11-481360.html

[2] M. Jinno, H. Takara, B. Kozicki, Y. Tsukishima, Y. Sone, and S. Matsuoka, "Spectrum-efficient and scalable elastic optical path network: architecture, benefits, and enabling technologies," *IEEE Communications Magazine*, vol. 47, pp. 66–73, Nov. 2009.

[3] K. Christodoulopoulos, I. Tomkos, and E. A. Varvarigos, "Routing and spectrum allocation in OFDM-based optical networks with elastic bandwidth allocation," in *Proc. IEEE Global Communications Conference*, 2010, pp. 1–6.

[4] B. C. Chatterjee, N. Sarma, and E. Oki, "Routing and spectrum allocation in elastic optical networks: A tutorial," *IEEE Communications Surveys and Tutorials*, vol. 17, no. 3, pp. 1776–1800, 2015.

[5] K. Christodoulopoulos, I. Tomkos, and E. Varvarigos, "Elastic bandwidth allocation in flexible OFDM-based optical networks," *IEEE/OSA Journal of Lightwave Technology*, vol. 29, no. 9, pp. 1354–1366, May 2011.

[6] S. Peng, R. Nejabati, and D. Simeonidou, "Role of optical network virtualization in cloud computing [invited]," *IEEE/OSA Journal of Optical Communications and Networking*, vol. 5, no. 10, pp. A162–A170, Oct. 2013.

[7] Y. Lui, G. Shen, and W. Shao, "Design for energy-efficient IP over WDM networks with joint lightpath bypass and router-card sleeping strategies," *IEEE/OSA Journal of Optical Communications and Networking*, vol. 5, no. 11, pp. 1122–1138, Nov. 2013.

[8] C. Wang, G. Shen, and S. K. Bose, "Distance adaptive dynamic routing and spectrum allocation in elastic optical networks with shared backup path protection," *IEEE/OSA Journal of Lightwave Technology*, vol. 33, no. 14, pp. 2955–2964, Jul. 2015.

[9] L. Chiaraviglio, M. Mellia, and F. Neri, "Energy-aware backbone networks: a case study," in *Proc. IEEE International Conference on Communications*, 2009, pp. 1–5.

[10] Cisco, "Cisco global cloud index: Forecast and methodology, 2015–2020," 2016. [Online]. Available: http://www.cisco.com/c/dam/en/us/solutions/collateral/service-provider/global-cloud-index-gci/white-paper-c11-738085.pdf

[11] R. Mijumbi, J. Serrat, J.-L. Gorricho, N. Bouten, F. De Turck, and R. Boutaba, "Network function virtualization: State-of-the-art and research challenges," *IEEE Communications Surveys and Tutorials*, vol. 18, no. 1, pp. 236–262, 2016.

[12] M. Jinno, H. Takara, and B. Kozicki, "Dynamic optical mesh networks: drivers, challenges and solutions for the future," in *Proc. European Conference on Optical Communication*, 2009, pp. 1–4.

[13] Cisco, "The zettabyte era: trends and analysis," 2017. [Online]. Available: https://www.cisco.com/c/en/us/solutions/collateral/service-provider/visual-networking-index-vni/vni-hyperconnectivity-wp.pdf

[14] O. Gerstel, M. Jinno, A. Lord, and S. J. B. Yoo, "Elastic optical networking: a new dawn for the optical layer?" *IEEE Communications Magazine*, vol. 50, no. 2, pp. s12–s20, Feb. 2012.

[15] A. Cai, Z. Fan, K. Xu, M. Zukerman, and C.-K. Chan, "Elastic versus WDM networks with dedicated multicast protection," *IEEE/OSA Journal of Optical Communications and Networking*, vol. 9, no. 11, pp. 921–933, Nov. 2017.

[16] L. H. Sahasrabuddhe and B. Mukherjee, "Multicast routing algorithms and protocols: A tutorial," *IEEE Network*, vol. 14, no. 1, pp. 90–102, 2000.

[17] G. N. Rouskas, "Optical layer multicast: rationale, building blocks, and challenges," *IEEE Network*, vol. 17, no. 1, pp. 60–65, Jan. 2003.

[18] Y. Zhou and G. S. Poo, "Optical multicast over wavelength-routed WDM networks: a survey," *Optical Switching and Networking*, vol. 2, no. 3, pp. 176–197, Nov. 2005.

[19] G. Zhang, M. D. Leenheer, A. Morea, and B. Mukherjee, "A survey on OFDM-based elastic core optical networking," *IEEE Communications Surveys and Tutorials*, vol. 15, no. 1, pp. 65–87, Mar. 2013.

[20] B. Mukherjee, *Optical WDM Networks*. Springer Science & Business Media, 2006.

[21] R. Ramaswami, K. Sivarajan, and G. Sasaki, *Optical networks: a practical perspective*. Morgan Kaufmann, 2009.

[22] ITU-T Recommendation G.694.1, "Spectral grids for WDM applications: DWDM frequency grid," Feb. 2016.

[23] A. Stavdas, C. Matrakidis, M. Gunkel, A. Asensio, L. Velasco, E. Varvarigos, and K. Christodoulopoulos, "Taking advantage of elastic optical networks," in *Elastic Optical Networks*. Springer, 2016, pp. 31–54.

[24] W. Shieh and I. Djordjevic, *OFDM for Optical Communications*. Academic Press, 2010.

[25] G. Bosco, A. Carena, V. Curri, P. Poggiolini, and F. Forghieri, "Performance limits of Nyquist-WDM and CO-OFDM in high-speed PM-QPSK systems," *IEEE Photonics Technology Letters*, vol. 22, no. 15, pp. 1129–1131, 2010.

[26] P. Wright, A. Lord, and S. Nicholas, "Comparison of optical spectrum utilization between flexgrid and fixed grid on a real network topology," in *Proc. Optical Fiber Communication Conference and Exposition/National Fiber Optic Engineers Conference*, 2012, pp. OTh3B–5.

[27] I. Tomkos, S. Azodolmolky, J. Solé-Pareta, D. Careglio, and E. Palkopoulou, "A tutorial on the flexible optical networking paradigm: state of the art, trends, and research challenges," *Proceedings of the IEEE*, vol. 102, no. 9, pp. 1317–1337, Sep. 2014.

[28] R. Schmogrow, M. Winter, M. Meyer, D. Hillerkuss, S. Wolf, B. Baeuerle, A. Ludwig, B. Nebendahl, S. Ben-Ezra, J. Meyer *et al.*, "Real-time Nyquist pulse generation beyond 100 Gbit/s and its relation to ofdm," *Optics Express*, vol. 20, no. 1, pp. 317–337, 2012.

[29] G. Bosco, "Spectrally efficient multiplexing: Nyquist-WDM," *Enabling Technologies for High Spectral-Efficiency Coherent Optical Communication Networks*, pp. 123–156, 2016.

[30] J.-X. Cai, Y. Cai, C. R. Davidson, D. G. Foursa, A. J. Lucero, O. V. Sinkin, W. W. Patterson, A. N. Pilipetskii, G. Mohs, and N. S. Bergano, "Transmission of 96 $\times$100-Gb/s bandwidth-constrained PDM-RZ-QPSK channels with 300% spectral efficiency over 10610 km and 400% spectral efficiency over 4370 km," *IEEE/OSA Journal of Lightwave Technology*, vol. 29, no. 4, pp. 491–498, Feb. 2011.

[31] J.-X. Cai, H. Zhang, H. G. Batshon, M. Mazurczyk, O. V. Sinkin, D. G. Foursa, A. N. Pilipetskii, G. Mohs, and N. S. Bergano, "200 Gb/s and dual wavelength 400 Gb/s transmission over transpacific distance at 6.0 b/s/hz spectral efficiency," *IEEE/OSA Journal of Lightwave Technology*, vol. 32, no. 4, pp. 832–839, Feb. 2014.

[32] W. Shieh, X. Yi, Y. Ma, and Q. Yang, "Coherent optical OFDM: has its time come? [Invited]," *Journal of Optical Networking*, vol. 7, no. 3, pp. 234–255, Mar. 2008.

[33] J. Armstrong, "OFDM for optical communications," *IEEE/OSA Journal of Lightwave Technology*, vol. 27, no. 3, pp. 189–204, 2009.

[34] X. Liu, S. Chandrasekhar, P. J. Winzer, B. Zhu, D. W. Peckham, S. Draving, J. Evangelista, N. Hoffman, C. J. Youn, Y.-H. Kwon *et al.*, "3$\times$ 485-Gb/s WDM transmission over 4800 km of ulaf and 12$\times$ 100-GHz wsss using CO-OFDM and single coherent detection with 80-GS/s adcs," in *Proc. Optical Fiber Communication Conference and Exposition/National Fiber Optic Engineers Conference*, 2011, pp. 1–3.

[35] S. Chandrasekhar and X. Liu, "OFDM based superchannel transmission technology," *IEEE/OSA Journal of Lightwave Technology*, vol. 30, no. 24, pp. 3816–3823, Dec. 2012.

[36] A. Napoli, D. Rafique, M. Bohn, M. Nölle, J. K. Fischer, and C. Schubert, "Transmission in elastic optical networks," in *Elastic Optical Networks*. Springer, 2016, pp. 83–116.

[37] A. N. Patel, P. N. Ji, J. P. Jue, and T. Wang, "Routing, wavelength assignment, and spectrum allocation in transparent flexible optical WDM (FWDM) networks," in *Proc. Photonics in Switching*, 2010, p. PDPWG1.

[38] O. Rival and A. Morea, "Elastic optical networks with 25–100g format-versatile WDM transmission systems," in *Proc. OptoElectronics and Communications Conference*, 2010, pp. 100–101.

[39] Y. Zhang, M. O'Sullivan, and R. Hui, "Digital subcarrier multiplexing for flexible spectral allocation in optical transport network," *Optics Express*, vol. 19, no. 22, pp. 21 880–21 889, 2011.

[40] M. Jinno, B. Kozicki, H. Takara, A. Watanabe, Y. Sone, T. Tanaka, and A. Hirano, "Distance-adaptive spectrum resource allocation in spectrum-sliced elastic optical path network," *IEEE Communications Magazine*, vol. 48, no. 8, pp. 138–145, Aug. 2010.

[41] N. M. K. Chowdhury and R. Boutaba, "A survey of network virtualization," *Computer Networks*, vol. 54, no. 5, pp. 862–876, 2010.

[42] M. Jinno, H. Takara, and B. Kozicki, "Concept and enabling technologies of spectrum-sliced elastic optical path network (SLICE)," in *Proc. Asia Communications and Photonics Conference and Exhibition*, 2009.

[43] M. Klinkowski, M. Ruiz, L. Velasco, D. Careglio, V. Lopez, and J. Comellas, "Elastic spectrum allocation for time-varying traffic in flexgrid optical networks," *IEEE Journal on Selected Areas in Communications*, vol. 31, no. 1, pp. 26–38, 2013.

[44] X. Zhao, A. Cai, G. Shen, and S. K. Bose, "Optimal time-dependent spectrum sharing between neighboring elastic optical channels over a single link," in *Proc. Asia Communications and Photonics Conference and Exhibition*, 2013, pp. AF4F–4.

[45] A. Cai, G. Shen, and L. Peng, "Optimal planning for electronic traffic grooming in ip over elastic optical networks," in *Proc. Asia Communications and Photonics Conference and Exhibition*, 2013, pp. AF4G–5.

[46] S. Zhang, C. Martel, and B. Mukherjee, "Dynamic traffic grooming in elastic optical networks," *IEEE Journal on Selected Areas in Communications*, vol. 31, no. 1, pp. 4–12, 2013.

[47] O. A. Gerstel, "Flexible use of spectrum and photonic grooming," in *Proc. Photonics in Switching*, 2010, p. PMD3.

[48] M. Jinno, H. Takara, Y. Sone, K. Yonenaga, and A. Hirano, "Multiflow optical transponder for efficient multilayer optical networking," *IEEE Communications Magazine*, vol. 50, no. 5, 2012.

[49] N. Sambo, A. D'Errico, C. Porzi, V. Vercesi, M. Imran, F. Cugini, A. Bogoni, L. Potì, and P. Castoldi, "Sliceable transponder architecture including multiwavelength source," *IEEE/OSA Journal of Optical Communications and Networking*, vol. 6, no. 7, pp. 590–600, 2014.

[50] G. Zhang, M. De Leenheer, and B. Mukherjee, "Optical grooming in OFDM-based elastic optical networks," in *Proc. Optical Fiber Communication Conference and Exposition/National Fiber Optic Engineers Conference*, 2012, pp. 1–3.

[51] ——, "Optical traffic grooming in OFDM-based elastic optical networks [invited]," *IEEE/OSA Journal of Optical Communications and Networking*, vol. 4, no. 11, pp. B17–B25, 2012.

[52] N. Amaya, G. Zervas, and D. Simeonidou, "Introducing node architecture flexibility for elastic optical networks," *IEEE/OSA Journal of Optical Communications and Networking*, vol. 5, no. 6, pp. 593–608, 2013.

[53] G. Baxter, S. Frisken, D. Abakoumov, H. Zhou, I. Clarke, A. Bartos, and S. Poole, "Highly programmable wavelength selective switch based on liquid crystal on silicon switching elements," in *Proc. Optical Fiber Communication Conference and Exposition/National Fiber Optic Engineers Conference*, 2006, pp. 3–pp.

[54] R. Ryf, Y. Su, L. Moller, S. Chandrasekhar, X. Liu, D. T. Neilson, and C. R. Giles, "Wavelength blocking filter with flexible data rates and channel spacing," *IEEE/OSA Journal of Lightwave Technology*, vol. 23, no. 1, pp. 54–61, 2005.

[55] B. Kozicki, H. Takara, Y. Tsukishima, T. Yoshimatsu, K. Yonenaga, and M. Jinno, "Experimental demonstration of spectrum-sliced elastic optical path network (slice)," *Optics Express*, vol. 18, no. 21, pp. 22 105–22 118, 2010.

[56] Y. Li, L. Gao, G. Shen, and L. Peng, "Impact of roadm colorless, directionless, and contentionless (cdc) features on optical network performance [invited]," *IEEE/OSA Journal of Optical Communications and Networking*, vol. 4, no. 11, pp. B58–B67, 2012.

[57] T. Takagi, H. Hasegawa, K.-i. Sato, Y. Sone, A. Hirano, and M. Jinno, "Disruption minimized spectrum defragmentation in elastic optical path networks that adopt distance adaptive modulation," in *Proc. European Conference on Optical Communication*, 2011, pp. Mo–2.

[58] H. Zang, J. P. Jue, and B. Mukherjee, "A review of routing and wavelength assignment approaches for wavelength-routed optical WDM networks," *Optical Networks Magazine*, vol. 1, no. 1, pp. 47–60, Jan. 2000.

[59] A. Rosa, C. Cavdar, S. Carvalho, J. Costa, and L. Wosinska, "Spectrum allocation policy modeling for elastic optical networks," in *Proc. International Conference on High Capacity Optical Networks and Enabling Technologies*, 2012, pp. 242–246.

[60] S. Azodolmolky, M. Klinkowski, E. Marand, D. Careglio, J. S. Pareta, and I. Tomkos, "A survey on physical layer impairments aware routing and wavelength assignment algorithms in optical networks," *Computer Networks*, vol. 53, no. 7, pp. 926–944, May 2009.

[61] Y. Wang, X. Cao, and Q. Hu, "Routing and spectrum allocation in spectrum-sliced elastic optical path networks," in *Proc. IEEE International Conference on Communications*, 2011, pp. 1–5.

[62] Y. Wang, X. Cao, and Y. Pan, "A study of the routing and spectrum allocation in spectrum-sliced elastic optical path networks," in *Proc. IEEE International Conference on Computer Communications (INFOCOM)*, 2011, pp. 1503–1511.

[63] Y. Wang, X. Cao, Q. Hu, and Y. Pan, "Towards elastic and fine-granular bandwidth allocation in spectrum-sliced optical networks," *IEEE/OSA Journal of Optical Communications and Networking*, vol. 4, no. 11, pp. 906–917, Nov. 2012.

[64] W. D. Grover, *Mesh-Based Survivable Networks: Options and Strategies for Optical, MPLS, SONET and ATM Networking*. New York, NY, USA: Prentice-Hall, 2003.

[65] L. Velasco, M. Klinkowski, M. Ruiz, and J. Comellas, "Modeling the routing and spectrum allocation problem for flexgrid optical networks," *Photonic Network Communications*, vol. 24, no. 3, pp. 177–186, Dec. 2012.

[66] A. Cai, G. Shen, L. Peng, and M. Zukerman, "Novel node-arc model and multiiteration heuristics for static routing and spectrum assignment in elastic optical networks," *IEEE/OSA Journal of Lightwave Technology*, vol. 31, no. 21, pp. 3402–3413, Nov. 2013.

[67] M. Klinkowski and K. Walkowiak, "Routing and spectrum assignment in spectrum sliced elastic optical path network," *IEEE Communications Letters*, vol. 15, no. 8, pp. 884–886, Aug. 2011.

[68] X. Wan, L. Wang, N. Hua, H. Zhang, and X. Zheng, "Dynamic routing and spectrum assignment in flexible optical path networks," in *Proc. Optical Fiber Communication Conference and Exposition/National Fiber Optic Engineers Conference*, 2011, p. JWA055.

[69] X. Wan, N. Hua, and X. Zheng, "Dynamic routing and spectrum assignment in spectrum-flexible transparent optical networks," *IEEE/OSA Journal of Optical Communications and Networking*, vol. 4, no. 8, pp. 603–613, 2012.

[70] Y. Liu, N. Hua, X. Wan, X. Zheng, and Z. Liu, "A spectrum-scan routing scheme in flexible optical networks," in *Proc. Asia Communications and Photonics Conference and Exhibition*, 2011, pp. 1–6.

[71] G. Shen, S. K. Bose, T. H. Cheng, C. Lu, and T. Y. Chai, "Efficient heuristic algorithms for light-path routing and wavelength assignment in WDM networks under dynamically varying loads," *Computer Communications*, vol. 24, no. 3, pp. 364–373, 2001.

[72] Y. Liu, N. Hua, X. Zheng, H. Zhang, and B. Zhou, "Discrete spectrum-scan routing based on spectrum discretization in flexible optical networks," in *Proc. Optical Fiber Communication Conference and Exposition/National Fiber Optic Engineers Conference*, 2012, pp. 1–3.

[73] W. Fawaz and K. Chen, "Survivability-oriented quality of service in optical networks," *End-to-End Quality of Service Engineering in Next Generation Heterogenous Networks*, pp. 197–211, 2010.

[74] D. Zhou and S. Subramaniam, "Survivability in optical networks," *IEEE Network*, vol. 14, no. 6, pp. 16–23, Nov. 2000.

[75] E. Mannie and D. Papadimitriou, "Recovery (protection and restoration) terminology for generalized multi-protocol label switching (GMPLS)," *Request for Comments: 4427*, 2006.

[76] R. Ramaswami, K. Sivarajan, and G. Sasaki, *Optical networks: a practical perspective*. Morgan Kaufmann, 2009.

[77] S. Ramamurthy and B. Mukherjee, "Survivable WDM mesh networks. part i-protection," in *Proc. IEEE International Conference on Computer Communications (INFOCOM)*, vol. 2, 1999, pp. 744–751.

[78] ——, "Survivable WDM mesh networks. ii. restoration," in *Proc. IEEE International Conference on Communications*, vol. 3, 1999, pp. 2023–2030.

[79] B. Mukherjee, *Optical Communication Networks*. McGraw-Hill New York, 1997.

[80] W. D. Grover and D. Stamatelakis, "Cycle-oriented distributed preconfiguration: Ring-like speed with mesh-like capacity for self-planning network restoration," in *Proc. IEEE International Conference on Communications*, vol. 1, 1998, pp. 537–543.

[81] C. Ou, H. Zang, N. K. Singhal, K. Zhu, L. H. Sahasrabuddhe, R. A. MacDonald, and B. Mukherjee, "Subpath protection for scalability and fast recovery in optical WDM mesh networks," *IEEE Journal on Selected Areas in Communications*, vol. 22, no. 9, pp. 1859–1875, 2004.

[82] X. Shao, Y.-K. Yeo, Z. Xu, X. Cheng, and L. Zhou, "Shared-path protection in OFDM-based optical networks with elastic bandwidth allocation," in *Proc. Optical Fiber Communication Conference and Exposition/National Fiber Optic Engineers Conference*, 2012, pp. 1–3.

[83] G. Shen, Y. Wei, and Q. Yang, "Shared backup path protection (SBPP) in elastic optical transport networks," in *Proc. Asia Communications and Photonics Conference and Exhibition*, 2012, pp. PAF4C–6.

[84] G. Shen, Y. Wei, and S. Bose, "Optimal design for shared backup path protected elastic optical networks under single-link failure," *IEEE/OSA Journal of Optical Communications and Networking*, vol. 6, no. 7, pp. 649–659, 2014.

[85] Y. Wei and G. Shen, "Span restoration for flexi-grid optical networks under different spectrum conversion capabilities," in *Proc. International Conference on Design of Reliable Communication Networks*, 2013, pp. 79–87.

[86] K. Walkowiak, M. Klinkowski, B. Rabiega, and R. Goścień, "Routing and spectrum allocation algorithms for elastic optical networks with dedicated path protection," *Optical Switching and Networking*, vol. 13, pp. 63–75, 2014.

[87] M. Klinkowski and K. Walkowiak, "Offline rsa algorithms for elastic optical networks with dedicated path protection consideration," in *Proc. International Congress on Ultra Modern Telecommunications and Control Systems and Workshops*, 2012, pp. 670–676.

[88] A. N. Patel, P. N. Ji, J. P. Jue, and T. Wang, "Survivable transparent flexible optical WDM (FWDM) networks," in *Proc. Optical Fiber Communication Conference and Exposition/National Fiber Optic Engineers Conference*, 2011, p. OTuI2.

[89] Y. Wei, G. Shen, and S. K. Bose, "Applying ring cover technique to elastic optical networks," in *Proc. Asia Communications and Photonics Conference and Exhibition*, 2013, pp. AF1I–4.

[90] Y. Wei, K. Xu, H. Zhao, and G. Shen, "Applying p-cycle technique to elastic optical networks," in *Proc. International Conference on Optical Network Design and Modeling*, 2014, pp. 1–6.

[91] Y. Wei, K. Xu, Y. Jiang, H. Zhao, and G. Shen, "Optimal design for p-cycle-protected elastic optical networks," *Photonic Network Communications*, vol. 29, no. 3, pp. 257–268, 2015.

[92] Y. Wei, G. Shen, and S. K. Bose, "Span-restorable elastic optical networks under different spectrum conversion capabilities," *IEEE Transactions on Reliability*, vol. 63, no. 2, pp. 401–411, Jun. 2014.

[93] K. Zhu and B. Mukherjee, "Traffic grooming in an optical WDM mesh network," *IEEE Journal on Selected Areas in Communications*, vol. 20, no. 1, pp. 122–133, 2002.

[94] R. Dutta and G. N. Rouskas, "Traffic grooming in WDM networks: Past and future," *IEEE Network*, vol. 16, no. 6, pp. 46–56, 2002.

[95] Y. Zhang, X. Zheng, Q. Li, N. Hua, Y. Li, and H. Zhang, "Traffic grooming in spectrum-elastic optical path networks," in *Proc. Optical Fiber Communication Conference and Exposition/National Fiber Optic Engineers Conference*, 2011, p. OTuI1.

[96] M. Liu, M. Tornatore, and B. Mukherjee, "Survivable traffic grooming in elastic optical networks—shared protection," *IEEE/OSA Journal of Lightwave Technology*, vol. 31, no. 6, pp. 903–909, 2013.

[97] A. N. Patel, P. N. Ji, J. P. Jue, and T. Wang, "Defragmentation of transparent flexible optical WDM (FWDM) networks," in *Proc. Optical Fiber Communication Conference and Exposition/National Fiber Optic Engineers Conference*, 2011, pp. 1–3.

[98] F. Cugini, F. Paolucci, G. Meloni, G. Berrettini, M. Secondini, F. Fresi, N. Sambo, L. Poti, and P. Castoldi, "Push-pull defragmentation without traffic disruption in flexible grid optical networks," *IEEE/OSA Journal of Lightwave Technology*, vol. 31, no. 1, pp. 125–133, 2013.

[99] R. Proietti, R. Yu, K. Wen, Y. Yin, and S. Yoo, "Quasi-hitless defragmentation technique in elastic optical networks by a coherent rx lo with fast tx wavelength tracking," in *Proc. Photonics in Switching*, 2012, pp. 1–3.

[100] R. Wang and B. Mukherjee, "Provisioning in elastic optical networks with non-disruptive defragmentation," *IEEE/OSA Journal of Lightwave Technology*, vol. 31, no. 15, pp. 2491–2500, 2013.

[101] Y. Yin, M. Zhang, Z. Zhu, and S. Yoo, "Fragmentation-aware routing, modulation and spectrum assignment algorithms in elastic optical networks," in *Proc. Optical Fiber Communication Conference and Exposition/National Fiber Optic Engineers Conference*, 2013, pp. 1–3.

[102] G. Shen, A. Cai, and L. Peng, "Benefits of sub-band virtual concatenation (vcat) in CO-OFDM optical networks," in *Proc. International Conference on Transparent Optical Networks*, 2012, pp. 1–4.

[103] A. Cai, L. Peng, and G. Shen, "Sub-band virtual concatenation lightpath blocking performance evaluation for CO-OFDM optical networks," in *Proc. Asia Communications and Photonics Conference and Exhibition*, 2012, pp. AS4D–3.

[104] X. Chen, A. Jukan, and A. Gumaste, "Multipath de-fragmentation: Achieving better spectral efficiency in elastic optical path networks," in *Proc. IEEE International Conference on Computer Communications (INFOCOM)*, 2013, pp. 390–394.

[105] Y. Yang, J. Wang, and C. Qiao, "Nonblocking WDM multicast switching networks," *IEEE Transactions on Parallel and Distributed Systems*, vol. 11, no. 12, pp. 1274–1287, 2000.

[106] L. H. Sahasrabuddhe and B. Mukherjee, "Light-trees: optical multicasting for improved performance in wavelength routed networks," *IEEE Communications Magazine*, vol. 37, no. 2, pp. 67–73, 1999.

[107] A. Gumaste and I. Chlamtac, "Light-trails: A novel conceptual framework for conducting optical communications," in *Proc. IEEE International Conference on High Performance Switching and Routing*, 2003, pp. 251–256.

[108] N. A. VanderHorn, S. Balasubramanian, M. Mina, and A. K. Somani, "Light-trail testbed for ip-centric applications," *IEEE Communications Magazine*, vol. 43, no. 8, pp. S5–10, Aug. 2005.

[109] M. Ali and J. S. Deogun, "Power-efficient design of multicast wavelength-routed networks," *IEEE Journal on Selected Areas in Communications*, vol. 18, no. 10, pp. 1852–1862, Oct. 2000.

[110] P. S. Khodashenas, J. M. Rivas-Moscoso, D. Klonidis, G. Thouénon, C. Betoule, and I. Tomkos, "Impairment-aware resource allocation over flexi-grid network with all-optical add/drop capability," in *Proc. European Conference on Optical Communication*, 2015.

[111] S. Sankaranarayanan and S. Subramaniam, "Comprehensive performance modeling and analysis of multicasting in optical networks," *IEEE Journal on Selected Areas in Communications*, vol. 21, no. 9, pp. 1399–1413, 2003.

[112] R. Malli, X. Zhang, and C. Qiao, "Benefits of multicasting in all-optical networks," in *Proceedings of SPIE*, vol. 3531, 1998, pp. 209–220.

[113] A. Ding and G. S. Poo, "A survey of optical multicast over WDM networks," *Computer Communications*, vol. 26, no. 2, pp. 193–200, 2003.

[114] F. Zhou, M. Molnár, and B. Cousin, "Light-hierarchy: the optimal structure for multicast routing in WDM mesh networks," in *Proc. IEEE International Conference on Communications*, 2010, pp. 611–616.

[115] Y. Li, J. Wang, A. Gumaste, Y. Xu, and Y. Xu, "Multicast routing in light-trail WDM networks," in *Proc. IEEE Global Communications Conference*, 2008, pp. 1–5.

[116] R. Lin, W. D. Zhong, S. K. Bose, and M. Zukerman, "Multicast traffic grooming in tap-and-continue WDM mesh networks," *IEEE/OSA Journal of Optical Communications and Networking*, vol. 4, no. 11, pp. 918–935, Nov. 2012.

[117] D. D. Le, M. Molnár, and J. Palaysi, "Multicast routing in WDM networks without splitters," *IEEE Communications Magazine*, vol. 52, no. 7, pp. 158–167, Jul. 2014.

[118] D. D. Le and M. Merabet, "Light-trail based hierarchy: the optimal multicast route in WDM networks without splitters and converters," in *Proc. International Conference on Photonics, Optics and Laser Technology*, 2014, p. 8.

[119] C. K. Constantinou, K. Manousakis, and G. Ellinas, "Multicast routing algorithms for sparse splitting optical networks," *Computer Communications*, vol. 77, pp. 100–113, 2016.

[120] D. D. Le, F. Zhou, and M. Molnár, "Minimizing blocking probability for the multicast routing and wavelength assignment problem in WDM networks: exact solutions and heuristic algorithms," *IEEE/OSA Journal of Optical Communications and Networking*, vol. 7, no. 1, pp. 36–48, Jan. 2015.

[121] P. Majumdar, A. Pal, and T. De, "Extending light-trail into elastic optical networks for dynamic traffic grooming," *Optical Switching and Networking*, vol. 20, pp. 1–15, 2016.

[122] W. Kmiecik, R. Goścień, K. Walkowiak, and M. Klinkowski, "Two-layer optimization of survivable overlay multicasting in elastic optical networks," *Optical Switching and Networking*, vol. 14, pp. 164–178, Aug. 2014.

[123] N. Sambo, A. D'Errico, C. Porzi, V. Vercesi, M. Imran, F. Cugini, A. Bogoni, L. Potì, and P. Castoldi, "Sliceable transponder architecture including multiwavelength source," *IEEE/OSA Journal of Optical Communications and Networking*, vol. 6, no. 7, pp. 590–600, 2014.

[124] Q. Wang and L. K. Chen, "Performance analysis of multicast traffic over spectrum elastic optical networks," in *Proc. Optical Fiber Communication Conference and Exposition/National Fiber Optic Engineers Conference*, 2012, pp. OTh3B–7.

[125] Z. Yu, Y. Zhao, J. Zhang, X. Yu, B. Chen, and X. Lin, "Multicast routing and spectrum assignment in elastic optical networks," in *Proc. Asia Communications and Photonics Conference and Exhibition*, 2012, p. AF3E.3.

[126] M. Ruiz and L. Velasco, "Performance evaluation of light-tree schemes in flexgrid optical networks," *IEEE Communications Letters*, vol. 18, pp. 1731–1734, Oct. 2014.

[127] L. Gong, X. Zhou, X. Liu, W. Zhao, W. Lu, and Z. Zhu, "Efficient resource allocation for all-optical multicasting over spectrum-sliced elastic optical networks," *IEEE/OSA Journal of Optical Communications and Networking*, vol. 5, no. 8, pp. 836–847, Aug. 2013.

[128] K. Walkowiak, R. Goscien, M. Klinkowski, and M. Wozniak, "Optimization of multicast traffic in elastic optical networks with distance-adaptive transmission," *IEEE Communications Letters*, vol. 18, no. 12, pp. 2117–2120, Dec. 2014.

[129] K. Walkowiak, A. Kasprzak, and M. Woźniak, "Algorithms for calculation of candidate trees for efficient multicasting in elastic optical networks," in *Proc. International Conference on Transparent Optical Networks*, 2015, pp. 1–4.

[130] K. Walkowiak, R. Goscien, M. Tornatore, and M. Wozniak, "Impact of fanout and transmission reach on performance of multicasting in elastic optical networks," in *Proc. Optical Fiber Communication Conference and Exposition/National Fiber Optic Engineers Conference*, 2015, pp. Th2A–44.

[131] Z. Zhu, X. Liu, Y. Wang, W. Lu, L. Gong, S. Yu, and N. Ansari, "Impairment- and splitting-aware cloud-ready multicast provisioning in elastic optical networks," *IEEE/ACM Transactions on Networking*, 2016.

[132] M. Moharami, A. Fallahpour, H. Beyranvand, and J. A. Salehi, "Resource allocation and multicast routing in elastic optical networks," *IEEE Transactions on Communications*, vol. 65, no. 5, pp. 2101–2113, 2017.

[133] L. Yang, L. Gong, F. Zhou, B. Cousin, M. Molnár, and Z. Zhu, "Leveraging light forest with rateless network coding to design efficient all-optical multicast schemes for elastic optical networks," *IEEE/OSA Journal of Lightwave Technology*, vol. 33, no. 18, pp. 3945–3955, 2015.

[134] Z. Fan, Y. Li, G. Shen, and C. C.-K. Chan, "Dynamic resource allocation for all-optical multicast based on sub-tree scheme in elastic optical networks," in *Proc. Optical Fiber Communication Conference and Exposition/National Fiber Optic Engineers Conference*, 2016, pp. 1–3.

[135] Z. Fan, Y. Li, G. Shen, and C.-K. Chan, "Distance-adaptive spectrum resource allocation using subtree scheme for all-optical multicasting in elastic optical networks," *IEEE/OSA Journal of Lightwave Technology*, 2016.

[136] M. Ruiz and L. Velasco, "Serving multicast requests on single-layer and multilayer flexgrid networks," *IEEE/OSA Journal of Optical Communications and Networking*, vol. 7, no. 3, pp. 146–155, Mar. 2015.

[137] A. Bocoi, M. Schuster, F. Rambach, M. Kiese, C.-A. Bunge, and B. Spinnler, "Reach-dependent capacity in optical networks enabled by OFDM," in *Proc. Optical Fiber Communication Conference and Exposition/National Fiber Optic Engineers Conference*, 2009.

[138] A. Klekamp, R. Dischler, and F. Buchali, "Limits of spectral efficiency and transmission reach of optical-OFDM superchannels for adaptive networks," *IEEE Photonics Technology Letters*, vol. 23, no. 20, pp. 1526–1528, Oct. 2011.

[139] C. T. Politi, V. Anagnostopoulos, C. Matrakidis, A. Stavdas, A. Lord, V. López, and J. P. Fernández-Palacios, "Dynamic operation of flexi-grid OFDM-based networks," in *Proc. Optical Fiber Communication Conference and Exposition/National Fiber Optic Engineers Conference*, 2012, pp. OTh3B–2.

[140] A. Tarhan and C. Cavdar, "Shared path protection for distance adaptive elastic optical networks under dynamic traffic," in *Proc. International Congress on Ultra Modern Telecommunications and Control Systems and Workshops*, 2013, pp. 62–67.

[141] K. Walkowiak, *Modeling and Optimization of Cloud-Ready and Content-Oriented Networks*. Cham: Springer International Publishing, 2016, ch. Elastic Optical Networks, pp. 101–193.

[142] A. Cai, J. Guo, R. Lin, G. Shen, and M. Zukerman, "Multicast routing and distance-adaptive spectrum allocation in elastic optical networks with shared protection," *IEEE/OSA Journal of Lightwave Technology*, vol. 34, no. 17, pp. 4076–4088, Sep. 2016.

[143] W. S. Hu and Q. J. Zeng, "Multicast optical cross connects employing splitter-and-delivery switch," *IEEE Photonics Technology Letters*, vol. 10, no. 7, pp. 970–972, 1998.

[144] M. Ali and J. S. Deogun, "Cost-effective implementation of multicasting in wavelength-routed networks," *IEEE/OSA Journal of Lightwave Technology*, vol. 18, no. 12, p. 1628, 2000.

[145] Gurobi Optimization, Inc., "Gurobi optimizer reference manual," 2015. [Online]. Available: http://www.gurobi.com

[146] A. Gumaste and S. Q. Zheng, "Protection and restoration scheme for light-trail WDM ring networks," in *Proc. International Conference on Optical Network Design and Modeling*, 2005.

[147] R. Fourer, D. Gay, and B. Kernighan, *AMPL: A Modeling Language for Mathematical Programming (2nd Edition)*. Cengage Learning, 2002.

[148] N. K. Singhal, L. H. Sahasrabuddhe, and B. Mukherjee, "Provisioning of survivable multicast sessions against single link failures in optical WDM mesh networks," *IEEE/OSA Journal of Lightwave Technology*, vol. 21, no. 11, pp. 2587–2594, Nov. 2003.

[149] H. Takahashi and A. Matsuyama, "An approximate solution for the Steiner problem in graphs," *Mathematica Japonica*, vol. 24, no. 6, pp. 573–577, Feb. 1980.

[150] Z. Fan, "Flexible spectrum resource allocation in elastic optical networks," PhD dissertation, The Chinese University of Hong Kong, Nov. 2016.

[151] M. Médard, S. G. Finn, and R. A. Barry, "Redundant trees for preplanned recovery in arbitrary vertex-redundant or edge-redundant graphs," *IEEE/ACM Transactions on Networking*, vol. 7, no. 5, pp. 641–652, Oct. 1999.

[152] N. K. Singhal and B. Mukherjee, "Protecting multicast sessions in WDM optical mesh networks," *IEEE/OSA Journal of Lightwave Technology*, vol. 21, no. 4, pp. 884–892, Apr. 2003.

[153] L. Long and A. E. Kamal, "Tree-based protection of multicast services in WDM mesh network," in *Proc. IEEE Global Communications Conference*, 2009, pp. 1–6.

[154] C. K. Constantinou and G. Ellinas, "A novel multicast routing algorithm and its application for protection against single-link and single-link/node failure scenarios in optical WDM mesh networks," *Optics Express*, vol. 19, no. 26, pp. B471–B477, Dec. 2011.

[155] T. Panayiotou, G. Ellinas, N. Antoniades, and A. Hadjiantoni, "A novel segment-based protection algorithm for multicast sessions in optical networks with mesh topologies," in *Proc. Optical Fiber Communication Conference and Exposition/National Fiber Optic Engineers Conference*, 2011, pp. 1–3.

[156] T. Panayiotou, G. Ellinas, and N. Antoniades, "Segment-based protection of multicast connections in metropolitan area optical networks with quality-of-transmission considerations," *IEEE/OSA Journal of Optical Communications and Networking*, vol. 4, no. 9, pp. 692–702, Sep. 2012.

[157] C. K. Constantinou, G. Ellinas, and K. Manousakis, "Survivability of multicast requests in mesh optical networks," in *Proc. International Conference on Transparent Optical Networks*, 2014.

[158] N. K. Singhal, C. Ou, and B. Mukherjee, "Cross-sharing vs. self-sharing trees for protecting multicast sessions in mesh networks," *Computer Networks*, vol. 50, no. 2, pp. 200–206, Feb. 2006.

[159] P. Leelarusmee, C. Boworntummarat, and L. Wuttisittikulkij, "Design and analysis of five protection schemes for preplanned recovery in multicast WDM networks," in *Proc. IEEE Sarnoff Symposium on Advances in Wired and Wireless Communications*, 2004, pp. 167–170.

[160] T. Rahman and G. Ellinas, "Protection of multicast sessions in WDM mesh optical networks," in *Proc. Optical Fiber Communication Conference and Exposition/National Fiber Optic Engineers Conference*, 2005.

[161] W. D. Zhong and F. Zhang, "An overview of *p*-cycle based optical multicast protection approaches in mesh WDM networks," *Optical Switching and Networking*, vol. 8, no. 4, pp. 259–274, Dec. 2011.

[162] F. Zhang, W. D. Zhong, and Y. H. Jin, "Optimizations of *p*-cycle-based protection of optical multicast sessions," *IEEE/OSA Journal of Lightwave Technology*, vol. 26, no. 19, pp. 3298–3306, Oct. 2008.

[163] F. Zhang and W. D. Zhong, "Performance evaluation of optical multicast protection approaches for combined node and link failure recovery," *IEEE/OSA Journal of Lightwave Technology*, vol. 27, no. 18, pp. 4017–4025, Sep. 2009.

[164] T. H. Cormen, C. E. Leiserson, R. L. Rivest, and C. Stein, *Introduction to Algorithms (3rd ed.)*. Cambridge, MA, London, England: The MIT Press, 2009.

[165] K. Bharath-Kumar and J. Jaffe, "Routing to multiple destinations in computer networks," *IEEE Transactions on Communications*, vol. 31, no. 3, pp. 343–351, Mar. 1983.

[166] J. W. Suurballe, "Disjoint paths in a network," *Networks*, vol. 4, no. 2, pp. 125–145, Jan. 1974.

[167] M. Mohandespour and A. E. Kamal, "Multicast 1+1 protection: the case for simple network coding," in *Proc. IEEE International Conference on Computing, Networking and Communication*, 2015, pp. 853–857.

[168] D. R. Din and I. R. Lai, "Multicast protection problem on elastic optical networks using segment-base protection," in *Proc. International Conference on Informatics, Electronics & Vision*, Jun. 2015, pp. 1–6.

[169] A. Cai, M. Zukerman, R. Lin, and G. Shen, "Survivable multicast routing and spectrum assignment in light-tree-based elastic optical networks," in *Proc. Asia Communications and Photonics Conference and Exhibition*, 2015.